Table of Contents (Continued)

2.7.2.5 Puncture Accident - Shielding Consequences 2.7-61
2.7.3 Thermal 2.7-62
2.7.3.1 Summary of Pressures and Temperatures 2.7-62
2.7.3.2 Differential Thermal Expansion Stress 2-7-62
2.7.4 Crush 2.7-66
2.7.5 Immersion - Fissile Material 2.7-66
2.7.6 Immersion - All Packages 2.7-66
2.7.6.1 Membrane Stresses in Cask Outer Shell (away from ends) 2.7-69
2.7.6.2 Bending Stress in the Bottom Forging (at center) 2.7-69
2.7.6.3 Bending Stress in the Cask Lid (at center) 2.7-70
2.7.6.4 Bending Stress in the Cask Bottom (at center) 2.7-70
2.7.6.5 Bending Stress in the Port Cover Plate (at center) 2.7-71
2.7.7 PWR Transportable Storage Canister Analysis - Accident Conditions 2.7-73
2.7.7.1 Analysis Description 2.7-74
2.7.7.2 Analysis Results - PWR Canister 2.7-74
2.7.7.3 Canister Buckling Evaluation for 30-Foot End Drop 2.7-88
2.7.8 PWR Basket Analysis - Accident Conditions 2.7-91
2.7.8.1 Stress Evaluation of Support Disk 2.7-91
2.7.8.2 Stress Evaluation of Tie Rods and Spacers 2.7-116
2.7.8.3 Buckling Evaluation of Support Disk 2.7-119
2.7.8.4 Fuel Tube Analysis 2.7-125
2.7.8.5 Basket Weldment Analysis for 30-Foot End Drop 2.7-132
2.7.9 BWR Transportable Storage Canister Analysis - Accident Conditions 2.7-136
2.7.9.1 Analysis Description 2.7-137
2.7.9.2 Analysis Results - BWR Canister 2.7-137
2.7.9.3 Canister Buckling Evaluation for 30-Foot End Drop 2.7-151
2.7.10 BWR Basket Analysis - Accident Conditions 2.7-153
2.7.10.1 Stress Evaluation of Support Disk 2.7-154
2.7.10.2 Stress Evaluation of Tie Rods and Spacers 2.7-181
2.7.10.3 Buckling Evaluation of Support Disk 2.7-183
2.7.10.4 Fuel Tube Analysis 2.7-189
2.7.10.5 Basket Weldment Analysis for 30-Foot End-Drop 2.7-194

Table of Contents (Continued)

2.7.11 Summary of Damage to Cask Due to Hypothetical Accident Conditions .. 2.7-198
2.7.12 Cask Inner Shell Buckling Analysis 2.7-201
2.7.12.1 Analysis Methodology 2.7-201
2.7.12.2 Analysis Results 2.7-202
2.7.12.3 Detailed Code Case N-284-1 Buckling Evaluation 2.7-202

2.8 Special Form 2.8-1

2.9 Fuel Rod Buckling Evaluation 2.9-1
2.9.1 UMS® Design Basis Fuel Buckling Evaluation 2.9.1-1
2.9.1.1 Design Basis PWR Fuel Rod Mode Shapes and Buckling Evaluation 2.9.1-2
2.9.1.2 Design Basis BWR Fuel Rod Mode Shapes and Buckling Evaluation 2.9.1-3
2.9.2 Buckling Evaluation for Maine Yankee Site Specific Fuel 2.9.2-1
2.9.2.1 Buckling Evaluation for Maine Yankee High Burnup Fuel 2.9.2-1
2.9.2.2 Buckling Evaluation for Maine Yankee High Burnup Fuel with Mechanical Damage 2.9.2-4

2.10 Appendices 2.10-1
2.10.1 Computer Program Descriptions 2.10.1-1
2.10.1.1 ANSYS 2.10.1-1
2.10.1.2 LS-DYNA 2.10.1-2
2.10.2 Finite Element Model - Universal Transport Cask 2.10.2-1
2.10.2.1 Load Application and Boundary Conditions 2.10.2-5
2.10.2.2 Post-Processing of Results 2.10.2-13
2.10.3 Confirmatory Testing Program – UMS® Impact Limiters and Attachments 2.10.3-1
2.10.3.1 Confirmatory Testing Program Results Summary 2.10.3-1
2.10.3.2 Acceptance Criteria for Model Performance 2.10.3-3

Table of Contents (Continued)

2.10.3.3 30-Foot Top End Drop and 30-Foot Top Corner Drop Tests Performed at ORNL 2.10.3-4
2.10.3.4 30-Foot Side Drop Test Performed at SNL 2.10.3-19
2.10.3.5 Evaluation of the 30-Foot Oblique Drop 2.10.3-26
2.10.3.6 Scale Model Drawings 2.10.3-26
2.10.3.7 LS-DYNA Analyses of the UMS® Quarter-Scale Model 2.10.3-27

2.10.4 Dynamic Load Factor (DLF) Evaluation for PWR and BWR Support Disks 2.10.4-1
2.10.4.1 1-Foot End Drop Analysis 2.10.4-1
2.10.4.2 Side Drop Analysis 2.10.4-7

2.11 Site Specific Contents Structural Evaluations 2.11-1
2.11.1 Site Specific Spent Fuel 2.11-1
2.11.1.1 Maine Yankee Site Specific Spent Fuel 2.11.1-1
2.11.2 Site Specific Greater Than Class C Waste 2.11.2-1
2.11.2.1 Maine Yankee Greater Than Class C Waste 2.11.2-1

2.12 References 2.12-1

List of Figures

Figure 2.5.1.1-1 Primary Lifting Trunnion Geometry 2.5-27
Figure 2.5.1.1-2 Secondary Lifting Trunnion Geometry 2.5-28
Figure 2.5.2.1-1 Front Support and Tiedown Geometry 2.5-37
Figure 2.5.2.1-2 Shear Ring Geometry 2.5-38
Figure 2.5.2.1-3 Free-Body Diagram of Cask Subjected to Lateral Load 2.5-39
Figure 2.6.7.5-1 Universal Transport Cask with Impact Limiters 2.6-73
Figure 2.6.7.5-2 Cross-Section of Lower Impact Limiter 2.6-74
Figure 2.6.7.5-3 LS-DYNA Finite Element Model 2.6-75
Figure 2.6.7.5-4 Impact Limiter Shell LS-DYNA Finite Element Model 2.6-76
Figure 2.6.7.5-5 Acceleration Time History for the Cold Condition 30-Foot Top End Drop 2.6-77
Figure 2.6.7.5-6 Acceleration Time History for the Cold Condition 30-Foot Top Corner Drop 2.6-78
Figure 2.6.7.5-7 Acceleration Time History for the Cold Condition 30-Foot Side Drop 2.6-79
Figure 2.6.7.5-8 Impact Limiter Attachment Geometry 2.6-80
Figure 2.6.7.7-1 Neutron Shield Geometry 2.6-93
Figure 2.6.12-1 PWR Transportable Storage Canister 2.6-118
Figure 2.6.12-2 PWR Transportable Storage Canister Shell and Lids 2.6-119
Figure 2.6.12.2-1 PWR Canister Assembly Finite Element Model 2.6-124
Figure 2.6.12.2-2 Canister Structural and Shield Lid Finite Element Mesh 2.6-125
Figure 2.6.12.2-3 Structural and Shield Lid Weld Regions Finite Element Mesh 2.6-126
Figure 2.6.12.2-4 Canister Bottom Plate Finite Element Mesh 2.6-127
Figure 2.6.12.3-1 Identification of Sections for Evaluating Linearized Stresses in Canister 2.6-132
Figure 2.6.13-1 PWR Fuel Assembly Basket 2.6-177
Figure 2.6.13-2 Support Disk Cross Section Configuration 2.6-178
Figure 2.6.13-3 PWR Fuel Tube Configuration 2.6-179
Figure 2.6.13.2-1 PWR Basket Model for Side-Drop 2.6-185
Figure 2.6.13.2-2 Side Drop Orientation 2.6-186

List of Figures (Continued)

Figure 2.6.15.13-1 Finite Element Model of the Top Weldment Plate 2.6-365
Figure 2.6.15.13-2 Finite Element Model of the Bottom Weldment Plate 2.6-366
Figure 2.7.1.5-1 Radial Lead Slump Model 2.7-31
Figure 2.7.2.1-1 Cask Body Model for Puncture Analysis 2.7-44
Figure 2.7.2.1-2 Location of Sections for Evaluation 2.7-45
Figure 2.7.2.2-1 ANSYS Model for Cask Lid 2.7-51
Figure 2.7.2.3-1 Bottom Puncture Finite Element Model and Boundary Conditions 2.7-56
Figure 2.7.2.3-2 Location of Sections for Evaluation 2.7-57
Figure 2.7.6-1 Cross Section of Cask Body 2.7-72
Figure 2.7.7.2-1 Identification of the Sections for Evaluating the Linearized Stresses in the PWR Canister 2.7-76
Figure 2.7.9.2-1 Identification of Sections for Evaluating Linearized Stresses in BWR Canister 2.7-139

Figure 2.9.1-1 Typical Fuel Rod Finite Element Model and Boundary Conditions 2.9.1-5
Figure 2.9.1-2 Typical First Lateral Mode Shape Plot for Fuel Rod 2.9.1-6
Figure 2.9.1-3 Typical First Buckling Mode Shape for Fuel Rod 2.9.1-7
Figure 2.9.2-1 Two-Dimensional Beam Finite Element Model for Maine Yankee Fuel Rod 2.9.2-9
Figure 2.9.2-2 Mode Shape and First Buckling Shape for the Maine Yankee Fuel Rod 2.9.2-10
Figure 2.9.2-3 Two-Dimensional Beam Finite Element Model for Fuel Rod with Missing Grid 2.9.2-11
Figure 2.9.2-4 Modal Shape and First Buckling Mode Shape for a Fuel Rod with a Missing Grid 2.9.2-12
Figure 2.10.2-1 Primary Components of the Universal Transport Cask 2.10.2-3
Figure 2.10.2-2 Universal Transport Cask 3-D Model 2.10.2-4
Figure 2.10.2.1-1 Cask Body Loading for Side-Drop Conditions 2.10.2-11
Figure 2.10.2.1-2 View of Cask Model Showing Pressure Distribution for Side-Drop Analysis 2.10.2-12
Figure 2.10.2.2-1 Lower Cask Body Section Locations 2.10.2-14
Figure 2.10.2.2-2 Sections Through Cask Body Ligaments 2.10.2-14

List of Figures (Continued)

Figure 2.10.2.2-3 Cask Body Sections at Center 2.10.2-15
Figure 2.10.2.2-4 Cask Body Sections in Upper Cask 2.10.2-15
Figure 2.10.3-1 Typical Filtered Acceleration Time History for the Quarter- Scale Model Top End Drop, Overlayed with the Unfiltered Data 2.10.3-30
Figure 2.10.3-2 Force-Deflection Curve for Static Test 1 (End Drop Orientation) for a 45° Section of the Quarter-Scale Model Upper Impact Limiter 2.10.3-31
Figure 2.10.3-3 Force-Deflection Curve for Static Test 2 (End Drop Orientation) for a 45° Section of the Quarter-Scale Model Upper Impact Limiter 2.10.3-32
Figure 2.10.3-4 Typical Filtered Acceleration Time History for the Quarter-Scale Model Top Corner Drop, Overlayed with the Unfiltered Data 2.10.3-33
Figure 2.10.3-5 UMS® Quarter-Scale Side Drop Accelerometer Locations 2.10.3-34
Figure 2.10.3-6 Typical Filtered Acceleration (Top Accelerometer) Time History for the Quarter-Scale Model Side Drop, Overlayed with the Unfiltered Data 2.10.3-35
Figure 2.10.3-7 Typical Filtered Acceleration (Bottom Accelerometer) Time History for the Quarter-Scale Model Side Drop, Overlayed with the Unfiltered Data 2.10.3-36
Figure 2.10.3-8 Comparison of Quarter-Scale Side Drop (LS-DYNA and Drop Test) Results (Upper Accelerometer) 2.10.3-37
Figure 2.10.3-9 Comparison of Quarter-Scale Side Drop (LS-DYNA and Drop Test) Results (Lower Accelerometer) 2.10.3-38
Figure 2.10.3-10 Quarter-Scale Side Drop Force-Displacement Curve 2.10.3-39
Figure 2.10.3-11 LS-DYNA Quarter-Scale Model 2.10.3-40
Figure 2.10.3-12 Comparison of Quarter-Scale Top End Drop (LS-DYNA and Drop Test) Results 2.10.3-41
Figure 2.10.3-13 Comparison of Quarter-Scale Top Corner Drop (LS-DYNA and Drop Test) Results 2.10.3-42
Figure 2.10.3-14 Comparison of Quarter-Scale Test Model and LS-DYNA Deformation During the Side Drop 2.10.3-43
Figure 2.10.4.1-1 ANSYS Finite Element Model of PWR Support Disk for End Drop Analysis 2.10.4-3
Figure 2.10.4.1-2 ANSYS Finite Element Model of BWR Support Disk for End Drop Analysis 2.10.4-3

List of Figures (Continued)

Figure 2.10.4.1-3 1-Foot End-Drop Acceleration Time History 2.10.4-4
Figure 2.10.4.1-4 1-Foot End-Drop Frequency Response Spectrum 2.10.4-4
Figure 2.10.4.2-1 ANSYS Finite Element Model of PWR Support Disk for Side Drop Analysis 2.10.4-9
Figure 2.10.4.2-2 ANSYS Finite Element Model of BWR Support Disk for Side Drop Analysis 2.10.4-9
Figure 2.10.4.2-3 LS-DYNA Finite Element Model for Side Drop Analysis 2.10.4-10
Figure 2.10.4.2-4 1-Foot Side-Drop Acceleration Time History 2.10.4-11
Figure 2.10.4.2-5 PWR Support Disk Acceleration Time History for 1-Foot Side-Drop 2.10.4-11
Figure 2.10.4.2-6 BWR Support Disk Acceleration Time History for 1-Foot Side-Drop 2.10.4-12
Figure 2.10.4.2-7 PWR Support Disk Frequency Response Spectrum for 1-Foot Side Drop 2.10.4-12
Figure 2.10.4.2-8 BWR Support Disk Frequency Response Spectrum for 1-Foot Side Drop 2.10.4-13
Figure 2.11.1.1-1 PWR Basket Drop Orientations and Case Study Loading Positions for Maine Yankee Consolidated Fuel 2.11.1-19
Figure 2.11.2.1-1 Maine Yankee GTCC Basket Finite Element Model 2.11.2-22
Figure 2.11.2.1-2 Maine Yankee GTCC Basket Finite Element Model Pressure Loading Locations 2.11.2-23
Figure 2.11.2.1-3 Maine Yankee GTCC Basket Finite Element Model Section Locations for Stress Evaluation 2.11.2-24
Figure 2.11.2.1-4 Finite Element Model for Maine Yankee GTCC Basket Support Wall 2.11.2-25
Figure 2.11.2.1-5 Finite Element Model for Maine Yankee GTCC Basket Separator Plate 2.11.2-26

List of Tables

Table 2.1.2-1 Exceptions to Codes and Standards 2.1-12
Table 2.1.2-2 Load Combinations: Normal and Hypothetical Accident Conditions 2.1-15
Table 2.1.2-3 Allowable Stress Limits for Containment Structures 2.1-16
Table 2.1.2-4 Allowable Stress Limits for Noncontainment Structures 2.1-17
Table 2.2-1 Calculated Weights and Centers of Gravity: Cask with Canister Containing PWR Fuel 2.2-2
Table 2.2-2 Calculated Weights and Centers of Gravity: Cask with Canister Containing BWR Fuel 2.2-3
Table 2.2-3 Calculated Weights and Centers of Gravity: Cask with Canister Containing Greater Than Class C (GTCC) Waste 2.2-4
Table 2.3.2-1 Mechanical Properties of SA-240, Type 304 Stainless Steel 2.3-4
Table 2.3.2-2 Mechanical Properties of SA-479, Type 304 Stainless Steel 2.3-5
Table 2.3.2-3 Mechanical Properties of SA-240, Type 304L Stainless Steel 2.3-6
Table 2.3.2-4 Mechanical Properties of SA-336, Type 304 Stainless Steel 2.3-7
Table 2.3.2-5 Mechanical Properties of Type XM-19 Stainless Steel 2.3-8
Table 2.3.3-1 Mechanical Properties of SA-564 and SA-693, Type 630, 17-4 PH Stainless Steel 2.3-10
Table 2.3.4-1 Mechanical Properties of SA-533, Type B, Class 2 Carbon Steel 2.3-12
Table 2.3.5-1 Mechanical Properties of SB-637, Grade N07718 Nickel Alloy Steel Bolting Material 2.3-14
Table 2.3.5-2 Mechanical Properties of SA-193, Grade B6, High Alloy Steel Bolting Material 2.3-15
Table 2.3.5-3 Mechanical Properties of SA-193, Grade B8S, High Alloy Steel Bolting Material 2.3-16
Table 2.3.6-1 Mechanical Properties of 6061-T651 Aluminum Alloy 2.3-18
Table 2.3.7-1 Static Mechanical Properties of Chemical Copper Lead 2.3-20
Table 2.3.7-2 Mechanical Properties of NS-4-FR 2.3-21
Table 2.4.4.2-1 Summary of Universal Transport Cask Materials Categories and Operating Environments 2.4-8
Table 2.5.1.1-1 Primary Trunnion/Top Forging Intersection Analysis Results 2.5-29
Table 2.5.2.1-1 Reactions Caused by Tiedown Devices (from 10 CFR 71.45(b)) 2.5-40
Table 2.5.2.1-2 Reactions Caused by Tiedown Devices (from AAR Field Manual Rule 88) 2.5-41

List of Tables (Continued)

Table 2.7.10.1-21 $P_m + P_b$ Stresses for Support Disk 30-Foot Side-Drop, 90° Orientation, Thermal Case 2 ..... 2.7-177
Table 2.7.10.1-22 Summary of Stress Evaluation of Support Disk - 30-Foot End-Drop 2.7-178
Table 2.7.10.1-23 $P_m + P_b$ Stresses for Support Disk 30-Foot End-Drop, Thermal Case 1 ..... 2.7-179
Table 2.7.10.1-24 $P_m + P_b$ Stresses for Support Disk -30-Foot End-Drop, Thermal Case 4 ..... 2.7-180
Table 2.7.10.3-1 Minimum Margins of Safety from Buckling Evaluation of BWR Support Disk (Weak Axis) 2.7-187
Table 2.7.10.3-2 Minimum Margins of Safety from Buckling Evaluation of BWR Support Disk (Strong Axis) 2.7-188
Table 2.7.11-1 Summary of Maximum Calculated Stresses in Cask 30-Foot Free Drop 2.7-199
Table 2.7.11-2 Summary of Maximum Calculated Stresses in Cask—Puncture 2.7-200
Table 2.7.12-1 Buckling Evaluation Load Cases and Results for the Universal Transport Cask 2.7-210
Table 2.7.12-2 Geometry Parameters for the Universal Transport Cask 2.7-211
Table 2.9.1-1 Location of Lateral Constraints – PWR Fuel Rods 2.9.1-8
Table 2.9.1-2 PWR Fuel Rod Analysis Summary 2.9.1-8
Table 2.9.1-3 Location of Lateral Constraints for BWR Fuel Rods 2.9.1-9
Table 2.9.1-4 BWR Fuel Rod Analysis Summary 2.9.1-9
Table 2.10.2.2-1 Component Section and Temperature Definition 2.10.2-16
Table 2.10.2.2-2 Stress Section Locations 2.10.2-17
Table 2.10.4.1-1 Response Acceleration for PWR Support Disk for 1-Foot End Drop 2.10.4-5
Table 2.10.4.1-2 Response Acceleration for BWR Support Disk for 1-Foot End Drop 2.10.4-6
Table 2.10.4.2-1 Response Acceleration for PWR Support Disk for 1-Foot Side Drop 2.10.4-14
Table 2.10.4.2-2 Response Acceleration for BWR Support Disk for 1-Foot Side Drop 2.10.4-15

Figure 2.6.12-2 PWR Transportable Storage Canister Shell and Lids

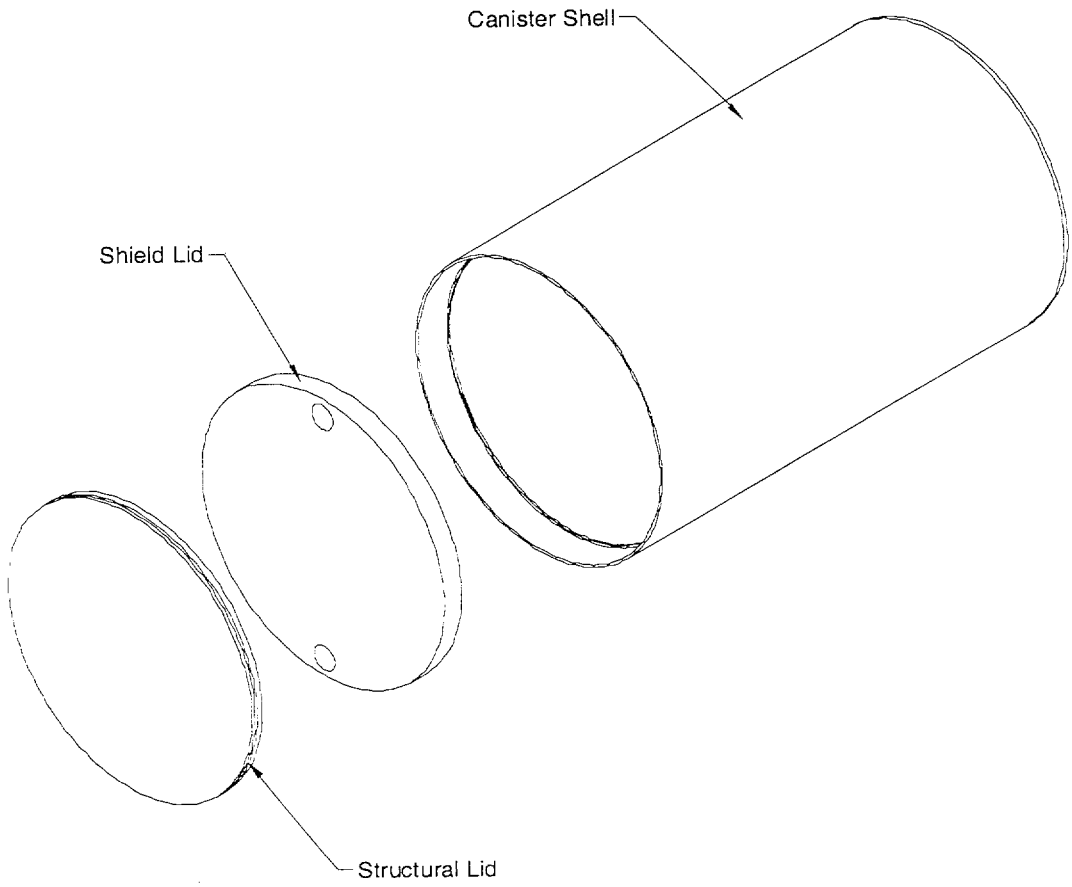

The maximum temperature in the canister shell central region is 399°F as determined in the thermal analysis presented in Section 3.4.2. This increase in temperature reduces the allowable S_m for Type 304L stainless steel from 16.0 ksi to 15.8 ksi. A review of the margins of safety for all cases evaluated indicates that the minimum margin for Sections 5 or 6 is 4.3 for the side-drop with pressure (Table 2.6.12.6-3). Using the allowable stress based on a temperature of 399°F reduces this minimum margin of safety to 4.23. Because this change in margin of safety is small, the increased peak temperature in the center of the canister has a negligible impact on the presented minimum margins.

The canister is analyzed by using the ANSYS [32] finite element computer program for the 1-ft free-drop condition in the top and bottom end, side, and top and bottom corner impact orientations. In addition, the effects of normal operating internal pressure and thermal stresses resulting from exposure of the cask to the hot (100°F ambient and solar insolance) and cold (-40°F ambient) normal conditions are evaluated. The worst-case stresses from these analyses are presented in Section 2.6.12.4.

2.6.12.2 Finite Element Model Description - PWR Canister

To evaluate the PWR Transportable Storage Canister for normal conditions of transport, ANSYS is used to construct and analyze a finite element model of the canister and its contents. The contents modeled consist of the fuel basket support disks and weldments. The fuel assemblies, fuel tubes, aluminum heat transfer disks, tie-rods, and related hardware are not explicitly modeled but rather are accounted for by applying pressure loads to the support disk slots as appropriate.

The finite element model of the canister is constructed by using ANSYS solid (SOLID45) elements. The model represents a one-half (180°) section of the canister and fuel basket. The basket support disks are modeled with three-dimensional shell (SHELL63) elements. The model uses gap-spring elements to simulate contact between adjacent components. Interaction between the basket and canister is accomplished by using three-dimensional gap elements (CONTAC52) along the periphery of the support disks. Contact between the canister and the cask inner shell is also modeled by using CONTAC52 gap elements. Contact between the canister structural lid and shield lid is modeled by using COMBIN40 combination elements in the axial degree of freedom. Simulation of the spacer ring is accomplished by using a ring of COMBIN40 spring

gap elements connecting the shield lid and the canister in the axial direction at the lid lower outside radius. In addition, CONTAC52 elements are used to model interaction between the structural lid and canister shell and the shield lid and canister shell just below the respective lid weld joints. The size of the CONTAC52 gaps are determined from the nominal dimensions of contacting components. The COMBIN40 elements used between the structural and shield lids and for the spacer ring are assigned small gap sizes of $1(10)^{-8}$ in. All gap-spring elements are assigned a stiffness of $1(10^{8})$ lb/in. Table 2.6.12.2-1 lists the element types assigned to specific gaps of the model. Table 2.6.12.2-2 lists the material properties used for the model.

Boundary conditions are applied to enforce symmetry at the cut boundary of the model. All nodes on the cask shell side of the canister-to-cask gap elements are fixed in all degrees of freedom. In addition, the axial and in-plane rotational degrees of freedom of the basket nodes are fixed.

Figure 2.6.12.2-1 is a plot of the entire canister finite element model including the support disks. An isolated view of the canister shield and structural lids portion of the model is presented in Figure 2.6.12.2-2, and an enlarged view of the model in the structural lid and shield lid weld regions is shown in Figure 2.6.12.2-3. The canister bottom plate portion of the model is shown in Figure 2.6.12.2-4.

The loading for the normal operating condition is based on 1-ft drops in conjunction with the internal pressure loading (to the canister). Drop orientations considered are the top and bottom end, side, and top and bottom corner-drops. In the end-drop orientation, the fuel contents load is transferred to the canister end and directly to the transport cask end through the cavity spacer. This corresponds to a compressive stress in the canister ends that is present in the finite element model. The canister shell is designed to be flush with the top surface of the structural lid with the worse case tolerance stack-up. This ensures that the content weight will be transferred through the lids to the transport cask during a top end or top corner drop condition. For the side-drop condition, the loads from the canister contents weight are transferred through the support disks into the canister wall, which is backed by the cask inner shell. Because the canister wall and the inner shell have different radii, a gap exists between the two surfaces. This gap results in the load passing only through regions in which the canister shell deflects to contact the inner shell. This load pattern is reflected in the side-drop analysis. For the corner-drop orientation, both the end-and side-load reactions with the cask inner shell are present.

The modeled contents weight includes 37,080 lb for all fuel assemblies (24 Class 1 PWR fuel assemblies), the fuel tube weight (3,417 lb), the aluminum heat transfer disk weight (1,946 lb), the disk spacer weight (1,879 lb), and the tie rod and nut and washer weights (783 + 94 lb). The weight of the support disks and weldments is accounted for by their being physically modeled. The PWR Class 1 configuration results in the largest load per support disk. The modeled canister length is 173.75 inches.

For the side and corner-drops, the weights of the fuel assemblies (W_{fuel}), aluminum heat transfer disks ($W_{ht\ disks}$), fuel tubes (W_{tubes}), tie rods (W_{rods}), nuts/washers (W_{nuts}), and spacers ($W_{spacers}$) are included in the model by applying a pressure load (F_{slot}) to the slot openings of the modeled support/weldment disks. This pressure load is calculated according to the following equation:

$$F_{slot} = \frac{W_{fuel} + W_{ht\,disks} + W_{tubes} + W_{rods} + W_{nuts} + W_{spacers}}{N_{slots} \times w_{slot} \times N_{disks}} \times g$$

where,

N_{slots} = number of slot openings in each support/weldment disk,
w_{slot} = width of each slot opening in each support/weldment disk,
N_{disks} = number of support/weldment disks, and
g = the associated g-loading for the drop height of interest.

For basket orientations other than 0°, the components of this resulting pressure load are applied to two faces of the slot opening. Additionally, for the corner-drops, the component resulting from accounting for the drop angle is used as the pressure load on the disk slot openings. For the PWR canister drop analyses, with 24 slot openings, a slot opening width of 9.272 inches, and a total of 34 support/weldment disks (32 support disks and 2 weldment disks), the resulting base pressure load used is:

$$F_{slot} = \frac{37{,}080 + 1{,}946 + 3{,}417 + 783 + 94 + 1{,}879}{24 \times 9.272 \times 34} \times g = 5.974 \times g$$

For the end drops, a uniform pressure representing the total weight of the fuel and fuel basket (52,369 lb) is applied to the canister shield lid (for top end-drop) or canister bottom plate (for

Figure 2.6.12.2-4 Canister Bottom Plate Finite Element Mesh

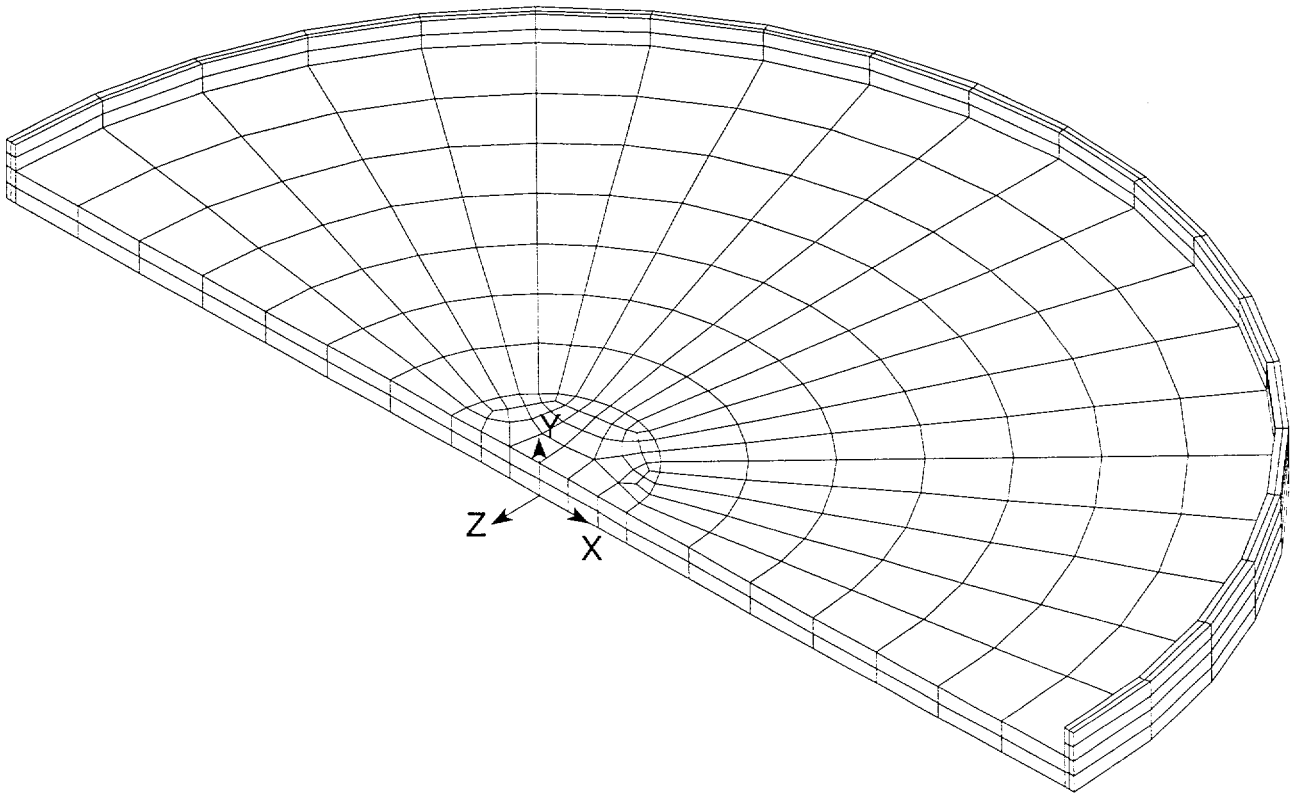

Table 2.6.12.2-1 Gap and Element Type Definition - Canister Model

Component
Axial Gaps from Canister Bottom Plate to Cask Shell (CONTAC52)
Radial Gaps from Canister Side to Cask Shell (CONTAC52)
Axial Gaps from Structural Lid Top to Cask Shell (CONTAC52)
Axial Gaps Between Structural and Shield Lid (COMBIN40)
Radial Gaps Between Shield Lid and Canister Inner Surface (CONTAC40)
Radial Gaps Between Shield Lid and Canister Inner Radius (CONTAC52)
Axial Gaps Between Shield Lid and Canister Wall to Simulate Spacer Ring (COMBIN40)
Radial Gaps Between Basket and Canister Inner Surface (CONTAC52)

Table 2.6.12.2-2 Material Definition - Canister Model

Component	Material
Canister Shell and Structural Lid	304L Stainless Steel; ASME SA240
Top and Bottom Weldments	304 Stainless Steel; ASME SA240
Shield Lid	304 Stainless Steel; ASME SA240
Support disk	17-4 PH, ASME SA693 Type 630 Stainless Steel

Table 2.6.14.2-1 Real Constant Sets Defined in Canister Model

Real Constant Set	Component
1	Canister Bottom Plate (SOLID45)
2-9	Canister Shell (SOLID45)
10-11	Shield Lid (SOLID45)
12-13	Structural Lid (SOLID45)
100	Axial Gaps from Canister Bottom Plate to Cask Shell (CONTAC52)
200	Radial Gaps from Canister Side to Cask Shell (CONTAC52)
300	Axial Gaps from Structural Lid Top to Cask Shell (CONTAC52)
400	Axial Gaps Between Structural and Shield Lid (COMBIN40)
500	Radial Gaps Between Shield Lid and Canister Inner Surface (CONTAC40)
600	Radial Gaps Between Shield Lid and Canister Inner Radius (CONTAC52)
700	Axial Gaps Between Shield Lid and Canister Wall to Simulate Spacer Ring (COMBIN40)
800	Radial Gaps Between Basket and Canister Inner Surface (CONTAC52)
1000	Intermediate Basket Thickness Real Constant
1100	End Basket Thickness Real Constant
1200	Weak Spring Real Constant

Table 2.6.14.2-2 Material Sets Defined in Canister Model

Material Property Set	Component	Material
1	Canister Shell and Structural Lid	304L Stainless Steel; ASME SA240
2	Top and Bottom End Basket Disk	304 Stainless Steel; ASME SA240
3	Shield Lid	304 Stainless Steel; ASME SA240
4	Support disk	ASME SA-533, Type B Class 2 Carbon Steel

2.6.14.3 Thermal Expansion and Thermal Stress Evaluation of Canister for BWR Fuel

A thermal stress evaluation is performed by using ANSYS to determine the differential thermal expansion and the associated thermal stresses that result from a heat load of 16 kW. In assessing the thermal stresses, the following three extreme conditions are considered:

Condition	Ambient Temperature	Solar Insolance Applied to Cask Surface	16 kW Fuel Load
1	100°F	Yes	Yes
2	-40°F	No	Yes
3	-40°F	No	No

The temperatures employed in the thermal stress analysis are obtained by applying temperatures at 36 key locations on the canister shell and ends to the thermal equivalent model of the structural canister model as thermal boundary conditions. These temperatures are taken from the thermal evaluation described in Section 3.4. The temperature distribution of the PWR canister is conservatively used in the BWR canister analyses since this produces the peak temperatures and temperature gradients. The structural finite element model is described in Section 2.6.14.2 and 2.6.12.2. The equivalent thermal model is obtained by changing the structural element SOLID45, which has three global displacements for degrees of freedom, to a SOLID70, which has temperature degrees of freedom at the individual nodes.

The temperature-dependent thermal conductivity for the canister material is employed in the thermal conduction analysis. The temperatures generated in this analysis are used in the thermal stress analysis to evaluate the properties at temperature as well as the stresses resulting from thermal expansion. Using this method, two separate cases are evaluated: a hot case (100°F ambient with solar heat load and maximum decay heat) and a cold case (-40°F ambient and maximum decay heat). Condition 3 is not evaluated because the entire assembly would be at -40°F for the conditions described.

According to the ASME Code, Section III, Subsection NB, the allowable stress criteria are based on the evaluation of linearized stresses across critical cross sections through the canister wall. For the evaluation of the thermal stresses, the criteria for the stresses are based on peak stresses. The stress values taken from the analyses are the nodal stresses at the surface. The sections used in this evaluation are shown in Figure 2.6.14.3-1. The thermal stresses reported in Tables 2.6.14.3-1 and 2.6.14.3-2 correspond to the maximum stresses for any circumferential section for the locations shown in Figure 2.6.14.3-1.

2.7 Hypothetical Accident Conditions

The Universal Transport Cask meets the standards specified in 10 CFR 71.51 when subjected to the conditions and tests specified in 10 CFR 71.73 for hypothetical accidents. In accordance with 10 CFR 71.73, the cask is structurally evaluated for hypothetical accident scenarios of free drop, puncture, fire, crush, and water immersion. In the free-drop analyses, the cask impact orientation evaluated is that which inflicts the maximum damage to the cask. The most unfavorable ambient temperature condition during operation in the range from -40°F to 100°F is assumed. The following sections contain the evaluation of the cask for structural integrity under the hypothetical accident conditions.

2.7.1 Free Drop (30 ft) - Cask Body Analysis

The Universal Transport Cask is required by 10 CFR 71.73(c)(1) to demonstrate structural adequacy for a free drop through a distance of 30 feet (9 meters) onto a flat, unyielding, horizontal surface. The cask payload is oriented to strike the surface to inflict the maximum damage. In determining the orientation that produces the maximum damage, the cask is evaluated for impact orientations in which the cask strikes the impact surface on its top end, bottom end, side, top corner, bottom corner, top-end oblique, and bottom-end oblique. Evaluation of each drop orientation is accomplished by using finite element analysis techniques. A complete description of the 3-D model used to analyze the cask body is presented in Appendix 2.10.2. The results of each drop orientation listed above is presented in this section. The impact limiters and the impact limiter attachments are evaluated in Section 2.6.7.5 for all loading conditions and orientations.

The mass of the contents is considered when evaluating impact. The environmental temperature for the drop is between -40°F and 100°F. For the accident condition, stresses arising from thermal expansion are not considered for the stress reevaluation. However, for determination of properties, the temperatures are considered. Heat generation from the contents and solar insolance are also considered. An internal pressure of 150 psig is applied in the finite element models to produce the bounding critical stress condition in conjunction with the other loads previously discussed. Eighty (80.0) psig is used in the cask closure analysis. As shown in Table 2.7.3.1-4, a pressure of 80 psig conservatively exceeds the maximum calculated internal pressures. Closure lid bolt preload is considered and fabrication stresses are discussed.

The following method and assumptions are adopted in all the drop analyses:

1. The finite element method is utilized to do the impact analyses. The analyses are performed using the ANSYS computer program.

2. The analyses assume linear elastic behavior of the cask.

3. The cask contents are applied to the cask as a pressure load. The pressure simulates the actual contents by applying the pressure as a cosine distribution.

4. The finite element model of the cask includes, geometrically, only the components of the cask body to be structurally analyzed; however, the weight of radial neutron shield spacers (as appropriate), and impact limiters are modeled as non-geometrical point mass elements. The payload and spacer (as appropriate) are modeled as distributed loads to attain a total weight of 252,444 pounds. To bound the loads produced during a 30-ft drop, an acceleration of 60 *g* was used for all 30-ft drop orientations presented in this section. Therefore, the weights presented for the cask body analysis are conservative and envelop the actual values presented in Section 2.2. Additionally, the stress results (worst case side and oblique drop stresses) were increased by a factor of 2.7% producing an effective cask weight of 259,260 lb (no credit taken for bounding acceleration).

5. To account for the lead slump during the drops, and for the differential thermal expansion between the cask stainless steel shells and lead shell, gap elements are used in the finite element model to simulate the multi-body contact between these components.

As discussed in Appendix 2.10.2, the loads and boundary conditions considered in the finite element analyses are: (1) Closure lid bolt preload, (2) internal pressure, (3) thermal, and (4) impact and inertial loads resulting from the impact event.

During fabrication of the Universal Transport Cask, thermal stresses can be introduced in the inner and outer shells as a result of pouring molten lead between them. However, any residual stresses in the containment vessel and the outer shell induced by shrinkage of the lead shielding after the lead pouring operation are relieved early in the life of the cask because of the low creep

2.9 Fuel Rod Buckling Evaluation

Regulatory Guide 7.9 [41] requires that analysis or test data be provided showing that the structural integrity of the fuel rod cladding justifies the amount of integrity claimed. An assessment of fuel rod buckling is performed. The bounding load condition for the assessment of fuel rod buckling is the end drop condition. The end drop orientation maximizes not only the axial force component that would buckle the fuel rod, but it is also the orientation that has the maximum axial acceleration. Both PWR and BWR fuel rod configurations are evaluated. The evaluations show that buckling of PWR or BWR fuel rods does not occur in the UMS® Transport Cask.

The UMS® design basis PWR and BWR fuel is evaluated for buckling in Section 2.9.1. Maine Yankee site specific fuel is evaluated for buckling in Section 2.9.2. The Maine Yankee evaluation includes high burnup fuel and fuel with a missing grid.

THIS PAGE INTENTIONALLY LEFT BLANK

2.9.1 UMS® Design Basis Fuel Buckling Evaluation

During the end drop, the fuel rod is expected to impact the fuel assembly base. The fuel rod itself will respond as an elastic bar under a sudden compression load at its bottom end. The duration of this impact is bounded by the first extensional mode shape of the fuel rod. Contribution of higher frequency extensional modes of the rod would tend to shorten the duration of impact of the fuel rod with the fuel assembly base. The fuel rod, upon initiation of the impact, corresponds to an undeformed state. In the process of the impact, the compression of the fuel rod will increase to a maximum and then return to a near uncompressed state. At this point, the time of impact is completed. This actually represents half of a cycle of the lowest frequency of an extensional mode shape of the fuel rod. The frequency of this mode shape is evaluated using ANSYS Revision 5.2. The shape of the time dependence of the deformation is sinusoidal. The single extensional mode shape can also be considered to be a single degree of freedom (SDOF) with a corresponding mass and stiffness. In viewing such an event as a spring mass system, the time variation of the deformation during the impact is expected to be sinusoidal.

The buckling mode for the fuel rod is governed by the boundary conditions. Lateral support is provided at the intermediate fuel bundle supports (grids). The only vertical restraint is considered to be at the point of contact of the fuel rod and the base of the assembly. The weight of the fuel rod pellets and cladding is assumed to be uniformly distributed along the length of the fuel rod. In the end drop, this results in the maximum compressive load occurring at the base of the fuel rod. The first buckling mode shape corresponding to these conditions is computed using ANSYS Revision 5.2.

Typically, eigenvalue buckling is applied for static environments. For dynamic loading, it is assumed that the duration of the loading is sufficiently long to allow the system to experience the complete load, even as the deformation associated with buckling is commenced. For dynamic loading, the lateral motion, which would correspond to the buckled shape, will correspond to the lowest mode shape. The similarity of the two shapes (the lateral dynamic mode shape and the buckling mode shape) is expected, since both have the same displacement boundary conditions, the same stiffness matrix and the same governing finite element equations, i.e.:

$$[K]\{\phi_i\} = \lambda_i[A]\{\phi_i\}$$

where:

K = structure stiffness matrix
ϕ_i = eigenvector
λ_i = eigenvalue
A = mass matrix for the mode shape calculation or stress stiffening matrix for the buckling evaluation.

Based on the time duration of the impact and the inherent inability of the fuel rod to rapidly displace in the lateral direction, the effect of the actual lateral motion of buckling can be computed with a dynamic load factor (DLF) [47]. The expression for the DLF for a half-sine loading for an SDOF is given by:

$$DLF = \frac{2\beta}{1-\beta^2}\cos\left(\frac{\pi}{2\beta}\right)$$

where:

β = ratio of first extensional model frequency to the first lateral mode frequency

The maximum dynamic acceleration (g-load), which may potentially result in the buckling of the fuel rod, is determined by applying the $|DLF|$ to the design acceleration of 60g for the 30-foot end drop condition (see Section 2.7.1).

The critical buckling load for the fuel rod is calculated using the same ANSYS model employed for the dynamic mode shape calculation. The maximum dynamic g-load is compared to the g-load first buckling mode shape. If the maximum dynamic g-load is less than the first buckling mode shape g-load, the fuel rod will not buckle under a 30-foot end drop.

2.9.1.1 Design Basis PWR Fuel Rod Mode Shapes and Buckling Evaluation

Of the PWR assemblies to be transported in the cask, the following four are identified as representative assemblies:

- Westinghouse 15 x 15 Std (Class 1)
- Westinghouse 17 x 17 Std (Class 1)
- Babcock & Wilcox 15 x 15 Mark B (Class 2)
- Combustion Engineering 16 x 16 System 80 (Class 3)

Characteristics of the PWR fuel rods are shown in Table 1.2-4 and Table 5.2-2.

Evaluation is performed for the four representative PWR fuel assemblies as described in Section 2.9.1. The fuel pellet weight is combined with the cladding weight in the evaluation. To be consistent with this approach, an effective cross-sectional property is used in the evaluation, which incorporates the properties of the fuel pellet and the fuel cladding. The model used in this evaluation is comprised of ANSYS two-dimensional beam elements (BEAM3). In the model, the beam elements considered the weight of the fuel pellet, as well as the cladding. The modulus of elasticity (E_x) for the fuel pellet has a nominal value of 27.5 x 10^6 psi [48]. To be conservative, the E_x for the fuel pellet used in the model is taken as 13.0 x 10^6 psi (less than 50% of the nominal value). The E_x used for the Zircaloy cladding is 10.47 x 10^6 psi [60]. Densities for cladding and fuel are 0.237 lb/in^3 and 0.396 lb/in^3, respectively [48]. Figure 2.9.1-1 shows a typical fuel rod model used for the buckling analysis. Location of constraints for the four PWR fuel types considered in the analysis can be found in Table 2.9.1-1. Only one vertical constraint is specified in the model, which is located at the bottom end of the fuel rod.

The results for the PWR fuel rod buckling evaluation are shown in Table 2.9.1-2. A typical dynamic mode shape plot and the buckling mode shape plot are shown in Figures 2.9.1-2 and 2.9.1-3, respectively. For the four PWR fuel classes evaluated, the maximum dynamic g-load is less than the first buckling mode g-load; therefore, the PWR fuel rods do not buckle during the 30-foot end drop condition.

2.9.1.2 Design Basis BWR Fuel Rod Mode Shapes and Buckling Evaluation

Of the BWR assemblies to be transported in the cask, the following are identified as representative assemblies:

- GE 7 x 7 BWR/2-3 version GE-2b (Class 4)
- GE 8 x 8-2 BWR/2-3 version GE-5 (Class 4)
- GE 8 x 8-4 BWR/2-3 version GE-8 (Class 4)
- GE 7 x 7 BWR/4-6 version GE-2 (Class 5)
- GE 8 x 8-2 BWR/4-6 version GE-5 (Class 5)
- GE 8 x 8-4 BWR/4-6 version GE-10 (Class 5)
- GE 9 x 9-2 BWR/4-6 version GE-11 (Class 5)

Characteristics of the BWR fuel rods are shown in Table 1.2-5 and Table 5.2-6.

The representative BWR fuel assemblies are further bounded by three BWR configurations (based on rod diameter and length), the GE 7x7 BWR/4-6, GE 8x8-2 BWR/4-6, and GE 9x9-2 BWR/4-6. Using the similar method for the PWR fuel rod evaluation as described in Section 2.9.1, ANSYS models are used to determine the critical buckling g-loads. Location of lateral constraints for the BWR fuel rods are shown in Table 2.9.1-3.

The buckling g-loads for BWR fuel rods are shown in Table 2.9.1-4. The buckling mode shapes are similar to those of the PWR fuel rods. For the three BWR fuel classes evaluated, the critical buckling g-load is greater than the design acceleration of 60g for the 30-foot end drop (the DLF is conservatively ignored); therefore, the BWR fuel rods do not buckle during a 30-foot end drop.

Figure 2.9.1-1 Typical Fuel Rod Finite Element Model and Boundary Conditions

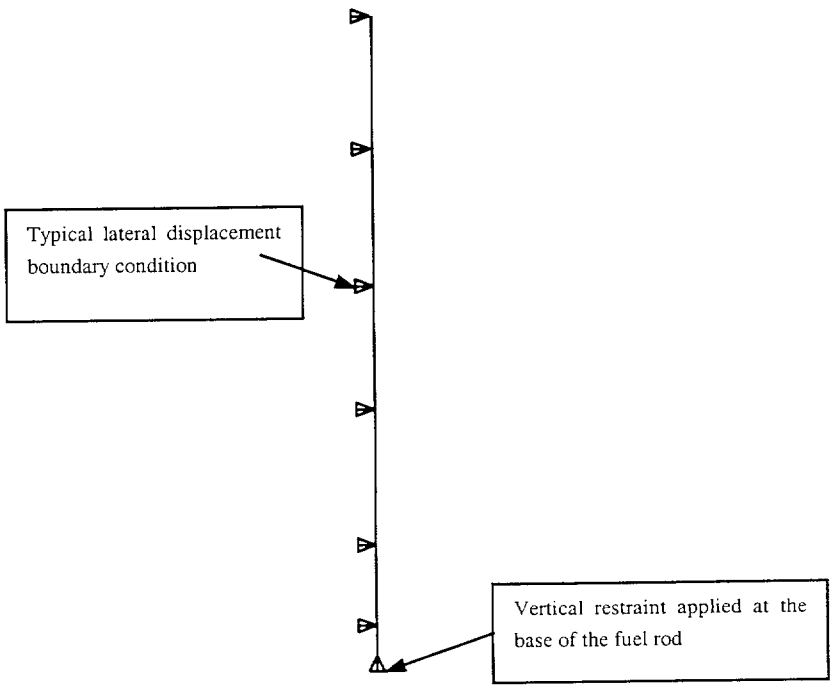

Figure 2.9.1-2 Typical First Lateral Mode Shape Plot for Fuel Rod

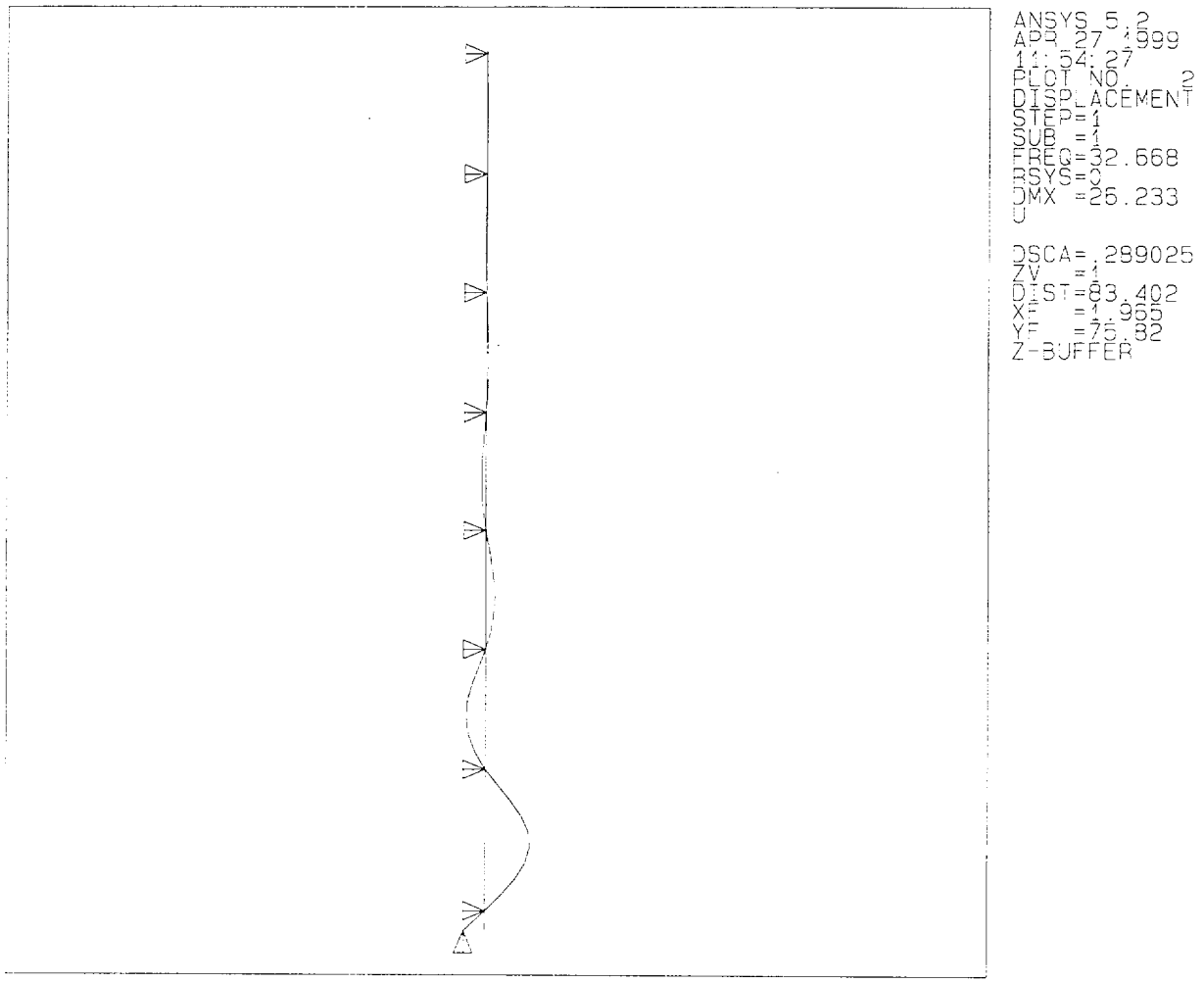

Figure 2.9.1-3 Typical First Buckling Mode Shape for Fuel Rod

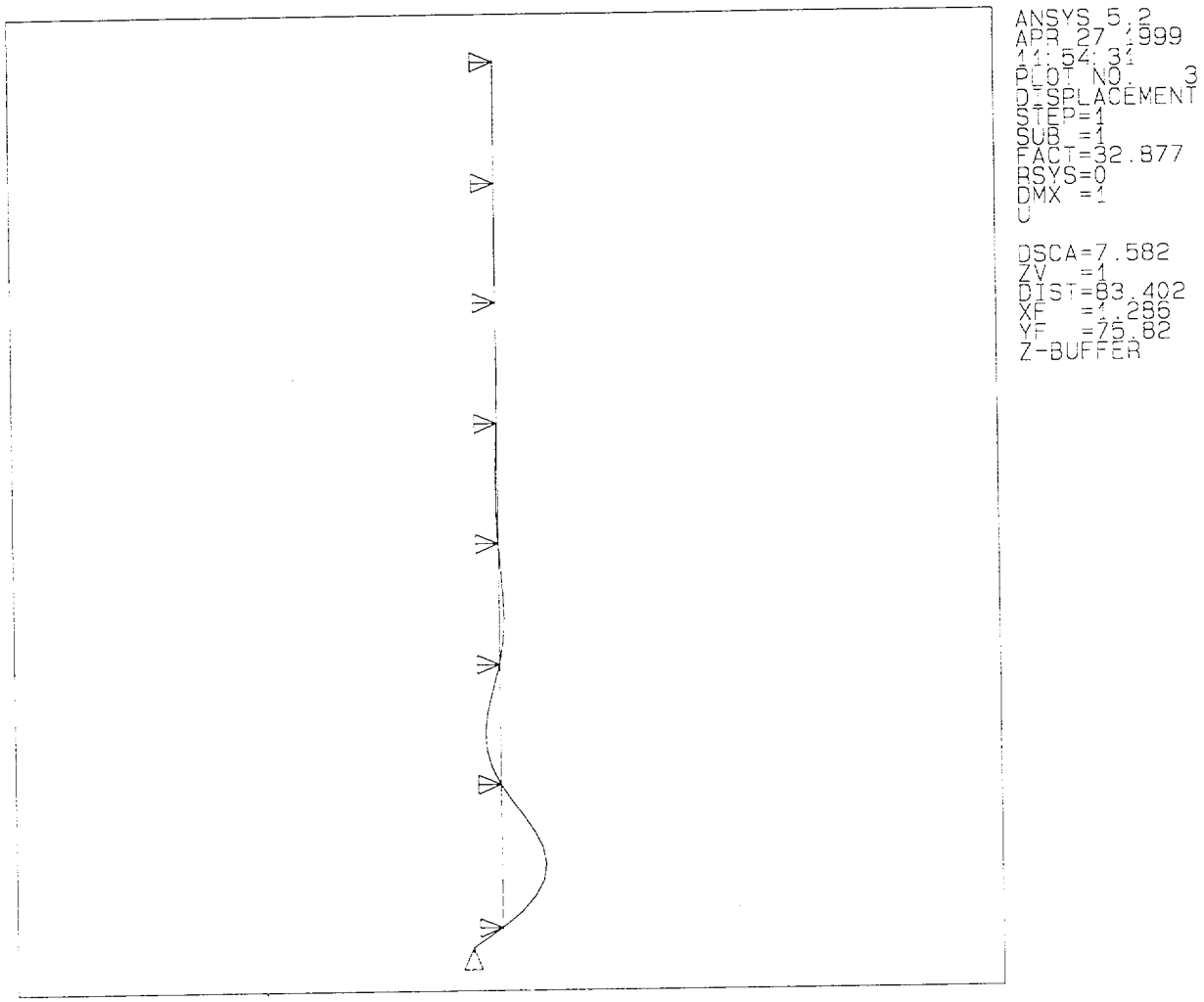

Table 2.9.1-1 Location of Lateral Constraints – PWR Fuel Rods

Fuel Assembly Type	Location of Lateral Constraints (inch)*										
Westinghouse 15x15 Std (Class 1) L_{rod}=151.88 in.	2.9	27.1	53.3	79.5	105.7	131.9	150.6				
Westinghouse 17x17 Std (Class 1) L_{rod}=151.64 in.	3.45	27.9	48.4	68.9	89.5	110.1	130.6	151.2			
Babcock & Wilcox 15x15 Mark B (Class 2) L_{rod}=153.68 in.	4.9	27.2	48.4	69.5	90.6	111.7	132.7	153.7			
Combustion Engineering 16x16 System 80 (Class 3) L_{rod}=161.00 in.	4.1	19.8	35.5	51.2	66.9	82.6	98.2	113.9	129.6	145.3	161.0

* Measured from the bottom end of the fuel rod.

Table 2.9.1-2 PWR Fuel Rod Analysis Summary

Fuel Assembly Class	First Extensional Frequency (Hz)	First Lateral Frequency (Hz)	Frequency Ratio, β	Dynamic Load Factor, DLF	Maximum Dynamic g-Load*	First Buckling Mode g-Load
Westinghouse 15 x 15	211.5	29.1	7.268	0.280	16.8	40.9
Westinghouse 17 x 17	212.2	32.7	6.490	0.316	18.9	32.9
Babcock &Wilcox 15 x 15	209.5	41.0	5.110	0.407	24.4	40.3
Combustion Engineering 16 x 16	200.4	68.9	2.909	0.780	46.8	53.7

* Maximum dynamic g- load = DLF x 60g.

Table 2.9.1-3 Location of Lateral Constraints for BWR Fuel Rods

Fuel Assembly Class	Location of Lateral Constraints (inch)*								
GE 7 x 7 BWR/4-6 L_{rod}=163.42 in.	0.00	22.88	43.03	63.18	83.33	103.48	123.63	143.78	163.42
GE 8 x 8-2 BWR/4-6 L_{rod}=163.42 in.	0.00	22.88	43.03	63.18	83.33	103.48	123.63	143.78	163.42
GE 9 x 9-2 BWR/4-6 L_{rod}=163.42 in.	0.00	22.88	43.03	63.18	83.33	103.48	123.63	143.78	163.42

* Measured from the bottom end of fuel rod.

Table 2.9.1-4 BWR Fuel Rod Analysis Summary

Fuel Assembly Class	Buckling g-Load
GE 7 x 7 BWR/4-6	104.3
GE 8 x 8-2 BWR/4-6	77.8
GE 9 x 9-2 BWR/4-6	64.6

THIS PAGE INTENTIONALLY LEFT BLANK

2.9.2 Buckling Evaluation for Maine Yankee Site Specific Fuel

This section presents the buckling evaluation for Maine Yankee high burnup fuel having oxide cladding layers that are 80 and 120 microns thick (Section 2.9.2.1). A similar evaluation is presented in Section 2.9.2.2 for Maine Yankee high burnup fuel with an oxide layer thickness of 80 microns that is also mechanically damaged. These analyses show that the high burnup fuel and the damaged high burnup fuel do not buckle in design basis accident events.

2.9.2.1 Buckling Evaluation for Maine Yankee High Burnup Fuel

This section presents the buckling evaluation for Combustion Engineering 14 x 14 fuel rods with a burnup between 45,000 and 50,000 MWD/MTU and having a cladding oxide layer thickness up to 80 microns (0.003 inch) thick. An assumed cladding oxide layer thickness of 120 microns is also evaluated. The fuel rod cladding thickness is assumed to be reduced by the amount of the oxide layer thickness.

An end drop orientation is considered with an acceleration of 60g, which subjects the fuel rod to axial loading. In the end drop orientation, the fuel rods are laterally restrained by the grids and may come into contact with the fuel assembly base. The only vertical constraint for the fuel rod is the base of the assembly. The weight of the fuel pellets is included in this evaluation, as the pellets are considered to be vertically supported by the cladding. A two-dimensional model comprised of ANSYS BEAM3 elements, shown in Figure 2.9.2-1, is used for the evaluation. This evaluation is considered to be the bounding condition (as opposed to an evaluation that considers the cladding only).

During the end drop, the fuel rod impacts the fuel assembly base. The fuel rod itself will respond as an elastic bar under a sudden compression load at its bottom end. The duration of this impact is bounded by the first extensional mode shape of the fuel rod. Contribution of higher frequency extensional modes of the rod would tend to shorten the duration of impact of the fuel rod with the fuel assembly base. The fuel rod, prior to impact, is in an undeformed state. In the process of the impact, the compression of the fuel rod will increase to a maximum and then return to a near uncompressed state, at which point the time of impact has been completed. This actually represents half of a cycle of the lowest frequency mode shape of the fuel rod. The shape of the time dependence of the deformation is sinusoidal. The single extensional mode shape can also be considered to be a single degree of freedom with a corresponding mass and stiffness. In

viewing such an event as a spring mass system, the time variation of the deformation during the impact is expected to be sinusoidal.

The buckling mode for the fuel rod is governed by the boundary conditions. For this configuration, the grids provide a lateral support, but no vertical support. The only vertical restraint is considered to be at the point of contact of the fuel rod and the base of the assembly. The weight of the fuel rod pellets and cladding is assumed to be uniformly distributed along the length of the fuel rod. In the end drop, this results in the maximum compressive load occurring at the base of the fuel rod. The first buckling mode shape corresponding to these conditions is computed as shown in Figure 2.9.2-2.

Typically, eigenvalue buckling is applied for static environments. For dynamic loading, it is assumed that the duration of the loading is sufficiently long to allow the system to experience the complete load, even as the deformation associated with the buckling is commenced. For dynamic loading, the lateral motion, which would correspond to the buckled shape, will correspond to the lowest mode shape. This lowest frequency mode shape is shown in Figure 2.9.2-2 and corresponds to a frequency of 25.9 Hz. The similarity of the two shapes shown in Figure 2.9.2-2 is expected, since both have the same displacement boundary conditions, the same stiffness matrix and the same governing finite element equations.

Based on the time duration of the impact and the inherent inability of the fuel rod to rapidly displace in the lateral direction, the effect of the actual lateral motion of buckling can be computed with a dynamic load factor (DLF). The expression for the DLF for a half-sine loading for a single degree of freedom is given by:

$$\mathrm{DLF} = \frac{2\beta}{1-\beta^2}\cos\left(\frac{\pi}{2\beta}\right)$$

where:

β = ratio of the first extensional mode frequency to the first lateral mode frequency

These values, computed in this section, are $\beta = 8.44$ and $|\mathrm{DLF}| = 0.24$.

This DLF is applied to the end drop acceleration of 60g, which is the bounding load to potentially result in the buckling of the fuel rod. The product of 60g × DLF = 14.4g is well below the

vertical acceleration corresponding to the first buckling mode shape, 37.9g, as computed in this section. This indicates that the time duration of the impact of the fuel onto the fuel assembly base is sufficiently short in nature so that buckling of the fuel rod cannot occur.

An effective cross-sectional property is used in the model to consider the properties of the fuel pellet and the fuel cladding. The modulus of elasticity (E_x) for the fuel pellet has a nominal value of 27.5×10^6 psi [48]. To be conservative, less than 50% of this value, or 13.0×10^6 psi, is used. The value of E_x (10.47×10^6 psi) is used for the irradiated Zircaloy cladding (ISG-12) [60]. Reference information shows that there is no additional reduction of the ductility of the cladding due to extended burnup into the 45,000 – 50,000 MWD/MTU range [61].

80 Micron Oxide Layer Evaluation

The bounding dimensions and physical data (minimum clad thickness, maximum rod length and minimum number of support grids) for the Maine Yankee fuel rod used in the model are:

Outer diameter of cladding (inches)	0.434
Cladding thickness (inches)	0.023
Cladding density (lb/in^3)	0.237
Fuel pellet density (lb/in^3)	0.396
Fuel pellet Modulus of Elasticity (psi)	13.0×10^6
Zircaloy cladding Modulus of Elasticity (psi)	10.47×10^6

The cladding is reduced from its nominal value of 0.026 inches by the assumed 80 micron oxidation layer thickness (0.003 inches) to 0.023 inches. Similarly, the fuel rod outer diameter is reduced from the nominal value of 0.44 inches to 0.434 inches. The elevations of the grids, measured from the bottom of the fuel assembly, are: 2.3, 33.0, 51.85, 70.7, 89.6, 108.4, 127.3 and 144.9 (inches).

The effective cross-sectional properties (EI_{eff}) for the beam are computed by adding the value of EI for the cladding and the pellet, where E and I are the modulus of elasticity (lb/in^2) and cross-sectional moment of inertia (in^4), respectively.

The lowest frequency for the extensional mode shape was computed to be 218.9 Hz. The first mode shape corresponds to a frequency of 25.9 Hz. Using the expression for the DLF previously discussed, the DLF is computed to be 0.24 ($\beta = 8.44$).

The buckling calculation used the same model employed for the mode shape calculation. The load that would potentially buckle the fuel rod in the end drop is due to the deceleration of the rod. This loading was implemented by applying a 1g acceleration in the direction that would result in compressive loading of the fuel rod. The acceleration required to buckle the fuel rod is computed to be 37.9g. This acceleration is much higher than the effective g-load of 14.4g corresponding to the end drop. Therefore, the fuel rods do not buckle during a 60g end drop.

120 Micron Oxide Layer Thickness Evaluation

The bounding dimensions and physical data (minimum clad thickness, maximum rod length and minimum number of support grids) are the same as those used for the 80 micron oxide layer thickness evaluation, except that the cladding is reduced from its nominal value of 0.026 inch by the assumed 120 micron oxidation layer thickness (0.0047 inch) to 0.0213 inch. Similarly, the fuel rod outer diameter is reduced from the nominal value of 0.44 inch to 0.4306 inch. The elevations of the grids, measured from the bottom of the fuel assembly, are: 2.3, 33.0, 51.85, 70.7, 89.6, 108.4, 127.3 and 144.9 (inches).

Using the same fuel rod model, the acceleration required to buckle the fuel rods is found to be 37.3g, which is much higher than the calculated effective g-load (14.3g) due to the 60g end drop. Therefore, the fuel rods with a 120 micron cladding oxide layer thickness do not buckle in the 60g end drop event.

2.9.2.2 Buckling Evaluation for Maine Yankee High Burnup Fuel with Mechanical Damage

This section presents the buckling evaluation for high burnup fuel having an 80 micron cladding oxide layer thickness and with mechanical damage consisting of one or more missing support grids up to an unsupported length of fuel rod of 60 inches.

End Drop Evaluation

As described in Section 2.9.2.1, the buckling load on the fuel rods is maximized at the bottom of the fuel assembly. The bounding evaluation is the removal of the grid strap that maximizes the spacing at the lowest possible vertical elevation. The elevations of the grids used in this model, measured from the bottom of the fuel assembly, are: 2.3, 51.85, 70.7, 89.6, 108.4, 127.3 and 144.9 (inches). The grid at the 33.0-inch elevation considered in the high burnup fuel model is removed, resulting in a grid spacing of approximately 50.0 inches. In addition, the grid located at

51.85 inches is conservatively assumed to be located at 62.3 inches, resulting in an unsupported fuel rod length of 60.0 inches.

The case of the missing grid is evaluated using the same methodology as for the fuel assembly with all the grids being present (Section 2.9.2.1). The dimensions and physical data used are those applied to the 80 micron cladding oxide thickness layer evaluation. The cladding thickness is reduced from its nominal value of 0.026 inches by an oxidation layer thickness of 80 microns (0.003 inch) to 0.023 inch. Similarly, the fuel rod outer diameter is reduced from the nominal value of 0.44 inch to 0.434 inch. The fuel pellet modulus of elasticity is conservatively reduced 50%. The modulus of elasticity of the cladding is taken from ISG-12.

Figures 2.9.2-3 and 2.9.2-4 show the finite element model's buckling results and mode shape. With the grid missing, the frequency of the fundamental lateral mode shape is 7.8 Hz. The natural frequency of the fundamental extensional mode is determined to be 218.9 Hz. The DLF is computed to be 0.072, resulting in an effective acceleration of 0.072 x 60 = 4.3g. Using the same method to compute the acceleration at which buckling occurs, the lowest buckling acceleration is 14.4g, which is significantly greater than 4.3g. Therefore, the fuel rod does not buckle during an end drop.

Side Drop Evaluation

The Maine Yankee fuel rod is evaluated for a 60g side drop with a missing support grid in the fuel assembly. Using the same assumptions as for the end drop evaluation, the span between support grids, the unsupported rod length, is 60.0 inches.

For this analysis, the dimensions and physical data used are:

Fuel Rod OD	0.434 in. (80 micron oxidation layer)
Clad ID	0.388 in.
E_{clad}	10.47E6 psi
E_{fuel}	13.0E6 psi
Clad density	0.237 lb/in^3
Fuel density	0.396 lb/in^3
A_{clad}	0.030 in^2 (cross-sectional area)
A_{fuel}	0.118 in^2 (cross-sectional area)

The mass of the fuel rod per unit length is:

$$m = \frac{0.396(0.122) + 0.237(0.030)}{386.4} = 0.000143\ \text{lb-s}^2/\text{in}^2$$

EI for the fuel rod is:

$$EI_{clad} = 10.47E6\frac{\pi\left(0.22^4 - 0.197^4\right)}{4} = 6{,}878\ \text{lb-in}^2$$

$$EI_{fuel} = 13.0E6\frac{\pi\left(0.197^4\right)}{4} = 15{,}378\ \text{lb-in}^2$$

$$EI = 6878 + 15378 = 22{,}256\ \text{lb-in}^2$$

During a side drop, the maximum deflection of a fuel rod is based on the fuel rod spacing of the fuel assembly. The pitch (center to center spacing) of fuel rods is 0.58 inch [62]. The maximum pitch is across the diagonal of the fuel assembly. The maximum pitch is:

$$dp = \frac{0.58}{\sin 45} = 0.82\ \text{in.}$$

The maximum deflection of a fuel rod is at the top of the fuel assembly and the minimum deflection is at the bottom of the fuel assembly.

Assuming a 17x17 array (which envelopes the Maine Yankee 14x14 array), the maximum fuel rod deflection is:

(17-1) x (0.82-0.43) = 6.18 inches.

The deflection of a simply supported beam with a distributed load is given by the equation:

$$\Delta = \frac{5\omega l^4}{384EI} = \frac{5(g\omega)l^4}{384(EI_{total})} \qquad [63]$$

$$g = \frac{384\Delta(EI_{total})}{5\omega l^4}$$

The cladding bending stress is given by the equation:

$$S = \frac{Mc}{I} = \frac{\left(\left(g\omega l^2\right)/8\right)c}{I_{clad}}\left(\frac{EI_{clad}}{EI_{total}}\right)$$

Inserting the equation for 'g':

$$S = \frac{384\Delta c E_{clad}}{40 \times L^2}$$

where:

c = 0.217 inch distance from center of fuel rod to extreme outer fiber
L = 60 inches (the unsupported fuel rod length)
Δ = 6.18 inches (the maximum deflection)

The bending stress in the fuel rod is:

$$S = \frac{384 \times 6.18 \times 0.217 \times 10.47E6}{40(60)^2} = 37.4 \text{ ksi}$$

The maximum hoop stress due to the fuel rod internal pressure is determined to be 19.1 ksi (131.4 Mpa per Table 3.4-7). Therefore, the maximum axial stress is 9.6 ksi (one half of the hoop stress [64]).

The bearing stress between two fuel rods under a 60g load is:

$$S_{brg} = 0.591\sqrt{\frac{\omega E}{K_D}} = 0.591\sqrt{\frac{(0.000143 \times 386.4) \times 60 \times 10.47E6}{0.22}} = 7.4 \text{ ksi} \quad [64]$$

where:

$$K_D = \frac{D_1 D_2}{D_1 + D_2} = \frac{0.434 \times 0.434}{0.434 + 0.434} = 0.22$$

The total stress is:

$$S = 37.4 + 9.6 + 7.4 = 54.4\,\text{ksi}$$

The ultimate strength allowable for irradiated Zircaloy–4 is 83.4 ksi (Figure 3-2 [65]). Therefore, the margin of safety for ultimate strength is:

$$MS = \frac{83.4}{54.4} - 1 = 0.53$$

The yield strength allowable for irradiated Zircaloy–4 is 78.3 ksi (Figure 3-2 [65]). Therefore, the margin of safety for yield strength is:

$$MS = \frac{78.3}{54.4} - 1 = 0.44$$

The maximum bearing stress occurs between the bottom fuel rod and the fuel tube. The bearing stress is:

$$S_{brg} = 0.591\sqrt{\frac{17 \times 0.000143 \times 386.4 \times 60 \times 10.47E6}{0.44}} = 21.6\,\text{ksi}$$

The bending stress is negligible because the maximum deflection is equal to the spacing of the fuel rods established by the grid. Therefore, the top fuel rod is bounding.

Consequently, the fuel rods are demonstrated to be structurally adequate for the 60g side drop loading condition.

Figure 2.9.2-1 Two-Dimensional Beam Finite Element Model for Maine Yankee Fuel Rod

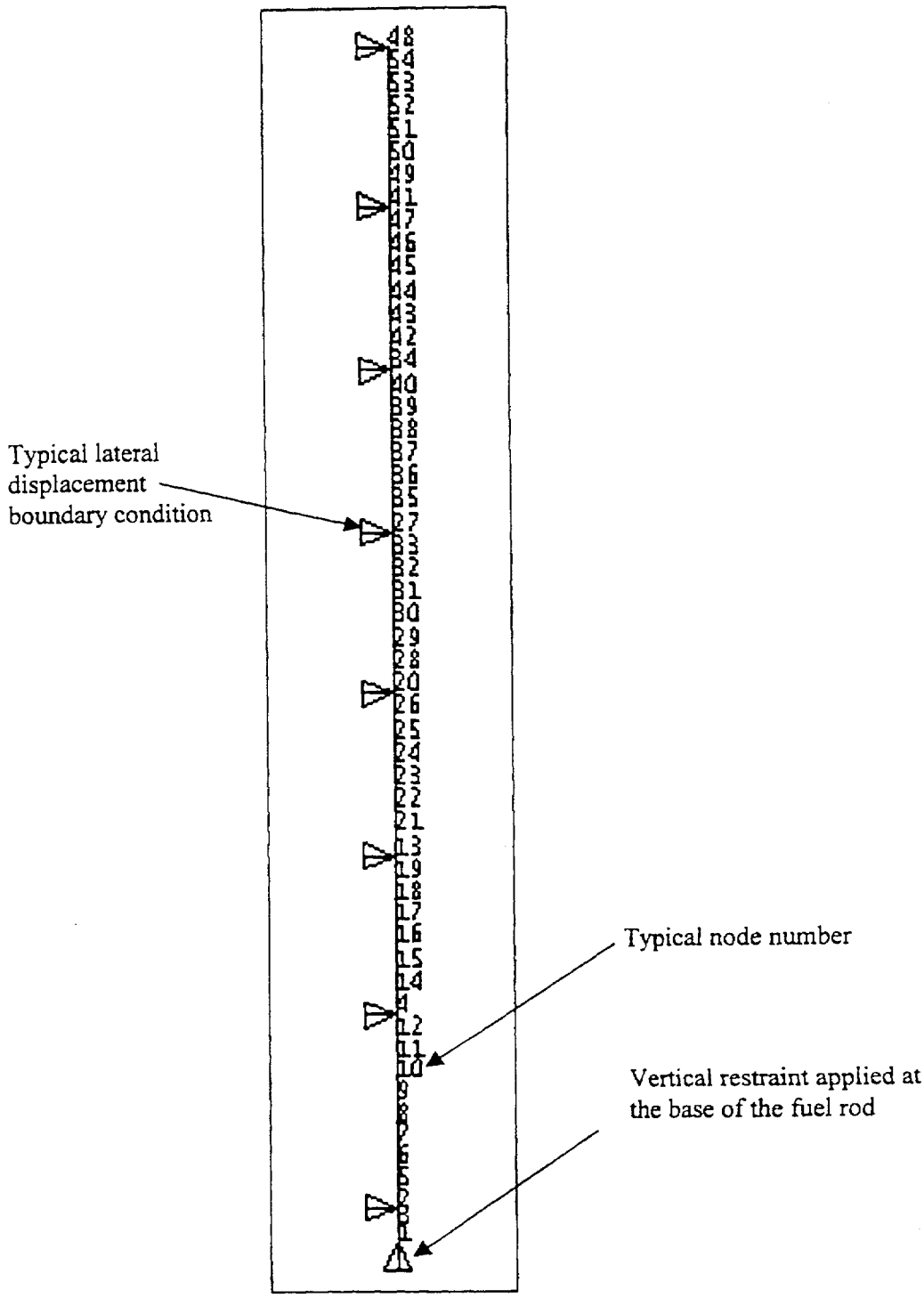

Figure 2.9.2-2 Mode Shape and First Buckling Shape for the Maine Yankee Fuel Rod

First Lateral Dynamic
Mode Shape at 25.9 Hz

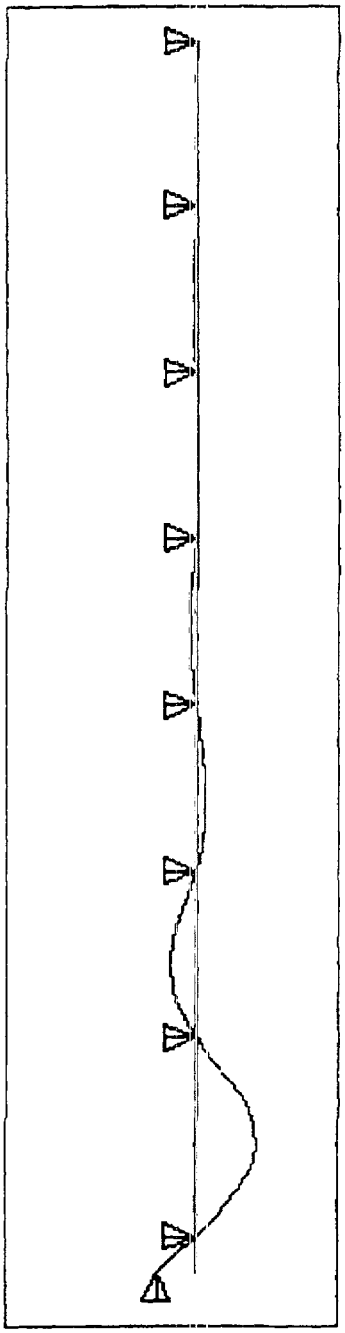

First Buckling
Shape at 37.9g

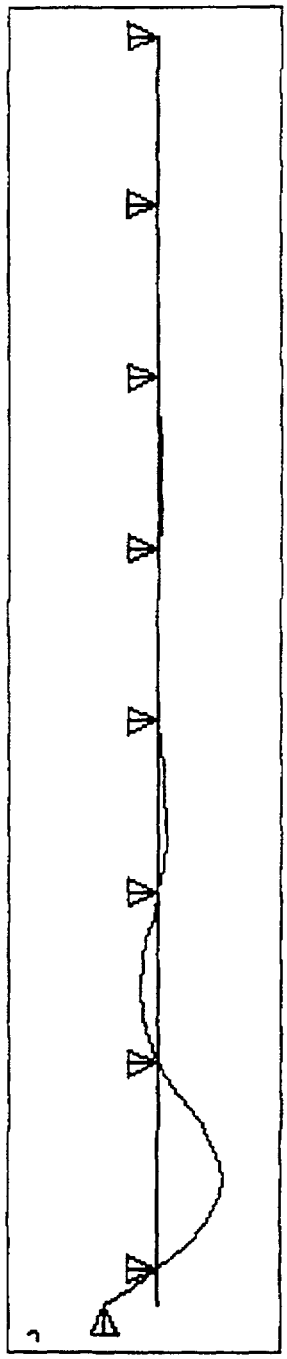

Figure 2.9.2-3 Two-Dimensional Beam Finite Element Model for Fuel Rod with Missing Grid

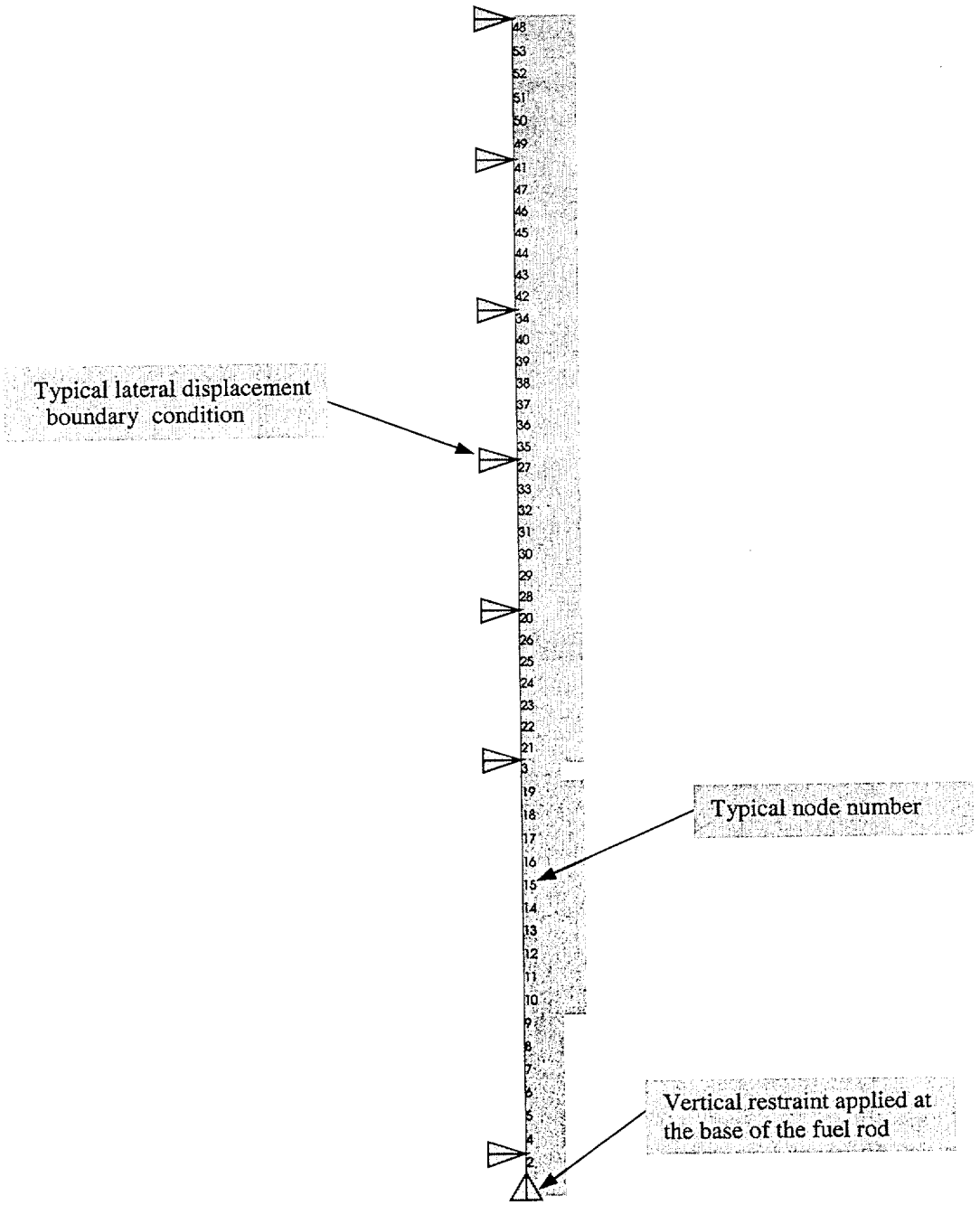

Figure 2.9.2-4 Modal Shape and First Buckling Mode Shape for a Fuel Rod with a Missing Grid

First Lateral Dynamic Mode Shape at 7.8 Hz

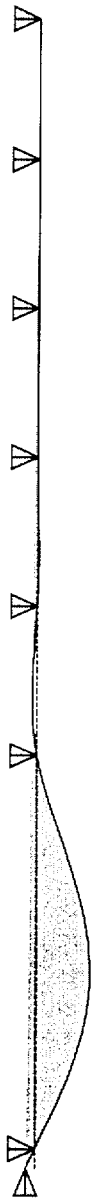

First Buckling Mode Shape at 14.4g

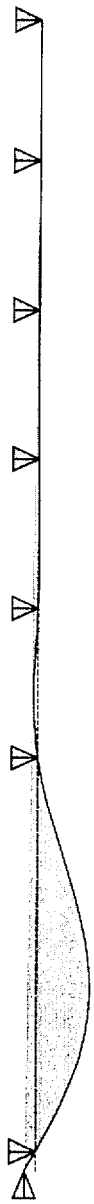

2.11.1.1 Maine Yankee Site Specific Spent Fuel

The standard spent fuel assembly for the Maine Yankee site is the Combustion Engineering (CE) 14x14 fuel assembly. Fuel of the same design has also been supplied by Westinghouse and by Exxon. The standard 14x14 fuel assemblies are included in the population of the design basis PWR fuel assemblies for the UMS® Transport System (see Table 1.2-4). The structural evaluation for the UMS® transport system loaded with the standard Maine Yankee fuels is bounded by the structural evaluations in Sections 2.6 and 2.7 for the normal conditions of transport and hypothetical accident conditions, respectively. The Maine Yankee site specific fuel is described in Section 1.3.1.

The weight of a standard 14x14 fuel assembly with the control element assembly inserted is 1,360 lbs. This weight is bounded by the weight of the design basis PWR fuel assembly (37,608/24 = 1,567 lbs) used in the PWR support disk analysis presented in Section 2.6.13. The fuel configurations with removed fuel rods, with fuel rods replaced by solid stainless steel or Zircaloy rods, or with poison rods replaced by hollow Zircaloy rods, all weigh less than the standard 14x14 fuel assembly. The configuration with instrument thimbles, CEA fingertips or neutron sources placed in the center guide tube positions weighs less than the design basis PWR fuel assembly. Since the weight of any of these fuel assembly configurations is bounded by the design basis fuel assembly weight, no additional analysis of these configurations is required.

Section 2.11.1.1.1 documents the structural evaluation of the basket support disk for the configuration holding consolidated fuel and damaged fuel inside the Maine Yankee fuel cans. The structural evaluation for the Maine Yankee fuel can is presented in Section 2.11.1.1.2.

2.11.1.1.1 Maine Yankee Support Disk Evaluation

A structural evaluation is required for the support disk for the configuration holding consolidated fuel. There are two consolidated fuel lattices, each constructed of 17x17 Zircaloy fuel grids and stainless steel end fittings, that are connected by 4 stainless steel support rods. One of the consolidated fuel lattices has 283 fuel rods with 2 empty positions. The other has 172 fuel rods with the remaining positions either empty or holding stainless steel rods. The calculated weight for the heaviest of the two consolidated fuel lattices is 2,100 pounds.

A parametric study is performed to show that the PWR support disk holding a Maine Yankee consolidated fuel lattice is bounded by the UMS® PWR support disk stress evaluation presented in Section 2.6.13. Note that only one consolidated fuel lattice will be loaded in any single Transportable Storage Canister and that the loading position of the consolidated fuel assembly is restricted to a basket corner position (see Section 1.3.1.1). However, Maine Yankee fuel cans holding other intact or damaged fuel can be loaded in the other three corner positions of the basket (Maine Yankee fuel cans may be loaded only in the four corner positions of the basket. See Figure 2.11.1.1-1 for corner positions). Therefore, the bounding case for Maine Yankee is the basket configuration with twenty (20) Maine Yankee fuel assemblies, three (3) fuel cans containing spent fuel, and one (1) fuel can containing consolidated fuel.

The two-dimensional ANSYS model used in the support disk evaluation (see Figure 2.6.13-2) in Section 2.6.13 is employed for the parametric study. The boundary condition of the model is modified by restraining the outer surface of the canister shell. The load from a PWR fuel assembly is modeled as a pressure load at the inner surface of each support disk slot opening. The design basis fuel pressure loading is 12.26 psi (see Section 2.6.13.2). Based on the same design parameters (slot size = 9.272 in., disk thickness = 0.5 inch, and the number of disks = 30), the pressure load corresponding to a Maine Yankee standard CE 14x14 fuel assembly is 10.3 psi. The pressure load is 11.3 psi for a Maine Yankee fuel can holding an intact or damaged fuel assembly. For a Maine Yankee fuel can holding consolidated fuel, the pressure load is 17.0 psi.

This study considers both the 1-foot (20g) and the 30-foot (60g) side drop conditions for four different drop orientations: 0°, 18.22°, 26.28°, and 45°, as shown in Figure 2.11.1.1-1. A total of five cases are considered in the study. Inertial loads are applied to the support disk in all cases. The base case considers that all 24 fuel positions hold design basis PWR fuel assemblies. The other four cases (Cases 1 through 4) represent four possible load combinations for the placement of four Maine Yankee fuel cans in the corner positions, one of which holds consolidated fuel. The remaining twenty (20) basket positions hold Maine Yankee standard 14×14 fuel assemblies. The basket loading positions are shown in Figure 2.11.1.1-1. The load combinations evaluated in the four Maine Yankee fuel can loading cases are:

Case	Basket Position 1	Basket Position 2	Basket Position 3	Basket Position 4
1	Consolidated	Damaged	Damaged	Damaged
2	Damaged	Consolidated	Damaged	Damaged
3	Damaged	Damaged	Damaged	Consolidated
4	Damaged	Damaged	Consolidated	Damaged

Table 2.11.1.1-1 provides a parametric comparison between the Base Case and the 4 cases evaluated, based on the maximum sectional stresses in the support disk. As shown in the table, the maximum stress in the UMS® basket support disk loaded with 20 standard fuel assemblies and four Maine Yankee fuel cans, including one holding consolidated fuel, is bounded by that for the support disk loaded with the design basis PWR fuel.

Additionally, a support disk analysis is performed for the Maine Yankee fuel configuration (20 standard fuel assemblies, three fuel cans containing spent fuel and one fuel can containing the consolidated fuel assembly), using the two-dimensional PWR support disk model for the governing case (45° basket orientation and thermal condition B) for the side drop condition (Section 2.6.13.6). The loading condition corresponds to Case 1 of the parametric study previously discussed. The analysis results of the P_m and $P_m + P_b$ stresses are summarized in Tables 2.11.1.1-2 and 2.11.1.1-3, respectively. The minimum margins of safety for the P_m and $P_m + P_b$ stresses are +0.82 and +0.24, respectively. The minimum margin of safety for the corresponding analysis for the support disk for the UMS® System design basis PWR configuration is +0.79 and +0.19 for P_m and $P_m + P_b$ stresses, respectively (see Tables 2.6.13.6-16 and 2.6.13.6-17). This comparison further substantiates the conclusion of the parametric study based on the normalized stress ratios using a two-dimensional model (Table 2.11.1.1-1).

Since no credit is taken for the structural integrity of the consolidated fuel or damaged fuel inside the fuel can, it is assumed that 100% of the fuel rods fail during an accident. For a Maine Yankee standard 14x14 fuel assembly, the volume of 176 fuel rods (100%) and 5 guide tubes will fill up 103.6 inches of the fuel can (span over 21 support disks) assuming a 50% volume compaction factor. For the consolidated fuel, the volume of 283 rods (100%) and 4 connector rods will fill up 109.6 inches of the fuel can (span over 22 support disks) assuming a 75% compaction factor. The compaction factor of 75% for the consolidated fuel considers that the

number of rods in the consolidated fuel is approximately 1.5 times the number of rods in the standard Maine Yankee fuel and these rods are initially more closely spaced.

The corresponding pressure load on the support disk ligament is 15.3 psi for the 100% failed Maine Yankee damaged fuel and 22.5 psi for the consolidated fuel. Since the fuel cans holding damaged fuel and consolidated fuel are limited to the corner locations of the basket, the total load per support disk for this Maine Yankee configuration remains bounded by the total load per support disk for the UMS® System design basis configuration. To demonstrate that there is no adverse impact on the maximum stress of the support disk, the PWR support disk analysis (Section 2.6.13.6) is reperformed for the Maine Yankee configuration (20 standard fuel assemblies, three fuel cans containing 100% failed fuel and one fuel can containing the 100% failed consolidated fuel) for the governing case of the side drop condition (45° basket drop orientation and thermal condition B). The analysis results indicate the minimum margins of safety for the P_m and $P_m + P_b$ stresses are +0.80 and +0.23, respectively. The minimum margin of safety for the corresponding analysis for the support disk for the UMS® System design basis PWR configuration is +0.79 and +0.19 for the P_m and $P_m + P_b$ stresses, respectively (Tables 2.6.13.6-16 and 2.6.13.6-17). Therefore, the maximum stress in the support disk for the Maine Yankee configuration, assuming 100% rod failure of the damaged and consolidated fuel in the fuel cans, is bounded by the maximum stress in the support disk calculated for the UMS® design basis fuel (Table 2.11.1.1-4).

2.11.1.1.2 Maine Yankee Fuel Can

The Maine Yankee fuel can, shown in Drawings 412-501 and 412-502, is provided to accommodate Maine Yankee damaged fuel in any condition. The fuel can fits within a standard PWR basket fuel tube. The primary function of the Maine Yankee fuel can is to confine the fuel material within the can to minimize the potential for dispersal of the fuel material into the canister cavity volume.

The Maine Yankee fuel can is designed to hold an intact fuel assembly, a damaged fuel assembly, a fuel assembly with a burnup between 45,000 and 50,000 MWD/MTU and having a cladding oxidation layer thickness greater than 80 microns, or consolidated fuel in the Maine Yankee fuel inventory.

The fuel can is a square cross-section tube made of Type 304 stainless steel with a total length of 162.8 inches. The can walls are 0.048-inch thick sheet (18 gauge). The minimum internal width of the can is 8.52 inches. The bottom of the can is a 0.63 inch thick plate. Four holes in the plates, screened with a Type 304 stainless steel wire screen (250 openings/inch x 250 openings/inch mesh), permit water to be drained from the can during loading operations. Since the bottom surface of the fuel can rests on the canister bottom plate, additional slots are machined in the fuel can (extending from the holes to the side of the bottom assembly) to allow the water to be drained from the can. At the top of the can, the wall thickness is increased to 0.15 inch to permit the can to be handled. Slots in the top assembly side plates allow the use of a handling tool to lift the can and contents. To confine the contents within the can, the top assembly consists of a 0.88-inch thick plate with screened drain holes identical to those in the bottom plate. Once the can is loaded, the can and contents are inserted into the basket, where the can may be supported by the sides of the fuel assembly tube, which are backed by the structural support disks. Alternately, the empty fuel can may be placed in the basket prior to having the designated contents inserted in the fuel can.

Structural evaluation of the Maine Yankee fuel can is shown below. The end drop and side drop conditions (both normal and accident conditions of transport) are considered in the evaluation.

End Drop Conditions

For the bottom end drop, the top assembly (lid), the side plates, and the tube body act against the bottom assembly. For the top end drop, the bottom assembly, tube body and side plates act against the top assembly. Because the top assembly is heavier, the bottom end drop is the governing case for tube body compression. The can contents bear against the bottom assembly through which the loads are transferred to the TSC bottom plate.

The Maine Yankee fuel can tube body is subjected to compressive stresses. Under normal operating conditions, the tube is evaluated for a 20g acceleration. This approach addresses the transport condition 1-foot drop and bounds the storage deadweight and handling condition, including a 10% dynamic load factor. The compressive load (P) on the tube is the combined weight of the lid, side plates and tube body times 20:

$$P = (17.89\ \text{lb} + 6.57\ \text{lb} + 78.77\ \text{lb}) \times 20 = 2{,}064.6\ \text{lb};\ \text{use } 3{,}000\ \text{lb for evaluation.}$$

The compressive stress (S_c) in the tube body is:

$$S_c = \frac{P}{A} = \frac{3{,}000\ \text{lb}}{1.714\ \text{in}^2} = 1{,}750\ \text{psi}$$

where:

$$A = 8.62^2 - 8.52^2 = 1.714\ \text{in}^2$$

The margin of safety (MS) is then:

$$MS = \frac{S_m}{S_c} - 1 = \frac{16{,}700\ \text{psi}}{1{,}750\ \text{psi}} - 1 = +8.5 \text{ for normal operating conditions at 600°F.}$$

Under accident conditions, the tube is evaluated for a 60g acceleration.

The compressive load (P) is:

$$P = (17.89\ \text{lb} + 6.57\ \text{lb} + 78.77\ \text{lb}) \times 60g = 6{,}193.8\ \text{lb; use 8,500 lb for evaluation.}$$

The compressive stress (S_c) in the tube body is:

$$S_c = \frac{P}{A} = \frac{8{,}500\ \text{lb}}{1.714\ \text{in}^2} = 4{,}959\ \text{psi}$$

where the margin of safety (MS) is then:

$$MS = \frac{0.7S_u}{S_c} - 1 = \frac{0.7(63{,}300)\ \text{psi}}{4{,}959\ \text{psi}} - 1 = +7.9 \text{ for accident conditions at 600°F.}$$

The tube is evaluated using the Euler formula to determine the critical buckling load (P_{cr}):

$$P_{cr} = \frac{\pi^2 EI}{L_e^2} = \frac{\pi^2 (25.2 \times 10^6)(20.98)}{2(157.8)} = 16.5 \times 10^6\ \text{lb}$$

where:

$E = 25.2 \times 10^6$ psi

$I = \frac{8.62^4 - 8.52^4}{12} = 20.98 \text{ in}^4$

$L_e = 2L$ (worst case condition)

L = tube body length (157.8 in)

Because the maximum compressive load (8,500 lb under the accident condition) is much less than the critical buckling load (16.5×10^6 lb), the tube has adequate resistance to buckling.

The lid is analyzed for compressive stresses in a top end drop where compressive loads are transferred through the lid structure to the TSC shield lid. The compressive load (P) is the weight of the fuel assembly plus the weight of the lid (18.01 lb; use 30 lb for analysis) times the appropriate acceleration factor.

Case 1: The Maine Yankee fuel can contents is in an intact (although damaged) Maine Yankee fuel assembly, a CF-1 fuel rod storage insert, or a consolidated fuel assembly. The compressive load for Case 1 acts directly through the support ring and the lift tee, which are directly in line with the axis of the upper end fitting posts in the top end drop configuration.

Case 2: The Maine Yankee fuel can contents is a fuel rod storage insert with a 3/4 – 10 threaded rod that transfers the compressive load to the center of the lid directly in line with the lift tee axis.

For Case 1, the contents weight is conservatively analyzed as the consolidated fuel weight (2,100 lb); Case 2 considers the heaviest standard Maine Yankee fuel assembly (1,300 lb).

Note: Because the lid thickness is greater than the free space between the top and the Maine Yankee fuel can and the bottom of the TSC shield lid, the lid cannot become disengaged from the can.

Case 1:

For normal operating conditions, the compressive stress (σ_c) is:

$$\sigma_c = \frac{P}{A} = \frac{2130\ (20)\ \text{lb}}{7.66\ \text{in}^2} = 5{,}561\ \text{psi} \qquad \text{(using 30 lb for lid weight)}$$

where A is the combined cross-sectional area of the support ring and the lift tee:

$$A = \frac{\pi}{4}\left(\left(6.63^2 - 6.07^2\right) + 1.625^2\right) = 7.66 \text{ in}^2$$

The margin of safety (MS) is:

$$MS = \frac{S_m}{\sigma_c} - 1 = \frac{16{,}700 \text{ psi}}{5{,}561 \text{ psi}} - 1 = +2.0 \text{ (normal operating condition)}$$

For accident conditions, the compressive stress (σ_c) is:

$$\sigma_c = \frac{P}{A} = \frac{2130(60)}{7.66} = 16{,}684 \text{ psi}$$

The margin of safety (MS) is:

$$MS = \frac{0.7S_u}{\sigma_c} - 1 = \frac{0.7(63{,}300 \text{ psi})}{16{,}684 \text{ psi}} - 1 = +1.66 \text{ (accident condition)}$$

Case 2:

For normal operating conditions, the compressive stress (σ_c) is:

$$\sigma_c = \frac{P}{A} = \frac{1330(20) \text{ lb}}{2.07 \text{ in}^2} = 12{,}850 \text{ psi}$$ (using 30 lb for lid weight)

where A is the cross-sectional area of the lift tee:

$$A = \frac{\pi}{4}(1.625)^2 = 2.07 \text{ in}^2$$

The margin of safety (MS) is:

$$MS = \frac{S_m}{\sigma_c} - 1 = \frac{16{,}700 \text{ psi}}{12{,}850 \text{ psi}} - 1 = +0.30 \text{ (normal operating condition)}$$

For accident conditions, the compressive stress (σ_c) is:

$$\sigma_c = \frac{P}{A} = \frac{1330(60)}{2.07} = 38{,}551 \text{ psi}$$

The margin of safety (MS) is:

$$MS = \frac{0.7S_u}{\sigma_c} - 1 = \frac{0.7(63{,}300 \text{ psi})}{38{,}551 \text{ psi}} - 1 = +0.15 \text{ (accident condition)}$$

Side Drop Conditions

The majority of the tube body is contained within the fuel tube in the basket assembly. Because both the tube body and the fuel tube have square cross-sections, they will be in full contact (for 153.0 inches longitudinally) during the side drop and no significant bending stress will be introduced into the tube body. The last 4.8 inches of the body tube and the 5.0-inch length of the side plates will be unsupported past the fuel tube flange in the side drop configuration.

The tube body will be evaluated as a cantilevered beam with the combined weight (P) of the overhanging tube body, top assembly, and side plates multiplied by the appropriate deceleration factor and, conservatively, concentrated at the top end of the side plates.

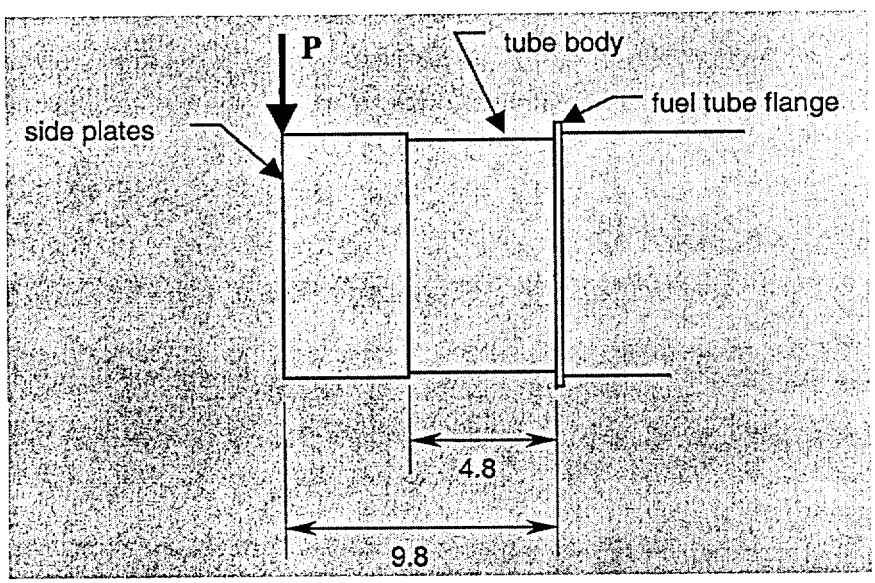

Normal condition (one-foot drop):

The maximum bending stress (f_b) is determined as follows:

$$f_b = \frac{M_{max}c}{I} = \frac{6{,}860(4.31)}{20.98} \cong 1{,}410 \text{ psi}$$

where:

M_{max} = $Pg \times L = 35(20)(9.8) = 6{,}860$ lb·in.

P = 35 lb; (side plates, 6.57 lb + tube body (0.5 lb/in. × 4.8 in. = 2.4) + top assembly, 17.89 lb, equals 26.86 lb; use 35 lb for this analysis.)

g = 20 (normal condition)

L = 9.8 in. (the total overhung length of the tube body and end plates)

c = 8.62/2 = 4.31 in.

$$I = \frac{bh^3 - b_i h_i^3}{12} = \frac{8.62^4 - 8.52^4}{12} = 20.98 \text{ in}^4$$

The shear stress (τ) is:

$$\tau = \frac{Pg}{A} = \frac{35(20)}{1.714} \cong 409 \text{ psi}$$

where:

$A = 8.62^2 - 8.52^2 = 1.714 \text{ in}^2$

$$\sigma_1, \sigma_2 = \frac{1}{2}\left(f_b \pm \sqrt{f_b^2 + 4\tau^2}\right) = \frac{1}{2}\left(1{,}410 \pm \sqrt{1{,}410^2 + 4(409)^2}\right) = 1{,}520 \text{ psi and } -110 \text{ psi}$$

The stress intensity (σ_{max}) = $|\sigma_1 - \sigma_2| = 1{,}630$ psi

The shear stress (τ) is:

$$\tau = \frac{(P + w(L - 2.38))g}{A} = \frac{(35 + 19.16(9.8 - 2.38))20}{1.714} \cong 2{,}068 \text{ psi}$$

$$\sigma_1, \sigma_2 = \frac{1}{2}\left(f_b \pm \sqrt{f_b^2 + 4\tau^2}\right) = \frac{1}{2}\left(3{,}577 \pm \sqrt{3{,}577^2 + 4(2{,}068)^2}\right) = 4{,}523 \text{ psi and } -946 \text{ psi}$$

The stress intensity (σ_{max}) = $|\sigma_1 - \sigma_2|$ = 5,469 psi

The margin of safety (MS) is:

$$MS = \frac{1.5S_m}{\sigma_{max}} - 1 = \frac{1.5(16{,}700) \text{ psi}}{5{,}469 \text{ psi}} - 1 = +3.58 \text{ for the normal condition (20g acceleration)}$$

Accident condition (30-foot drop):

The maximum bending stress (f_b) is determined as follows:

$$f_b = \frac{M_{max}c}{I} = \frac{52{,}226(4.31)}{20.98} = 10{,}729 \text{ psi}$$

where:

$$M_{max} = \left(PL + \frac{w(L - 2.38)^2}{2}\right)(60g) = \left(35(9.8) + \frac{19.16(9.8 - 2.38)^2}{2}\right)(60g) = 52{,}226 \text{ lb} \cdot \text{in}$$

The shear stress (τ) is:

$$\tau = \frac{(P + w(L - 2.38))g}{A} = \frac{(35 + 19.16(9.8 - 2.38))60}{1.714} \cong 6{,}202 \text{ psi}$$

g = 60 (accident condition)

$$\sigma_1, \sigma_2 = \frac{1}{2}\left(f_b \pm \sqrt{f_b^2 + 4\tau^2}\right) = \frac{1}{2}\left(10{,}729 \pm \sqrt{10{,}729^2 + 4(6{,}202)^2}\right) = 13{,}565 \text{ psi and } -2{,}836 \text{ psi}$$

The stress intensity (σ_{max}) = $|\sigma_1 - \sigma_2|$ = 16,401 psi

The margin of safety (MS) is:

$$MS = \frac{1.0\ S_u}{\sigma_{max}} - 1 = \frac{1.0(63{,}300)}{16{,}401} - 1 = +2.86 \text{ for the accident condition (60g acceleration)}$$

The welds joining the tube body to the side plates are full penetration welds (Type III NG-3352.3). Per Table NG-3352-1, the weld quality factor (n) for a Type III weld with visual surface inspection is 0.5.

The margin of safety (MS) for the welds is:

$$MS = \frac{n \cdot 1.5 \cdot S_m}{\sigma_{max}} - 1 = \frac{0.5(1.5)(16{,}700 \text{ psi})}{5{,}469 \text{ psi}} - 1 = +1.29 \text{ (normal condition)}$$

$$MS = \frac{n \cdot 1.0 \cdot S_u}{\sigma_{max}} - 1 = \frac{0.5(1.0)(63{,}300 \text{ psi})}{16{,}401 \text{ psi}} - 1 = +0.93 \text{ (accident condition)}$$

100% Failed Fuel Analysis

Normal Conditions:

To ensure that the Maine Yankee fuel can (fuel can) is structurally adequate to withstand the impact and to prevent the loss of the confinement capability, the fuel can is evaluated for a 1-foot side drop event. The fuel can is considered to hold 100% failed consolidated fuel, which is the worst case loading condition for the can for the normal conditions of transport. The evaluation is performed using the LS-DYNA program. As shown below, a finite element model is constructed

for the evaluation. The model consists of a half-symmetry section of the fuel can containing the fuel mass and the fuel tube supported by the support disks. Four support disks (three spans) are considered in the model.

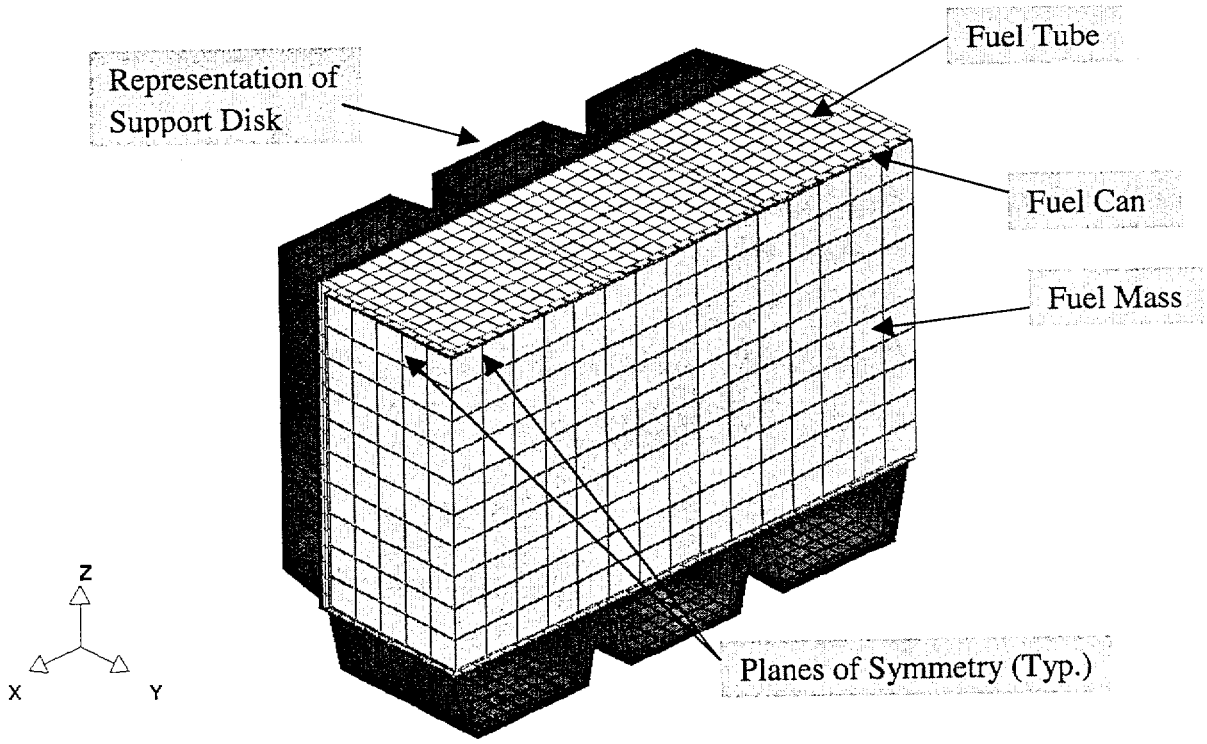

The global X-axis aligns with the longitudinal axis of the fuel can. The Z-axis of the model aligns with the gravitational force direction. The gravitational body force acts in the negative Z-direction. Symmetry boundary conditions are applied at the planes of symmetry. All nodes for the support disk in the model are fully restrained.

For the normal operating conditions, the governing ASME Code requires that the stress limits given in Paragraph NB-3221 be satisfied. However, in accordance with Paragraph NB-3222, the provision of NB-3228 is applicable if plastic analysis techniques are applied. Per NB-3228.3 (Plastic Analysis), the stress limits given in NB-3221 need not be satisfied at a specific location if it is shown that the specified loads do not exceed two-thirds of the plastic analysis collapse load, i.e., the collapse load is greater than 1.5 times the applied load. For the evaluation of the Maine Yankee fuel can, this process is simplified by demonstrating that the fuel can remains structurally stable when the fuel can is subjected to a conservative impact loading (maximum g-load = 30g) of 1.5 times the impact loading (maximum g-load = 20g) for the 1-foot side drop condition.

The fuel mass used in the finite element model corresponds to a maximum weight of 2,100 pounds for the consolidated fuel, occupying a length of 109.6 inches inside the fuel can. The material properties for Type 304 stainless steel at 600°F are used for both the fuel can and the fuel tube. The dynamic force input applied to the model has a maximum g-load of 30g and a duration of 32.1 milliseconds, which is derived from the deceleration time-history of the transport cask for the 1-foot side drop condition.

The analysis results indicate that, at 1.5 times the design loading (30g), the model remains structurally stable and the maximum strain in the fuel can is less than 1%. Consequently, it is conservative to conclude that the design loading does not exceed two-thirds of the collapse load that is specified in NB-3228.3, and that the fuel can and the fuel tube meet the ASME Code requirement of Level A (normal operating) conditions. The deformation analysis also indicates that after the impact, there is enough clearance between the fuel can and fuel tube, and between fuel tube and the support disk, to allow removal of the fuel can from the package.

Accident Conditions:

The Maine Yankee fuel can may hold 100% failed/damaged fuel or consolidated fuel. An evaluation is performed to demonstrate that the fuel can maintains its integrity during a tip-over accident for this condition.

The fuel can is designed to hold either Maine Yankee standard fuel assemblies (1300 lb) or consolidated fuel assemblies (2100 lb). For 100% failed fuel, the pressure load applied to the fuel can is:

standard fuel: $$P_s = \frac{1300}{8.52 \times 103.6} = 1.47 \text{ psi}$$

consolidated fuel: $$P_c = \frac{2100}{8.52 \times 109.6} = 2.25 \text{ psi}$$

where:

1300 lbs = Maine Yankee standard fuel weight

2100 lbs = maximum consolidated fuel weight

8.52 in = inside width of fuel can

103.6 in = height occupied by 100% failed standard fuel

109.6 in = height occupied by 100% failed consolidated fuel

Therefore, the bounding pressure load on the fuel can is the consolidated fuel, 2.25 psi, multiplied by 60g (135 psi).

An ANSYS model of the Maine Yankee fuel can (8.57 in × 8.57 in) is constructed to evaluate the fuel can for a 60g loading. Note that 8.57 inches is the dimension of the fuel can based on the centerlines of its side walls.

It should be noted that the fuel tube, the BORAL plate and its cover are not included in the model. Therefore, the fuel can analysis is conservative.

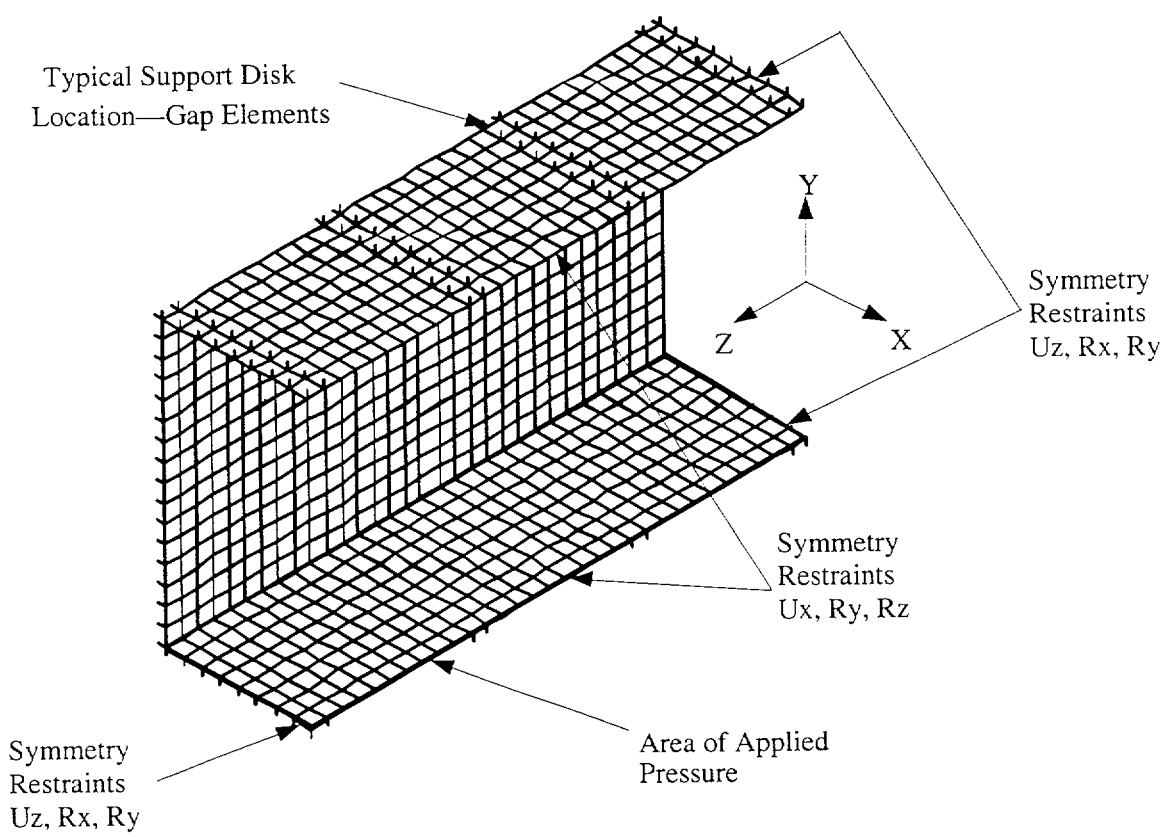

The finite element analysis results show that the maximum stress in the fuel can is 25.4 ksi, which is local to the sections of the tube resting on the support disks. At 750°F, the ultimate strength for Type 304 stainless steel is 63.1 ksi. The margin of safety is:

$$MS = \frac{63.1}{25.4} - 1 = +1.48$$

The analysis shows that the maximum total strain is 0.050 inch/inch. Defining the acceptable elastic-plastic response of the stainless steel as one-half of the material failure strain of 0.40 inch/inch at 750°F, the resulting margin of safety is:

$$MS = \frac{0.40/2}{0.05} - 1 = +3.0$$

Similarly, the margin of safety for elastic-plastic stress becomes:

$$MS = \frac{63.1 - 17.3}{25.4 - 17.3} - 1 = +4.65$$

where the yield strength of Type 304 stainless steel is 17.3 ksi at 750°F.

Figure 2.11.1.1-1 PWR Basket Drop Orientations and Case Study Loading Positions for Maine Yankee Consolidated Fuel

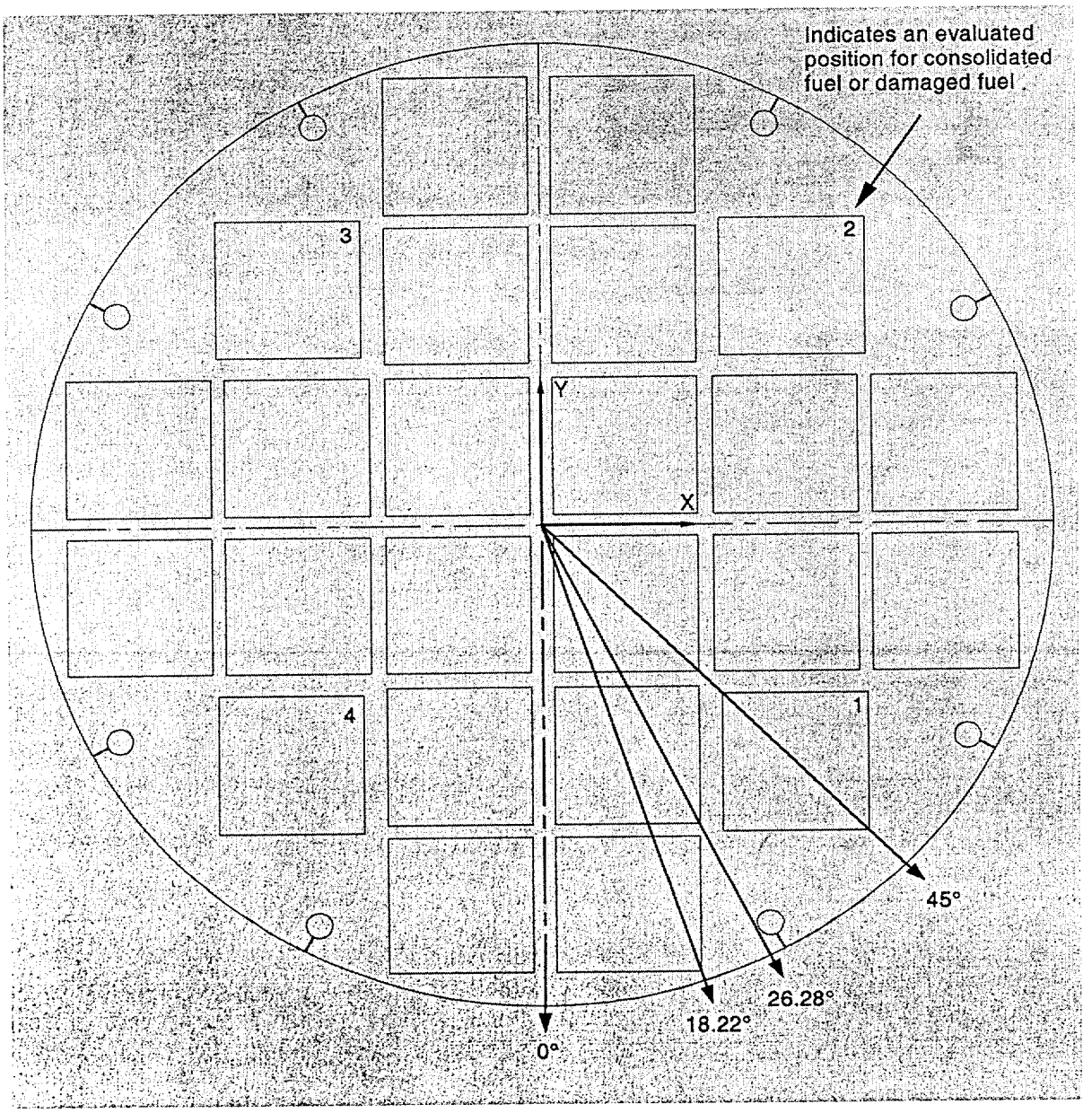

Table 2.11.1.1-1 Normalized Stress Ratios - UMS® PWR Basket Support Disk Sectional Stresses Due to Maine Yankee Consolidated Fuel Compared to the Design Basis PWR Fuel Basket Maximum Stresses (Base Case)

Case	Support Disk Sectional Stress Intensity (ksi) – Membrane							
	Normal Conditions, 20g				Accident Conditions, 60g			
	0°	18.22°	26.28°	45°	0°	18.22°	26.28°	45°
Base Case[1]	1.00	1.00	1.00	1.00	1.00	1.00	1.00	1.00
Case 1	0.96	0.91	0.96	0.96	0.91	0.94	0.94	0.94
Case 2	0.95	0.92	0.96	0.96	0.91	0.94	0.94	0.95
Case 3	0.96	0.93	0.97	0.96	0.91	0.95	0.95	0.95
Case 4	0.95	0.93	0.97	0.96	0.91	0.95	0.95	0.96
Case	**Support Disk Sectional Stress Intensity (ksi) – Membrane + Bending**							
	Normal Conditions, 20g				**Accident Conditions, 60g**			
	0°	**18.22°**	**26.28°**	**45°**	**0°**	**18.22°**	**26.28°**	**45°**
Base Case[1]	1.00	1.00	1.00	1.00	1.00	1.00	1.00	1.00
Case 1	0.96	0.92	0.96	0.95	0.96	0.94	0.94	0.94
Case 2	0.96	0.92	0.96	0.96	0.95	0.95	0.95	0.95
Case 3	0.96	0.93	0.96	0.95	0.96	0.95	0.95	0.95
Case 4	0.96	0.93	0.97	0.97	0.96	0.98	0.98	0.97

1. Tables 2.6.13.6-16 and 2.6.13.6-17.

Table 2.11.1.1-2 P_m Stresses for Support Disk for 1-Foot Side Drop – Maine Yankee Consolidated Fuel

Section	Sx (ksi)	Sy (ksi)	Sxy (ksi)	Stress Intensity (ksi)	Allowable Stress (ksi)	Margin of Safety
120	9.7	-9.8	7.6	24.8	45	0.82
114	-9.9	9.7	7.6	24.8	45	0.82
35	13.9	-1.5	6.4	20	45	1.25
23	-1.4	14.1	6.3	20	45	1.25
21	-7.6	-15.9	6.6	19.5	45	1.31
37	15.8	-7.8	6.6	19.5	45	1.31
112	7.1	-5.9	6.1	17.8	45	1.52
111	-5.8	7.1	6.1	17.7	45	1.54
63	1.6	-9.8	5.5	15.9	45	1.83
96	-9.5	1.6	5.6	15.7	45	1.86
9	-0.5	-11.2	5.6	15.5	45	1.91
49	11	-0.5	5.6	15.4	45	1.92
28	-9	2.8	4.3	14.7	45	2.07
40	2.8	-8.9	4.4	14.6	45	2.07
7	3	11.6	5.5	14.3	45	2.15
104	-7	0.2	6.1	14.2	45	2.17
51	11.3	3	5.5	14.1	45	2.19
66	0.2	-7.1	6	14.1	45	2.2
72	10.6	-9.6	3.8	14	45	2.23
98	-9.7	-10.7	3.7	13.9	45	2.23
95	-3.2	-11.6	4.1	13.3	45	2.4
42	-6.3	-10.2	4.6	13.2	45	2.4
26	10.3	-6.2	4.5	13.2	45	2.4
110	13.2	-0.1	-0.5	13.2	45	2.41
64	11.3	-3.3	4.2	13.1	45	2.43
119	-0.1	-13.1	-0.5	13.1	45	2.43
94	12.1	-0.1	-0.3	12.2	45	2.7
71	-0.1	-12	-0.3	12	45	2.74
79	1	8.9	3.7	10.8	45	3.17
80	8.6	1	3.7	10.7	45	3.2
124	3.6	-6.5	1.3	10.4	45	3.34
108	-4.1	5	2.2	10.1	45	3.44
22	-2.5	-0.8	-4.9	10	45	3.5
36	-0.8	-2.6	-4.9	9.9	45	3.53
74	-0.2	-9	2.1	9.8	45	3.6
99	-9	-0.2	2.1	9.8	45	3.61
115	0.5	-4.6	3.9	9.3	45	3.82
122	-4.5	0.5	3.9	9.3	45	3.85
116	-0.1	-9.1	0	9.1	45	3.96
92	2.2	-6.8	0.2	9	45	4.02

Table 2.11.1.1-3 $P_m + P_b$ Stresses for Support Disk for 1-Foot Side Drop – Maine Yankee Consolidated Fuel

Section	Sx (ksi)	Sy (ksi)	Sxy (ksi)	Stress Intensity (ksi)	Allowable Stress (ksi)	Margin of Safety
37	-38.5	-45.1	12	54.2	67.5	0.24
21	-44.9	-38.5	12	54.1	67.5	0.25
23	33.4	36.6	10.2	45.3	67.5	0.49
35	36.5	33.4	10.1	45.2	67.5	0.49
34	-40.7	-41.2	3.2	44.2	67.5	0.53
20	-41	-40.8	3.2	44.1	67.5	0.53
4	37.9	41.6	3	43.3	67.5	0.56
1	41.6	37.9	3	43.3	67.5	0.56
112	-18.1	-42	3.7	42.5	67.5	0.59
111	-41.6	-18	3.6	42.2	67.5	0.6
51	30.9	34.8	9	42.1	67.5	0.6
7	34.6	31.1	9.1	42	67.5	0.61
2	-37.8	-37.2	2.6	40.1	67.5	0.68
3	-37.2	-37.8	2.6	40.1	67.5	0.68
49	-30.8	-31	8.6	39.6	67.5	0.71
9	-30.9	-30.9	8.7	39.5	67.5	0.71
64	-31	-30.4	8.2	38.9	67.5	0.73
95	-30.1	-31.2	8.2	38.8	67.5	0.74
63	-30.2	-30.7	8.3	38.8	67.5	0.74
96	-30.4	-30.5	8.3	38.8	67.5	0.74
120	0.2	-34.9	5.5	36.7	67.5	0.84
114	-34.8	0.2	5.4	36.6	67.5	0.84
42	-18.9	-33	7.6	36.3	67.5	0.86
26	-32.9	-18.7	7.5	36.1	67.5	0.87
6	32.1	33.1	1.6	34.3	67.5	0.97
48	32.9	32.3	1.6	34.2	67.5	0.98
36	-4	-32	-4.1	32.6	67.5	1.07
22	-31.7	-3.7	-4.2	32.4	67.5	1.09
80	25	25	6.5	31.5	67.5	1.14
79	24.7	25.2	6.5	31.5	67.5	1.14
72	-18	-25.2	8.8	31.1	67.5	1.17
98	-25	-17.9	8.7	30.8	67.5	1.19
40	-9.7	-29.6	4.8	30.7	67.5	1.2
28	-29.3	-9.5	4.7	30.4	67.5	1.22
108	7.8	28.1	6.3	29.9	67.5	1.26
75	13.4	19.9	-12.3	29.4	67.5	1.3
39	-18.8	-28	1.6	28.3	67.5	1.39
25	-27.9	-18.6	1.6	28.1	67.5	1.4
123	-14.5	-18.3	-11.1	27.6	67.5	1.44
115	-12.4	-27.6	-0.3	27.6	67.5	1.44

Table 2.11.1.1-4 Normalized Stress Ratios - UMS® PWR Basket Support Disk Sectional Stresses Due to Maine Yankee Consolidated Fuel (100% Failed) Compared to the Design Basis PWR Fuel Basket Maximum Stresses (Base Case)

Case	Support Disk Sectional Stress Intensity Ratio - Membrane							
	Normal Conditions, 20g				Accident Conditions, 60g			
	0°	18.22°	26.28°	45°	0°	18.22°	26.28°	45°
Design Basis	1.00	1.00	1.00	1.00	1.00	1.00	1.00	1.00
Case 1	0.98	0.93	0.97	0.96	0.92	0.95	0.95	0.96
Case 2	0.98	0.94	0.97	0.97	0.93	0.95	0.95	0.97
Case 3	0.98	0.95	0.98	0.97	0.92	0.96	0.96	0.96
Case 4	0.98	0.95	0.98	0.97	0.93	0.97	0.96	0.98
Case	**Support Disk Sectional Stress Intensity Ratio – Membrane + Bending**							
	Normal Conditions, 20g, Cold				**Accident Conditions, 60g, Hot**			
	0°	**18.22°**	**26.28°**	**45°**	**0°**	**18.22°**	**26.28°**	**45°**
Design Basis	1.00	1.00	1.00	1.00	1.00	1.00	1.00	1.00
Case 1	1.00	0.93	0.97	0.97	0.96	0.98	0.98	0.97
Case 2	0.99	0.94	0.97	0.98	0.96	0.99	0.99	0.98
Case 3	1.00	0.95	0.97	0.98	0.96	0.99	0.99	0.97
Case 4	0.99	0.95	0.98	0.99	0.96	1.03	1.02	1.00

Table 2.11.1.1-5 P_m Stresses for Support Disk for 1-Foot Side Drop – Maine Yankee 100% Failed Consolidated Fuel

Section	Sx (ksi)	Sy (ksi)	Sxy (ksi)	Stress Intensity (ksi)	Allowable Stress (ksi)	Margin of Safety
120	9.9	-9.7	7.8	24.9	45	0.80
114	-9.7	9.8	7.7	24.9	45	0.81
35	14.0	-1.6	6.9	20.8	45	1.16
23	-1.5	14.2	6.8	20.7	45	1.17
21	-7.9	-16.7	6.7	20.3	45	1.22
37	16.6	-8.1	6.7	20.3	45	1.22
112	7.2	-6.2	6.2	18.3	45	1.46
111	-6.0	7.2	6.2	18.1	45	1.48
9	-0.9	-12.8	6.2	17.1	45	1.63
49	12.5	-0.9	6.2	17.1	45	1.64
63	1.5	-11.0	5.8	17.0	45	1.64
96	10.6	1.5	5.9	16.8	45	1.67
7	3.1	12.7	5.8	15.4	45	1.92
51	12.4	3.1	5.8	15.2	45	1.97
72	11.2	-9.6	4.4	14.9	45	2.02
40	2.2	-8.9	4.9	14.9	45	2.02
98	-9.7	-11.3	4.3	14.9	45	2.02
28	-9.0	2.2	4.8	14.8	45	2.03
104	-7.4	-0.3	6.2	14.4	45	2.13
66	-0.3	-7.5	6.1	14.3	45	2.16
95	-3.3	-12.0	4.5	13.9	45	2.23
64	11.8	-3.5	4.6	13.8	45	2.25
26	10.1	-6.4	4.6	13.2	45	2.40
42	-6.5	-10.0	4.6	13.2	45	2.40
110	13.0	-0.1	-0.5	13.0	45	2.46
119	-0.1	-12.9	-0.5	12.9	45	2.49
94	12.1	-0.1	-0.4	12.2	45	2.70
71	-0.1	-12.0	-0.4	12.0	45	2.74
79	0.7	9.4	4.0	11.9	45	2.79
80	9.1	0.7	4.1	11.8	45	2.83
74	-0.2	-9.6	2.3	10.5	45	3.30
99	-9.6	-0.3	2.3	10.4	45	3.32
22	-3.1	-1.4	-5.1	10.3	45	3.36
36	-1.5	-3.3	-5.1	10.3	45	3.37
108	-4.1	5.3	2.1	10.3	45	3.38
124	3.2	-6.8	0.9	10.2	45	3.41
92	2.6	-7.2	0.4	9.9	45	3.57
115	0.8	-4.8	4.0	9.7	45	3.65
122	-4.7	0.8	3.9	9.6	45	3.69
116	-0.1	-9.4	0.0	9.4	45	3.77

Note: Analysis corresponds to the 1-foot side drop with 45° basket orientation and thermal case B (See Section 2.6.13.6.2).

Table 2.11.1.1-6 $P_m + P_b$ Stresses for Support Disk for 1-Foot Side Drop – Maine Yankee 100% Failed Consolidated Fuel

Section	Sx (ksi)	Sy (ksi)	Sxy (ksi)	Stress Intensity (ksi)	Allowable Stress (ksi)	Margin of Safety
37	-40.2	-46.2	12.3	55.9	67.5	0.21
21	-46.0	-40.2	12.3	55.8	67.5	0.21
23	35.6	37.9	10.7	47.5	67.5	0.42
35	37.8	35.7	10.7	47.5	67.5	0.42
34	-42.8	-42.4	3.2	45.8	67.5	0.47
20	-42.2	-42.8	3.3	45.8	67.5	0.48
1	-44.4	-38.2	2.9	45.5	67.5	0.48
4	-38.2	-44.2	2.8	45.3	67.5	0.49
7	36.4	33.5	9.7	44.7	67.5	0.51
51	33.3	36.5	9.6	44.6	67.5	0.51
49	-34.0	-34.6	9.7	44.0	67.5	0.53
9	-34.4	-34.1	9.7	44.0	67.5	0.53
112	-18.5	-43.0	3.8	43.6	67.5	0.55
2	-40.0	-41.0	2.9	43.5	67.5	0.55
3	-41.0	-39.8	2.9	43.4	67.5	0.56
111	-42.8	-18.5	3.7	43.3	67.5	0.56
64	-32.8	-32.8	8.8	41.6	67.5	0.62
95	-32.4	-32.9	8.7	41.4	67.5	0.63
63	-31.9	-33.0	8.9	41.4	67.5	0.63
96	-32.7	-32.1	8.9	41.3	67.5	0.64
6	-33.1	-36.6	1.9	37.4	67.5	0.81
48	-36.4	-33.2	1.8	37.2	67.5	0.81
120	0.1	-35.3	5.5	37.0	67.5	0.82
114	-35.2	0.0	5.5	36.9	67.5	0.83
42	-19.6	-33.4	7.6	36.8	67.5	0.84
26	-33.3	-19.4	7.6	36.6	67.5	0.84
36	-5.1	-34.2	-4.1	34.7	67.5	0.94
80	27.4	27.3	7.1	34.5	67.5	0.96
79	27.0	27.7	7.1	34.4	67.5	0.96
22	-33.8	-4.7	-4.1	34.4	67.5	0.96
72	-19.4	-27.4	9.6	33.8	67.5	1.00
98	-27.1	-19.3	9.5	33.4	67.5	1.02
40	-11.4	-32.0	5.5	33.4	67.5	1.02
28	-31.7	-11.2	5.4	33.0	67.5	1.04
108	7.9	28.6	6.3	30.3	67.5	1.23
50	4.4	29.3	-3.6	29.8	67.5	1.27
75	13.7	20.1	-12.5	29.8	67.5	1.27
8	29.0	4.0	-3.7	29.5	67.5	1.29
74	-18.6	-23.7	7.8	29.4	67.5	1.30
99	-23.4	-18.6	7.8	29.2	67.5	1.31

Note: Analysis corresponds to the 1-foot side drop with 45° basket orientation and thermal case B (See Section 2.6.13.6.2).

THIS PAGE INTENTIONALLY LEFT BLANK

45. Parker Seals "O-Ring Handbook," ORD-5700, 1992.

46. Oberg, Erik, et al, Machinery's Handbook, 25th Edition, First Printing, Industrial Press, Inc., New York, New York, 1984.

47. Clough, Ray W. and Joseph Penzien, "Dynamics of Structures," 2nd Edition, 1993.

48. Rust, James H., "Nuclear Power Plant Engineering," 1979.

49. ISG-4, Revision 1, "Cask Closure Weld Inspections," May 1999.

50. Blevins, R.D., *Formulas for Natural Frequency and Mode Shape*, Krieger Publishing Co., Malabar, Florida, 1995.

51. ARMCO Product Data Bulletin No. S-22, "17-4PH, Precipitation Hardening Stainless Steel," ARMCO, Inc., 1988.

52. ASTM B733-97, "Standard Specification for Autocatalytic (Electroless) Nickel-Phosphorus Coatings on Metal," Annual Book of ASTM Standards, Vol. 02.05, American Society for Testing and Materials, Conshohocken, PA, 1996.

53. American Society for Metals, "Metals Handbook," 1985.

54. Duncan, R.N., "Corrosion Resistance of High-Phosphorus Electroless Nickel Coatings," Plating and Surface Finishing, July 1986, pages 52-56.

55. Weaver, William Jr. and James M. Gere, "Matrix Analysis of Framed Structures," Second Edition, D. Van Nostrand Company, New York, 1980.

56. Marks' Standard Handbook for Mechanical Engineers, 9th Edition, McGraw-Hill Book Company, New York, New York.

57. NUREG-1617, "Standard Review Plan for Transportation Packages for Spent Nuclear Fuel," U.S. Nuclear Regulatory Commission, Washington, DC.

58. Sandia Report SAND90-2187, TTC-1012, UC-80, "An Analysis of Parameters Affecting Slapdown of Transportation Packages," Sandia National Laboratories, Albuquerque, NM, 1991.

59. US NRC Regulatory Guide 1.92, "Combining Modal Responses and Spatial Components in Seismic Response Analysis," Revision 1, February 1976.

60. ISG-12, "Buckling of Irradiated Fuel Under Bottom End Drop Conditions," May 1999.

61. NUREG/CR-5009, "Assessment of the Use of Extended Burnup Fuel in Light Water Power Reactors," Battelle Pacific Northwest Labs, Richland, Washington, February 1988.

62. "Maine Yankee Atomic Power Company Specification for Independent Spent Fuel Storage Installation and Transport Facility," NAC Document 12412-DI-01, NAC International, Atlanta, Georgia.

63. Blake, Alexander, "Practical Stress Analysis in Engineering Design," 2nd Edition, Marcell Dekker, Inc., New York, 1990.

64. Young, Warren C., "Roark's Formula for Stress & Strain," 6th Edition, McGraw-Hill, 1989.

65. "Fuel-Assembly Behavior Under Dynamic Impact Loads Due to Dry-Storage Cask Mishandling," EPRI NP-7419, ABB Combustion Engineering, Inc., Windsor, Conn., July 1991.

EA790-SAR-001

DOCKET NO. 71-9270

UMS®

UNIVERSAL MPC SYSTEM®

SAFETY ANALYSIS REPORT

for the

UMS® Universal Transport Cask

MAY 2001 UMST-01C

VOLUME 2 OF 2

NAC INTERNATIONAL

List of Effective Pages

Master Table of Contents

i.....Revision UMST-00A
ii.....Revision UMST-00A
iii .....Revision UMST-00A
iv.....Revision UMST-01B
v.....Revision UMST-01B
vi.....Revision UMST-01B
vii.....Revision UMST-01B
viii .....Revision UMST-00A
ix.....Revision UMST-01C
x.....Revision UMST-01C
xi.....Revision UMST-00A
xii.....Revision UMST-01A
xiii .....Revision UMST-00A
xiv.....Revision UMST-00A
xv.....Revision UMST-01C
xvi.....Revision UMST-00A
xvii.....Revision UMST-00A
xviii .....Revision UMST-00A
xix.....Revision UMST-00A

Chapter 1

1-i .....Revision UMST-99A
1-ii .....Revision UMST-01C
1-1.....Revision UMST-00A
1-2.....Revision UMST-01C
1-3.....Revision UMST-00A
1-4.....Revision UMST-01C
1-5.....Revision UMST-01C
1-6.....Revision UMST-01C
1-7.....Revision UMST-01C
1.1-1.....Revision UMST-99A
1.1-2.....Revision UMST-99A
1.1-3.....Revision UMST-00A
1.1-4.....Revision UMST-99A
1.1-5.....Revision UMST-99A
1.1-6.....Revision UMST-99A
1.2-1.....Revision UMST-00A
1.2-2.....Revision UMST-99A
1.2-3.....Revision UMST-00A
1.2-4.....Revision UMST-99A
1.2-5.....Revision UMST-00A
1.2-6.....Revision 0
1.2-7.....Revision UMST-99A
1.2-8.....Revision UMST-99A
1.2-9.....Revision UMST-00A
1.2-10.....Revision UMST-00A
1.2-11.....Revision UMST-00A
1.2-12.....Revision UMST-00A
1.2-13.....Revision UMST-00A
1.2-14.....Revision UMST-00A
1.2-15.....Revision UMST-00A
1.2-16.....Revision UMST-99A
1.2-17.....Revision UMST-99A
1.2-18.....Revision UMST-99A
1.2-19.....Revision UMST-00A
1.2-20.....Revision UMST-00A
1.2-21.....Revision UMST-99A
1.2-22.....Revision UMST-01C
1.2-23.....Revision UMST-00A
1.2-24.....Revision UMST-99A
1.2-25.....Revision UMST-99A
1.3-1.....Revision UMST-99A
1.3.1-1.....Revision UMST-99A
1.3.1-2.....Revision UMST-01C

List of Effective Pages (Continued)

1.3.1-3.....Revision UMST-01C
1.3.1-4.....Revision UMST-01C
1.3.1-5.....Revision UMST-01C
1.3.1-6.....Revision UMST-01C
1.3.1-7.....Revision UMST-00A
1.3.1-8.....Revision UMST-01C
1.3.2-1.....Revision UMST-99A
1.3.3-1.....Revision UMST-00A
1.3.4-1.....Revision UMST-01B
1.3.4-2.....Revision UMST-01C

License Drawings
34 drawings
Revised as shown in Chapter 1

Chapter 2

2-i .....Revision UMST-00A
2-ii .....Revision UMST-00A
2-iii .....Revision UMST-01B
2-iv .....Revision UMST-01B
2-v.....Revision UMST-01B
2-vi .....Revision UMST-01B
2-vii .....Revision UMST-00A
2-viii .....Revision UMST-01C
2-ix .....Revision UMST-01C
2-x .....Revision UMST-01B
2-xi .....Revision UMST-01B
2-xii .....Revision UMST-01B
2-xiii .....Revision UMST-01C
2-xiv .....Revision UMST-01C
2-xv .....Revision UMST-01C
2-xvi .....Revision UMST-00A
2-xvii .....Revision UMST-00A
2-xviii .....Revision UMST-00A
2-xix .....Revision UMST-00A
2-xx .....Revision UMST-01B
2-xxi .....Revision UMST-01B
2-xxii .....Revision UMST-01B
2-xxiii .....Revision UMST-01B
2-xxiv .....Revision UMST-01B
2-xxv .....Revision UMST-01B
2-xxvi .....Revision UMST-01B
2-xxvii .....Revision UMST-01B
2-xxviii .....Revision UMST-00A
2-xxix .....Revision UMST-00A
2-xxx .....Revision UMST-00A
2-xxxi .....Revision UMST-00A
2-xxxii .....Revision UMST-00A
2-xxxiii .....Revision UMST-01C
2-xxxiv .....Revision UMST-01C
2-1.....Revision UMST-00A
2.1-1.....Revision UMST-00A
2.1-2.....Revision 0
2.1-3.....Revision 0
2.1-4.....Revision 0
2.1-5.....Revision 0
2.1-6.....Revision UMST-00A
2.1-7.....Revision 0
2.1-8.....Revision 0
2.1-9.....Revision UMST-00A
2.1-10.....Revision UMST-00A
2.1-11.....Revision UMST-00A
2.1-12.....Revision UMST-00A
2.1-13.....Revision UMST-00A
2.1-14.....Revision UMST-00A

List of Effective Pages (Continued)

2.1-15.....Revision UMST-00A
2.1-16.....Revision UMST-00A
2.1-17.....Revision UMST-00A
2.1-18.....Revision UMST-00A
2.1-19.....Revision UMST-00A
2.1-20.....Revision UMST-00A
2.1-21.....Revision UMST-00A
2.1-22.....Revision UMST-00A
2.1-23.....Revision UMST-00A
2.1-24.....Revision UMST-00A
2.2-1.....Revision UMST-00A
2.2-2.....Revision UMST-00A
2.2-3.....Revision UMST-00A
2.2-4.....Revision UMST-00A
2.3-1.....Revision 0
2.3-2.....Revision UMST-00A
2.3-3.....Revision 0
2.3-4.....Revision 0
2.3-5.....Revision 0
2.3-6.....Revision 0
2.3-7.....Revision 0
2.3-8.....Revision 0
2.3-9.....Revision 0
2.3-10.....Revision UMST-99A
2.3-11.....Revision 0
2.3-12.....Revision 0
2.3-13.....Revision 0
2.3-14.....Revision 0
2.3-15.....Revision UMST-00A
2.3-16.....Revision UMST-99A
2.3-17.....Revision UMST-00A
2.3-18.....Revision UMST-00A
2.3-19.....Revision UMST-00A
2.3-20.....Revision UMST-00A
2.3-21.....Revision UMST-99A
2.3-22.....Revision UMST-00A
2.4-1.....Revision UMST-00A
2.4-2.....Revision UMST-00A
2.4-3.....Revision UMST-00A
2.4-4.....Revision UMST-00A
2.4-5.....Revision UMST-00A
2.4-6.....Revision UMST-00A
2.4-7.....Revision UMST-00A
2.4-8.....Revision UMST-00A
2.4-9.....Revision UMST-00A
2.5-1.....Revision UMST-97A
2.5-2.....Revision UMST-97A
2.5-3.....Revision UMST-97A
2.5-4.....Revision UMST-97A
2.5-5.....Revision 0
2.5-6.....Revision UMST-97A
2.5-7.....Revision UMST-97A
2.5-8.....Revision UMST-97A
2.5-9.....Revision UMST-97A
2.5-10.....Revision UMST-97A
2.5-11.....Revision UMST-97A
2.5-12.....Revision UMST-97A
2.5-13.....Revision UMST-97A
2.5-14.....Revision UMST-97A
2.5-15.....Revision 0
2.5-16.....Revision 0
2.5-17.....Revision UMST-01B
2.5-18.....Revision UMST-01B
2.5-19.....Revision UMST-00A
2.5-20.....Revision UMST-00A
2.5-21.....Revision UMST-00A

List of Effective Pages (Continued)

2.5-22.....Revision UMST-00A
2.5-23.....Revision UMST-97A
2.5-24.....Revision UMST-97A
2.5-25.....Revision UMST-97A
2.5-26.....Revision UMST-97A
2.5-27.....Revision 0
2.5-28.....Revision 0
2.5-29.....Revision UMST-97A
2.5-30.....Revision UMST-97A
2.5-31.....Revision UMST-97A
2.5-32.....Revision 0
2.5-33.....Revision 0
2.5-34.....Revision 0
2.5-35.....Revision 0
2.5-36.....Revision 0
2.5-37.....Revision 0
2.5-38.....Revision 0
2.5-39.....Revision 0
2.5-40.....Revision 0
2.5-41.....Revision 0
2.5-42.....Revision 0
2.5-43.....Revision 0
2.5-44.....Revision 0
2.5-45.....Revision 0
2.5-46.....Revision 0
2.5-47.....Revision 0
2.5-48.....Revision 0
2.5-49.....Revision 0
2.5-50.....Revision 0
2.5-51.....Revision UMST-00A
2.5-52.....Revision UMST-00A
2.6-1.....Revision UMST-00A
2.6-2.....Revision UMST-00A
2.6-3.....Revision UMST-00A
2.6-4.....Revision UMST-00A
2.6-5.....Revision UMST-00A
2.6-6.....Revision UMST-00A
2.6-7.....Revision UMST-00A
2.6-8.....Revision UMST-00A
2.6-9.....Revision UMST-00A
2.6-10.....Revision UMST-00A
2.6-11.....Revision UMST-00A
2.6-12.....Revision UMST-00A
2.6-13.....Revision UMST-00A
2.6-14.....Revision UMST-00A
2.6-15.....Revision UMST-00A
2.6-16.....Revision UMST-00A
2.6-17.....Revision 0
2.6-18.....Revision UMST-00A
2.6-19.....Revision UMST-00A
2.6-20.....Revision UMST-00A
2.6-21.....Revision UMST-00A
2.6-22.....Revision UMST-00A
2.6-23.....Revision UMST-00A
2.6-24.....Revision UMST-00A
2.6-25.....Revision UMST-00A
2.6-26.....Revision UMST-00A
2.6-27.....Revision UMST-00A
2.6-28.....Revision 0
2.6-29.....Revision UMST-00A
2.6-30.....Revision UMST-00A
2.6-31.....Revision 0
2.6-32.....Revision UMST-00A
2.6-33.....Revision UMST-00A
2.6-34.....Revision UMST-00A
2.6-35.....Revision UMST-00A

List of Effective Pages (Continued)

2.6-36.....Revision UMST-00A
2.6-37.....Revision UMST-00A
2.6-38.....Revision UMST-00A
2.6-39.....Revision UMST-00A
2.6-40.....Revision UMST-00A
2.6-41.....Revision UMST-00A
2.6-42.....Revision 0
2.6-43.....Revision UMST-00A
2.6-44.....Revision 0
2.6-45.....Revision UMST-00A
2.6-46.....Revision UMST-00A
2.6-47.....Revision 0
2.6-48.....Revision 0
2.6-49.....Revision UMST-00A
2.6-50.....Revision UMST-00A
2.6-51.....Revision UMST-00A
2.6-52.....Revision UMST-00A
2.6-53.....Revision UMST-00A
2.6-54.....Revision 0
2.6-55.....Revision UMST-00A
2.6-56.....Revision UMST-00A
2.6-57.....Revision 0
2.6-58.....Revision UMST-00A
2.6-59.....Revision UMST-00A
2.6-60.....Revision 0
2.6-61.....Revision UMST-01B
2.6-62.....Revision UMST-01B
2.6-63.....Revision UMST-01B
2.6-64.....Revision UMST-01B
2.6-65.....Revision UMST-01B
2.6-66.....Revision UMST-01B
2.6-67.....Revision UMST-01B
2.6-68.....Revision UMST-01B
2.6-69.....Revision UMST-01B
2.6-70.....Revision UMST-01B
2.6-71.....Revision UMST-01B
2.6-72.....Revision UMST-01B
2.6-73.....Revision UMST-01B
2.6-74.....Revision UMST-01B
2.6-75.....Revision UMST-01B
2.6-76.....Revision UMST-01B
2.6-77.....Revision UMST-01B
2.6-78.....Revision UMST-01B
2.6-79.....Revision UMST-01B
2.6-80.....Revision UMST-01B
2.6-81.....Revision UMST-01B
2.6-82.....Revision UMST-01B
2.6-83.....Revision UMST-01B
2.6-84.....Revision UMST-01B
2.6-85.....Revision UMST-01B
2.6-86.....Revision UMST-01B
2.6-87.....Revision UMST-01B
2.6-88.....Revision UMST-01B
2.6-89.....Revision UMST-01B
2.6-90.....Revision UMST-01B
2.6-91.....Revision UMST-01B
2.6-92.....Revision UMST-01B
2.6-93.....Revision UMST-01B
2.6-94.....Revision UMST-01B
2.6-95.....Revision UMST-01B
2.6-96.....Revision UMST-01B
2.6-97.....Revision UMST-01B
2.6-98.....Revision UMST-01B
2.6-99.....Revision UMST-01B
2.6-100.....Revision UMST-01B
2.6-101.....Revision UMST-01B

List of Effective Pages (Continued)

2.6-102.....Revision UMST-01B
2.6-103.....Revision UMST-01B
2.6-104.....Revision UMST-01B
2.6-105.....Revision UMST-01B
2.6-106.....Revision UMST-01B
2.6-107.....Revision UMST-01B
2.6-108.....Revision UMST-01B
2.6-109.....Revision UMST-01B
2.6-110.....Revision UMST-01B
2.6-111.....Revision UMST-01B
2.6-112.....Revision UMST-01B
2.6-113.....Revision UMST-01B
2.6-114.....Revision UMST-01B
2.6-115.....Revision UMST-01B
2.6-116.....Revision UMST-01B
2.6-117.....Revision UMST-01B
2.6-118.....Revision UMST-01B
2.6-119.....Revision UMST-01B
2.6-120.....Revision UMST-01C
2.6-121.....Revision UMST-01C
2.6-122.....Revision UMST-01B
2.6-123.....Revision UMST-01B
2.6-124.....Revision UMST-01B
2.6-125.....Revision UMST-01B
2.6-126.....Revision UMST-01B
2.6-127.....Revision UMST-01B
2.6-128.....Revision UMST-01C
2.6-129.....Revision UMST-01B
2.6-130.....Revision UMST-01B
2.6-131.....Revision UMST-01B
2.6-132.....Revision UMST-01B
2.6-133.....Revision UMST-01B
2.6-134.....Revision UMST-01B
2.6-135.....Revision UMST-01B
2.6-136.....Revision UMST-01B
2.6-137.....Revision UMST-01B
2.6-138.....Revision UMST-01B
2.6-139.....Revision UMST-01B
2.6-140.....Revision UMST-01B
2.6-141.....Revision UMST-01B
2.6-142.....Revision UMST-01B
2.6-143.....Revision UMST-01B
2.6-144.....Revision UMST-01B
2.6-145.....Revision UMST-01B
2.6-146.....Revision UMST-01B
2.6-147.....Revision UMST-01B
2.6-148.....Revision UMST-01B
2.6-149.....Revision UMST-01B
2.6-150.....Revision UMST-01B
2.6-151.....Revision UMST-01B
2.6-152.....Revision UMST-01B
2.6-153.....Revision UMST-01B
2.6-154.....Revision UMST-01B
2.6-155.....Revision UMST-01B
2.6-156.....Revision UMST-01B
2.6-157.....Revision UMST-01B
2.6-158.....Revision UMST-01B
2.6-159.....Revision UMST-01B
2.6-160.....Revision UMST-01B
2.6-161.....Revision UMST-01B
2.6-162.....Revision UMST-01B
2.6-163.....Revision UMST-01B
2.6-164.....Revision UMST-01B
2.6-165.....Revision UMST-01B
2.6-166.....Revision UMST-01B
2.6-167.....Revision UMST-01B

List of Effective Pages (Continued)

2.6-168.....Revision UMST-01B
2.6-169.....Revision UMST-01B
2.6-170.....Revision UMST-01B
2.6-171.....Revision UMST-01B
2.6-172.....Revision UMST-01B
2.6-173.....Revision UMST-01B
2.6-174.....Revision UMST-01B
2.6-175.....Revision UMST-01B
2.6-176.....Revision UMST-01B
2.6-177.....Revision UMST-01B
2.6-178.....Revision UMST-01B
2.6-179.....Revision UMST-01B
2.6-180.....Revision UMST-01B
2.6-181.....Revision UMST-01B
2.6-182.....Revision UMST-01B
2.6-183.....Revision UMST-01B
2.6-184.....Revision UMST-01B
2.6-185.....Revision UMST-01B
2.6-186.....Revision UMST-01B
2.6-187.....Revision UMST-01B
2.6-188.....Revision UMST-01B
2.6-189.....Revision UMST-01B
2.6-190.....Revision UMST-01B
2.6-191.....Revision UMST-01B
2.6-192.....Revision UMST-01B
2.6-193.....Revision UMST-01B
2.6-194.....Revision UMST-01B
2.6-195.....Revision UMST-01B
2.6-196.....Revision UMST-01B
2.6-197.....Revision UMST-01B
2.6-198.....Revision UMST-01B
2.6-199.....Revision UMST-01B
2.6-200.....Revision UMST-01B
2.6-201.....Revision UMST-01B
2.6-202.....Revision UMST-01B
2.6-203.....:Revision UMST-01B
2.6-204.....Revision UMST-01B
2.6-205.....Revision UMST-01B
2.6-206.....Revision UMST-01B
2.6-207.....Revision UMST-01B
2.6-208.....Revision UMST-01B
2.6-209.....Revision UMST-01B
2.6-210.....Revision UMST-01B
2.6-211.....Revision UMST-01B
2.6-212.....Revision UMST-01B
2.6-213.....Revision UMST-01B
2.6-214.....Revision UMST-01B
2.6-215.....Revision UMST-01B
2.6-216.....Revision UMST-01B
2.6-217.....Revision UMST-01B
2.6-218.....Revision UMST-01B
2.6-219.....Revision UMST-01B
2.6-220.....Revision UMST-01B
2.6-221.....Revision UMST-01B
2.6-222.....Revision UMST-01B
2.6-223.....Revision UMST-01B
2.6-224.....Revision UMST-01B
2.6-225.....Revision UMST-01B
2.6-226.....Revision UMST-01B
2.6-227.....Revision UMST-01B
2.6-228.....Revision UMST-01B
2.6-229.....Revision UMST-01B
2.6-230.....Revision UMST-01B
2.6-231.....Revision UMST-01B
2.6-232.....Revision UMST-01B
2.6-233.....Revision UMST-01B

List of Effective Pages (Continued)

2.6-234.....Revision UMST-01B
2.6-235.....Revision UMST-01B
2.6-236.....Revision UMST-01B
2.6-237.....Revision UMST-01B
2.6-238.....Revision UMST-01B
2.6-239.....Revision UMST-01B
2.6-240.....Revision UMST-01B
2.6-241.....Revision UMST-01B
2.6-242.....Revision UMST-01B
2.6-243.....Revision UMST-01B
2.6-244.....Revision UMST-01B
2.6-245.....Revision UMST-01B
2.6-246.....Revision UMST-01B
2.6-247.....Revision UMST-01B
2.6-248.....Revision UMST-01B
2.6-249.....Revision UMST-01B
2.6-250.....Revision UMST-01B
2.6-251.....Revision UMST-01B
2.6-252.....Revision UMST-01B
2.6-253.....Revision UMST-01C
2.6-254.....Revision UMST-01B
2.6-255.....Revision UMST-01B
2.6-256.....Revision UMST-01B
2.6-257.....Revision UMST-01B
2.6-258.....Revision UMST-01B
2.6-259.....Revision UMST-01B
2.6-260.....Revision UMST-01B
2.6-261.....Revision UMST-01B
2.6-262.....Revision UMST-01B
2.6-263.....Revision UMST-01B
2.5-264.....Revision UMST-01B
2.6-265.....Revision UMST-01B
2.6-266.....Revision UMST-01B
2.6-267.....Revision UMST-01B
2.6-268.....Revision UMST-01B
2.6-269.....Revision UMST-01B
2.6-270.....Revision UMST-01B
2.6-271.....Revision UMST-01B
2.6-272.....Revision UMST-01B
2.6-273.....Revision UMST-01B
2.6-274.....Revision UMST-01B
2.6-275.....Revision UMST-01B
2.6-276.....Revision UMST-01B
2.6-277.....Revision UMST-01B
2.6-278.....Revision UMST-01B
2.6-279.....Revision UMST-01B
2.6-280.....Revision UMST-01B
2.6-281.....Revision UMST-01B
2.6-282.....Revision UMST-01B
2.6-283.....Revision UMST-01B
2.6-284.....Revision UMST-01B
2.6-285.....Revision UMST-01B
2.6-286.....Revision UMST-01B
2.6-287.....Revision UMST-01B
2.6-288.....Revision UMST-01B
2.6-289.....Revision UMST-01B
2.6-290.....Revision UMST-01B
2.6-291.....Revision UMST-01B
2.6-292.....Revision UMST-01B
2.6-293.....Revision UMST-01B
2.6-294.....Revision UMST-01B
2.6-295.....Revision UMST-01B
2.6-296.....Revision UMST-01B
2.6-297.....Revision UMST-01B
2.6-298.....Revision UMST-01B
2.6-299.....Revision UMST-01B

List of Effective Pages (Continued)

2.6-300.....Revision UMST-01B
2.6-301.....Revision UMST-01B
2.6-302.....Revision UMST-01B
2.6-303.....Revision UMST-01B
2.6-304.....Revision UMST-01B
2.6-305.....Revision UMST-01B
2.6-306.....Revision UMST-01B
2.6-307.....Revision UMST-01B
2.6-308.....Revision UMST-01B
2.6-309.....Revision UMST-01B
2.6-310.....Revision UMST-01B
2.6-311.....Revision UMST-01B
2.6-312.....Revision UMST-01B
2.6-313.....Revision UMST-01B
2.6-314.....Revision UMST-01B
2.6-315.....Revision UMST-01B
2.6-316.....Revision UMST-01B
2.6-317.....Revision UMST-01B
2.6-318.....Revision UMST-01B
2.6-319.....Revision UMST-01B
2.6-320.....Revision UMST-01B
2.6-321.....Revision UMST-01B
2.6-322.....Revision UMST-01B
2.6-323.....Revision UMST-01B
2.6-324.....Revision UMST-01B
2.6-325.....Revision UMST-01B
2.6-326.....Revision UMST-01B
2.6-327.....Revision UMST-01B
2.6-328.....Revision UMST-01B
2.6-329.....Revision UMST-01B
2.6-330.....Revision UMST-01B
2.6-331.....Revision UMST-01B
2.6-332.....Revision UMST-01B
2.6-333.....Revision UMST-01B
2.6-334.....Revision UMST-01B
2.6-335.....Revision UMST-01B
2.6-336.....Revision UMST-01B
2.6-337.....Revision UMST-01B
2.6-338.....Revision UMST-01B
2.6-339.....Revision UMST-01B
2.6-340.....Revision UMST-01B
2.6-341.....Revision UMST-01B
2.6-342.....Revision UMST-01B
2.6-343.....Revision UMST-01B
2.6-344.....Revision UMST-01B
2.6-345.....Revision UMST-01B
2.6-346.....Revision UMST-01B
2.6-347.....Revision UMST-01B
2.6-348.....Revision UMST-01B
2.6-349.....Revision UMST-01B
2.6-350.....Revision UMST-01B
2.6-351.....Revision UMST-01B
2.6-352.....Revision UMST-01B
2.6-353.....Revision UMST-01B
2.6-354.....Revision UMST-01B
2.6-355.....Revision UMST-01B
2.6-356.....Revision UMST-01B
2.6-357.....Revision UMST-01B
2.6-358.....Revision UMST-01B
2.6-359.....Revision UMST-01B
2.6-360.....Revision UMST-01B
2.6-361.....Revision UMST-01B
2.6-362.....Revision UMST-01B
2.6-363.....Revision UMST-01B
2.6-364.....Revision UMST-01B
2.6-365.....Revision UMST-01B

List of Effective Pages (Continued)

2.6-366.....Revision UMST-01B
2.6-367.....Revision UMST-01B
2.6-368.....Revision UMST-01B
2.6-369.....Revision UMST-01B
2.6-370.....Revision UMST-01B
2.6-371.....Revision UMST-01B
2.6-372.....Revision UMST-01B
2.6-373.....Revision UMST-01B
2.6-374.....Revision UMST-01B
2.6-375.....Revision UMST-01B
2.6-376.....Revision UMST-01B
2.6-377.....Revision UMST-01B
2.6-278.....Revision UMST-01B
2.6-379.....Revision UMST-01B
2.6-380.....Revision UMST-01B
2.6-381.....Revision UMST-01B
2.6-382.....Revision UMST-01B
2.6-383.....Revision UMST-01B
2.7-1.....Revision UMST-00A
2.7-2.....Revision UMST-01C
2.7-3.....Revision 0
2.7-4.....Revision UMST-00A
2.7-5.....Revision 0
2.7-6.....Revision 0
2.7-7.....Revision UMST-00A
2.7-8.....Revision UMST-00A
2.7-9.....Revision UMST-00A
2.7-10.....Revision UMST-00A
2.7-11.....Revision 0
2.7-12.....Revision 0
2.7-13.....Revision 0
2.7-14.....Revision UMST-00A
2.7-15.....Revision 0
2.7-16.....Revision 0
2.7-17.....Revision 0
2.7-18.....Revision UMST-00A
2.7-19.....Revision 0
2.7-20.....Revision 0
2.7-21.....Revision UMST-00A
2.7-22.....Revision 0
2.7-23.....Revision 0
2.7-24.....Revision 0
2.7-25.....Revision UMST-00A
2.7-26.....Revision 0
2.7-27.....Revision 0
2.7-28.....Revision UMST-00A
2.7-29.....Revision UMST-00A
2.7-30.....Revision UMST-01B
2.7-31.....Revision UMST-00A
2.7-32.....Revision UMST-00A
2.7-33.....Revision UMST-00A
2.7-34.....Revision UMST-00A
2.7-35.....Revision UMST-00A
2.7-36.....Revision UMST-00A
2.7-37.....Revision UMST-00A
2.7-38.....Revision UMST-00A
2.7-39.....Revision UMST-00A
2.7-40.....Revision UMST-00A
2.7-41.....Revision UMST-00A
2.7-42.....Revision UMST-00A
2.7-43.....Revision UMST-00A
2.7-44.....Revision UMST-00A
2.7-45.....Revision UMST-00A
2.7-46.....Revision UMST-00A
2.7-47.....Revision UMST-00A
2.7-48.....Revision UMST-00A

List of Effective Pages (Continued)

2.7-49.....Revision UMST-00A
2.7-50.....Revision UMST-00A
2.7-51.....Revision UMST-00A
2.7-52.....Revision UMST-00A
2.7-53.....Revision UMST-00A
2.7-54.....Revision UMST-00A
2.7-55.....Revision UMST-00A
2.7-56.....Revision UMST-00A
2.7-57.....Revision UMST-00A
2.7-58.....Revision UMST-00A
2.7-59.....Revision UMST-00A
2.7-60.....Revision UMST-00A
2.7-61.....Revision UMST-00A
2.7-62.....Revision UMST-00A
2.7-63.....Revision UMST-00A
2.7-64.....Revision UMST-00A
2.7-65.....Revision UMST-00A
2.7-66.....Revision UMST-00A
2.7-67.....Revision UMST-00A
2.7-68.....Revision UMST-00A
2.7-69.....Revision UMST-00A
2.7-70.....Revision UMST-00A
2.7-71.....Revision UMST-00A
2.7-72.....Revision UMST-00A
2.7-73.....Revision UMST-00A
2.7-74.....Revision UMST-00A
2.7-75.....Revision UMST-00A
2.7-76.....Revision UMST-00A
2.7-77.....Revision UMST-00A
2.7-78.....Revision UMST-00A
2.7-79.....Revision UMST-00A
2.7-80.....Revision UMST-00A
2.7-81.....Revision UMST-00A
2.7-82.....Revision UMST-00A
2.7-83.....Revision UMST-00A
2.7-84.....Revision UMST-00A
2.7-85.....Revision UMST-00A
2.7-86.....Revision UMST-00A
2.7-87.....Revision UMST-00A
2.7-88.....Revision UMST-00A
2.7-89.....Revision UMST-00A
2.7-90.....Revision UMST-00A
2.7-91.....Revision UMST-00A
2.7-92.....Revision UMST-00A
2.7-93.....Revision UMST-00A
2.7-94.....Revision UMST-00A
2.7-95.....Revision UMST-00A
2.7-96.....Revision UMST-00A
2.7-97.....Revision UMST-00A
2.7-98.....Revision UMST-00A
2.7-99.....Revision UMST-00A
2.7-100.....Revision UMST-00A
2.7-101.....Revision UMST-00A
2.7-102.....Revision UMST-00A
2.7-103.....Revision UMST-00A
2.7-104.....Revision UMST-00A
2.7-105.....Revision UMST-00A
2.7-106.....Revision UMST-00A
2.7-107.....Revision UMST-00A
2.7-108.....Revision UMST-00A
2.7-109.....Revision UMST-00A
2.7-110.....Revision UMST-00A
2.7-111.....Revision UMST-00A
2.7-112.....Revision UMST-00A
2.7-113.....Revision UMST-00A
2.7-114.....Revision UMST-00A

List of Effective Pages (Continued)

2.7-115.....Revision UMST-00A
2.7-116.....Revision UMST-00A
2.7-117.....Revision UMST-00A
2.7-118.....Revision UMST-00A
2.7-119.....Revision UMST-00A
2.7-120.....Revision UMST-00A
2.7-121.....Revision UMST-00A
2.7-122.....Revision UMST-00A
2.7-123.....Revision UMST-00A
2.7-124.....Revision UMST-00A
2.7-125.....Revision UMST-00A
2.7-126.....Revision UMST-00A
2.7-127.....Revision UMST-00A
2.7-128.....Revision UMST-00A
2.7-129.....Revision UMST-00A
2.7-130.....Revision UMST-00A
2.7-131.....Revision UMST-00A
2.7-132.....Revision UMST-00A
2.7-133.....Revision UMST-00A
2.7-134.....Revision UMST-00A
2.7-135.....Revision UMST-00A
2.7-136.....Revision UMST-00A
2.7-137.....Revision UMST-00A
2.7-138.....Revision UMST-00A
2.7-139.....Revision UMST-00A
2.7-140.....Revision UMST-00A
2.7-141.....Revision UMST-00A
2.7-142.....Revision UMST-00A
2.7-143.....Revision UMST-00A
2.7-144.....Revision UMST-00A
2.7-145.....Revision UMST-00A
2.7-146.....Revision UMST-00A
2.7-147.....Revision UMST-00A
2.7-148.....Revision UMST-00A
2.7-149.....Revision UMST-00A
2.7-150.....Revision UMST-00A
2.7-151.....Revision UMST-00A
2.7-152.....Revision UMST-00A
2.7-153.....Revision UMST-00A
2.7-154.....Revision UMST-00A
2.7-155.....Revision UMST-00A
2.7-156.....Revision UMST-00A
2.7-157.....Revision UMST-00A
2.7-158.....Revision UMST-00A
2.7-159.....Revision UMST-00A
2.7-160.....Revision UMST-00A
2.7-161.....Revision UMST-00A
2.7-162.....Revision UMST-00A
2.7-163.....Revision UMST-00A
2.7-164.....Revision UMST-00A
2.7-165.....Revision UMST-00A
2.7-166.....Revision UMST-00A
2.7-167.....Revision UMST-00A
2.7-168.....Revision UMST-00A
2.7-169.....Revision UMST-00A
2.7-170.....Revision UMST-00A
2.7-171.....Revision UMST-00A
2.7-172.....Revision UMST-00A
2.7-173.....Revision UMST-00A
2.7-174.....Revision UMST-00A
2.7-175.....Revision UMST-00A
2.7-176.....Revision UMST-00A
2.7-177.....Revision UMST-00A
2.7-178.....Revision UMST-00A
2.7-179.....Revision UMST-00A
2.7-180.....Revision UMST-00A

List of Effective Pages (Continued)

2.7-181.....Revision UMST-00A
2.7-182.....Revision UMST-00A
2.7-183.....Revision UMST-00A
2.7-184.....Revision UMST-00A
2.7-185.....Revision UMST-00A
2.7-186.....Revision UMST-00A
2.7-187.....Revision UMST-00A
2.7-188.....Revision UMST-00A
2.7-189.....Revision UMST-00A
2.7-190.....Revision UMST-00A
2.7-191.....Revision UMST-00A
2.7-192.....Revision UMST-00A
2.7-193.....Revision UMST-00A
2.7-194.....Revision UMST-00A
2.7-195.....Revision UMST-00A
2.7-196.....Revision UMST-00A
2.7-197.....Revision UMST-00A
2.7-198.....Revision UMST-00A
2.7-199.....Revision UMST-00A
2.7-200.....Revision UMST-00A
2.7-201.....Revision UMST-00A
2.7-202.....Revision UMST-00A
2.7-203.....Revision UMST-00A
2.7-204.....Revision UMST-00A
2.7-205.....Revision UMST-00A
2.7-206.....Revision UMST-00A
2.7-207.....Revision UMST-00A
2.7-208.....Revision UMST-00A
2.7-209.....Revision UMST-00A
2.7-210.....Revision UMST-00A
2.7-211.....Revision UMST-00A
2.8-1.....Revision 0
2.9-1.....Revision UMST-01C
2.9.1-1.....Revision UMST-01C
2.9.1-2.....Revision UMST-01C
2.9.1-3.....Revision UMST-01C
2.9.1-4.....Revision UMST-01C
2.9.1-5.....Revision UMST-01C
2.9.1-6.....Revision UMST-01C
2.9.1-7.....Revision UMST-01C
2.9.1-8.....Revision UMST-01C
2.9.1-9.....Revision UMST-01C
2.9.2-1.....Revision UMST-01C
2.9.2-2.....Revision UMST-01C
2.9.2-3.....Revision UMST-01C
2.9.2-4.....Revision UMST-01C
2.9.2-5.....Revision UMST-01C
2.9.2-6.....Revision UMST-01C
2.9.2-7.....Revision UMST-01C
2.9.2-8.....Revision UMST-01C
2.9.2-9.....Revision UMST-01C
2.9.2-10.....Revision UMST-01C
2.9.2-11.....Revision UMST-01C
2.9.2-12.....Revision UMST-01C
2.10-1.....Revision UMST-01B
2.10.1-1.....Revision UMST-01B
2.10.1-2.....Revision UMST-01B
2.10.2-1.....Revision UMST-99A
2.10.2-2.....Revision UMST-99A
2.10.2-3.....Revision UMST-99A
2.10.2-4.....Revision UMST-99A
2.10.2-5.....Revision UMST-99A
2.10.2-6.....Revision UMST-99A
2.10.2-7.....Revision UMST-99A
2.10.2-8.....Revision UMST-99A
2.10.2-9.....Revision UMST-00A

List of Effective Pages (Continued)

2.10.2-10.....Revision UMST-00A
2.10.2-11.....Revision UMST-99A
2.10.2-12.....Revision UMST-99A
2.10.2-13.....Revision UMST-00A
2.10.2-14.....Revision UMST-00A
2.10.2-15.....Revision UMST-00A
2.10.2-16.....Revision UMST-00A
2.10.2-17.....Revision UMST-00A
2.10.3-1.....Revision UMST-01B
2.10.3-2.....Revision UMST-01B
2.10.3-3.....Revision UMST-01B
2.10.3-4.....Revision UMST-01B
2.10.3-5.....Revision UMST-01B
2.10.3-6.....Revision UMST-01B
2.10.3-7.....Revision UMST-01B
2.10.3-8.....Revision UMST-01B
2.10.3-9.....Revision UMST-01B
2.10.3-10.....Revision UMST-01B
2.10.3-11.....Revision UMST-01B
2.10.3-12.....Revision UMST-01B
2.10.3-13.....Revision UMST-01B
2.10.3-14.....Revision UMST-01B
2.10.3-15.....Revision UMST-01B
2.10.3-16.....Revision UMST-01B
2.10.3-17.....Revision UMST-01B
2.10.3-18.....Revision UMST-01B
2.10.3-19.....Revision UMST-01B
2.10.3-20.....Revision UMST-01B
2.10.3-21.....Revision UMST-01B
2.10.3-22.....Revision UMST-01B
2.10.3-23.....Revision UMST-01B
2.10.3-24.....Revision UMST-01B
2.10.3-25.....Revision UMST-01B
2.10.3-26.....Revision UMST-01B
2.10.3-27.....Revision UMST-01B
2.10.3-28.....Revision UMST-01B
2.10.3-29.....Revision UMST-01B
2.10.3-30.....Revision UMST-01B
2.10.3-31.....Revision UMST-01B
2.10.3-32.....Revision UMST-01B
2.10.3-33.....Revision UMST-01B
2.10.3-34.....Revision UMST-01B
2.10.3-35.....Revision UMST-01B
2.10.3-36.....Revision UMST-01B
2.10.3-37.....Revision UMST-01B
2.10.3-38.....Revision UMST-01B
2.10.3-39.....Revision UMST-01B
2.10.3-40.....Revision UMST-01B
2.10.3-41.....Revision UMST-01B
2.10.3-42.....Revision UMST-01B
2.10.3-43.....Revision UMST-01B
2.10.4-1.....Revision UMST-99A
2.10.4-2.....Revision UMST-99A
2.10.4-3.....Revision UMST-00A
2.10.4-4.....Revision UMST-00A
2.10.4-5.....Revision UMST-00A
2.10.4-6.....Revision UMST-00A
2.10.4-7.....Revision UMST-99A
2.10.4-8.....Revision UMST-00A
2.10.4-9.....Revision UMST-99A
2.10.4-10.....Revision UMST-99A
2.10.4-11.....Revision UMST-00A
2.10.4-12.....Revision UMST-00A
2.10.4-13.....Revision UMST-00A
2.10.4-14.....Revision UMST-00A
2.10.4-15.....Revision UMST-00A

List of Effective Pages (Continued)

Model Drawings
9 drawings
Revised as shown in Section 2.10.3.6.2

2.11-1.....Revision UMST-99A
2.11.1-1.....Revision UMST-01C
2.11.1-2.....Revision UMST-01C
2.11.1-3.....Revision UMST-01C
2.11.1-4.....Revision UMST-01C
2.11.1-5.....Revision UMST-01C
2.11.1-6.....Revision UMST-01C
2.11.1-7.....Revision UMST-01C
2.11.1-8.....Revision UMST-01C
2.11.1-9.....Revision UMST-01C
2.11.1-10.....Revision UMST-01B
2.11.1-11.....Revision UMST-01B
2.11.1-12.....Revision UMST-01B
2.11.1-13.....Revision UMST-01B
2.11.1-14.....Revision UMST-01C
2.11.1-15.....Revision UMST-01C
2.11.1-16.....Revision UMST-01C
2.11.1-17.....Revision UMST-01C
2.11.1-18.....Revision UMST-01C
2.11.1-19.....Revision UMST-01C
2.11.1-20.....Revision UMST-01C
2.11.1-21.....Revision UMST-01C
2.11.1-22.....Revision UMST-01C
2.11.1-23.....Revision UMST-01C
2.11.1-24.....Revision UMST-01C
2.11.1-25.....Revision UMST-01C
2.11.2-1.....Revision UMST-00A
2.11.2-2.....Revision UMST-00A
2.11.2-3.....Revision UMST-00A
2.11.2-4.....Revision UMST-99A
2.11.2-5.....Revision UMST-99A
2.11.2-6.....Revision UMST-99A
2.11.2-7.....Revision UMST-00A
2.11.2-8.....Revision UMST-99A
2.11.2-9.....Revision UMST-99A
2.11.2-10.....Revision UMST-99A
2.11.2-11.....Revision UMST-99A
2.11.2-12.....Revision UMST-99A
2.11.2-13.....Revision UMST-99A
2.11.2-14.....Revision UMST-99A
2.11.2-15.....Revision UMST-00A
2.11.2-16.....Revision UMST-99A
2.11.2-17.....Revision UMST-99A
2.11.2-18.....Revision UMST-99A
2.11.2-19.....Revision UMST-99A
2.11.2-20.....Revision UMST-99A
2.11.2-21.....Revision UMST-99A
2.11.2-22.....Revision UMST-00A
2.11.2-23.....Revision UMST-00A
2.11.2-24.....Revision UMST-00A
2.11.2-25.....Revision UMST-00A
2.11.2-26.....Revision UMST-00A
2.11.2-27.....Revision UMST-00A
2.11.2-28.....Revision UMST-00A
2.12-1.....Revision UMST-99A
2.12-2.....Revision UMST-99A
2.12-3.....Revision UMST-99A
2.12-4.....Revision UMST-01B
2.12-5.....Revision UMST-01C
2.12-6.....Revision UMST-01C

List of Effective Pages (Continued)

Chapter 3

3-i .....Revision UMST-00A
3-ii .....Revision UMST-01A
3-iii .....Revision UMST-00A
3-iv .....Revision UMST-00A
3-v.....Revision UMST-01A
3-vi .....Revision UMST-01A
3-vii .....Revision UMST-00A
3-viii .....Revision UMST-01A
3.1-1.....Revision UMST-00A
3.1-2.....Revision UMST-00A
3.1-3.....Revision UMST-00A
3.1-4.....Revision 0
3.1-5.....Revision 0
3.1-6.....Revision 0
3.2-1.....Revision 0
3.2-2.....Revision 0
3.2-3.....Revision 0
3.2-4.....Revision 0
3.2-5.....Revision 0
3.2-6.....Revision 0
3.2-7.....Revision UMST-00A
3.2-8.....Revision 0
3.2-9.....Revision UMST-00A
3.2-10.....Revision UMST-00A
3.2-11.....Revision 0
3.2-12.....Revision 0
3.2-13.....Revision 0
3.2-14.....Revision 0
3.2-15.....Revision 0
3.2-16.....Revision 0
3.2-17.....Revision 0
3.2-18.....Revision UMST-00A
3.2-19.....Revision 0
3.3-1.....Revision UMST-00A
3.3-2.....Revision UMST-00A
3.3-3.....Revision UMST-00A
3.4-1.....Revision UMST-00A
3.4-2.....Revision 0
3.4-3.....Revision 0
3.4-4.....Revision 0
3.4-5.....Revision UMST-00A
3.4-6.....Revision UMST-00A
3.4-7.....Revision UMST-00A
3.4-8.....Revision UMST-00A
3.4-9.....Revision UMST-00A
3.4-10.....Revision 0
3.4-11.....Revision 0
3.4-12.....Revision 0
3.4-13.....Revision UMST-00A
3.4-14.....Revision 0
3.4-15.....Revision UMST-00A
3.4-16.....Revision 0
3.4-17.....Revision 0
3.4-18.....Revision 0
3.4-19.....Revision UMST-00A
3.4-20.....Revision UMST-00A
3.4-21.....Revision UMST-00A
3.4-22.....Revision 0
3.4-23.....Revision UMST-99A
3.4-24.....Revision 0
3.4-25.....Revision UMST-00A
3.4-26.....Revision UMST-99A
3.4-27.....Revision UMST-00A
3.4-28.....Revision UMST-00A

List of Effective Pages (Continued)

3.4-29.....Revision UMST-00A
3.4-30.....Revision UMST-99A
3.4-31.....Revision UMST-99A
3.4-32.....Revision UMST-00A
3.4-33.....Revision UMST-00A
3.4-34.....Revision UMST-99A
3.4-35.....Revision 0
3.4-36.....Revision UMST-00A
3.4-37.....Revision UMST-00A
3.4-38.....Revision UMST-00A
3.4-39.....Revision UMST-00A
3.4-40.....Revision UMST-99A
3.4-41.....Revision UMST-99A
3.4-42.....Revision UMST-99A
3.4-43.....Revision UMST-00A
3.4-44.....Revision UMST-00A
3.4-45.....Revision UMST-00A
3.4-46.....Revision UMST-00A
3.4-47.....Revision UMST-00A
3.4-48.....Revision UMST-00A
3.4-49.....Revision UMST-00A
3.4-50.....Revision UMST-00A
3.4-51.....Revision UMST-00A
3.4-52.....Revision UMST-00A
3.4-53.....Revision UMST-00A
3.4-54.....Revision UMST-00A
3.4-55.....Revision UMST-00A
3.4-56.....Revision UMST-00A
3.4-57.....Revision UMST-00A
3.4-58.....Revision UMST-00A
3.4-59.....Revision UMST-00A
3.4-60.....Revision UMST-00A
3.4-61.....Revision UMST-00A
3.4-62.....Revision UMST-00A
3.4-63.....Revision UMST-00A
3.4-64.....Revision UMST-00A
3.4-65.....Revision UMST-00A
3.4-66.....Revision UMST-00A
3.4-67.....Revision UMST-00A
3.4-68.....Revision UMST-00A
3.4-69.....Revision UMST-00A
3.4-70.....Revision UMST-00A
3.5-1.....Revision UMST-00A
3.5-2.....Revision UMST-00A
3.5-3.....Revision 0
3.5-4.....Revision 0
3.5-5.....Revision 0
3.5-6.....Revision UMST-99A
3.5-7.....Revision UMST-00A
3.5-8.....Revision UMST-00A
3.5-9.....Revision 0
3.5-10.....Revision 0
3.5-11.....Revision 0
3.5-12.....Revision 0
3.5-13.....Revision 0
3.5-14.....Revision 0
3.5-15.....Revision 0
3.5-16.....Revision 0
3.5-17.....Revision 0
3.5-18.....Revision 0
3.5-19.....Revision 0
3.5-20.....Revision 0
3.5-21.....Revision 0
3.5-22.....Revision 0
3.5-23.....Revision 0
3.5-24.....Revision 0

List of Effective Pages (Continued)

3.5-25.....Revision 0
3.5-26.....Revision 0
3.5-27.....Revision 0
3.5-28.....Revision 0
3.5-29.....Revision UMST-00A
3.5-30.....Revision UMST-00A
3.5-31.....Revision UMST-99A
3.6-1.....Revision UMST-99A
3.6-2.....Revision UMST-01C
3.6-3.....Revision UMST-99A
3.6-4.....Revision UMST-00A
3.6-5.....Revision UMST-00A
3.6-6.....Revision UMST-00A
3.6-7.....Revision UMST-01A
3.6-8.....Revision UMST-01C
3.6-9.....Revision UMST-01A
3.6-10.....Revision UMST-01A
3.6-11.....Revision UMST-01A
3.6-12.....Revision UMST-01A
3.6-13.....Revision UMST-01A
3.6-14.....Revision UMST-01A
3.6-15.....Revision UMST-01A
3.6-16.....Revision UMST-01A
3.7-1.....Revision UMST-00A
3.7-2.....Revision UMST-00A
3.7-3.....Revision UMST-00A

Chapter 4

4-i .....Revision UMST-00A
4-ii .....Revision UMST-00A
4-iii .....Revision UMST-00A
4-iv .....Revision UMST-00A
4-1.....Revision UMST-00A
4-2.....Revision UMST-00A
4.1-1.....Revision UMST-00A
4.1-2.....Revision UMST-00A
4.1-3.....Revision UMST-00A
4.1-4.....Revision UMST-00A
4.1-5.....Revision UMST-00A
4.2-1.....Revision UMST-00A
4.2-2.....Revision UMST-00A
4.2-3.....Revision 0
4.2-4.....Revision UMST-00A
4.2-5.....Revision UMST-00A
4.2-6.....Revision UMST-00A
4.2-7.....Revision UMST-00A
4.2-8.....Revision UMST-00A
4.2-9.....Revision UMST-00A
4.2-10.....Revision UMST-00A
4.2-11.....Revision UMST-00A
4.3-1.....Revision UMST-00A
4.3-2.....Revision UMST-00A
4.3-3.....Revision UMST-00A
4.3-4.....Revision UMST-00A
4.3-5.....Revision UMST-00A
4.4-1.....Revision 0
4.5-1.....Revision UMST-00A
4.5.1-1.....Revision UMST-99A
4.5.2-1.....Revision UMST-99A
4.5.2-2.....Revision UMST-99A
4.5.2-3.....Revision UMST-99A
4.5.2-4.....Revision UMST-99A
4.5.2-5.....Revision UMST-99A
4.5.2-6.....Revision UMST-99A
4.5.2-7.....Revision UMST-99A

List of Effective Pages (Continued)

4.5.2-8.....Revision UMST-99A
4.5.2-9.....Revision UMST-99A
4.5.2-10.....Revision UMST-99A
4.5.2-11.....Revision UMST-99A
4.5.3-1.....Revision UMST-00A
4.5.3-2.....Revision UMST-00A
4.5.3-3.....Revision UMST-00A
4.5.3-4.....Revision UMST-00A
4.5.3-5.....Revision UMST-00A
4.5.3-6.....Revision UMST-00B
4.5.3-7.....Revision UMST-00B
4.5.3-8.....Revision UMST-00B
4.5.3-9.....Revision UMST-00B
4.5.3-10.....Revision UMST-00A
4.5.3-11.....Revision UMST-00A
4.5.3-12.....Revision UMST-00A
4.5.3-13.....Revision UMST-00A
4.6-1.....Revision UMST-00A

Chapter 5

5-i .....Revision UMST-99A
5-ii .....Revision UMST-01C
5-iii .....Revision UMST-01C
5-iv .....Revision UMST-01C
5-v.....Revision UMST-01C
5-vi .....Revision UMST-97A
5-vii .....Revision UMST-00A
5-viii .....Revision UMST-01C
5-ix .....Revision UMST-01C
5-x .....Revision UMST-01C
5-1.....Revision UMST-01C
5-2.....Revision UMST-99A
5.1-1.....Revision 0
5.1-2.....Revision 0
5.1-3.....Revision UMST-97A
5.1-4.....Revision UMST-01C
5.1-5.....Revision UMST-01C
5.1-6.....Revision UMST-00A
5.1-7.....Revision UMST-01C
5.1-8.....Revision UMST-01C
5.1-9.....Revision UMST-01C
5.1-10.....Revision UMST-01C
5.2-1.....Revision UMST-97A
5.2-2.....Revision UMST-97A
5.2-3.....Revision UMST-97A
5.2-4.....Revision 0
5.2-5.....Revision 0
5.2-6.....Revision UMST-97A
5.2-7.....Revision 0
5.2-8.....Revision UMST-97A
5.2-9.....Revision UMST-97A
5.2-10.....Revision 0
5.2-11.....Revision 0
5.2-12.....Revision UMST-97A
5.2-13.....Revision UMST-97A
5.2-14.....Revision 0
5.2-15.....Revision 0
5.2-16.....Revision UMST-01A
5.2-17.....Revision UMST-01A
5.2-18.....Revision 0
5.2-19.....Revision 0
5.2-20.....Revision 0
5.2-21.....Revision 0
5.2-22.....Revision 0
5.2-23.....Revision 0

List of Effective Pages (Continued)

5.2-24.....Revision UMST-97A
5.2-25.....Revision UMST-97A
5.2-26.....Revision 0
5.3-1.....Revision UMST-00A
5.3-2.....Revision UMST-00A
5.3-3.....Revision 0
5.3-4.....Revision UMST-97A
5.3-5.....Revision UMST-97A
5.3-6.....Revision UMST-97A
5.3-7.....Revision UMST-97A
5.3-8.....Revision UMST-97A
5.3-9.....Revision UMST-97A
5.3-10.....Revision UMST-99A
5.3-11.....Revision 0
5.3-12.....Revision 0
5.3-13.....Revision 0
5.3-14.....Revision UMST-97A
5.3-15.....Revision 0
5.3-16.....Revision 0
5.3-17.....Revision UMST-97A
5.3-18.....Revision UMST-97A
5.3-19.....Revision UMST-97A
5.3-20.....Revision UMST-97A
5.3-21.....Revision UMST-00A
5.3-22.....Revision UMST-00A
5.3-23.....Revision 0
5.3-24.....Revision UMST-00A
5.3-25.....Revision UMST-00A
5.3-26.....Revision 0
5.3-27.....Revision UMST-99A
5.3-28.....Revision UMST-97A
5.3-29.....Revision UMST-97A
5.3-30.....Revision UMST-97A
5.3-31.....Revision UMST-97A
5.3-32.....Revision UMST-97A
5.3-33.....Revision UMST-97A
5.3-34.....Revision UMST-97A
5.3-35.....Revision 0
5.4-1.....Revision 0
5.4-2.....Revision UMST-00A
5.4-3.....Revision UMST-00A
5.4-4.....Revision UMST-00A
5.4-5.....Revision UMST-00A
5.4-6.....Revision UMST-00A
5.4-7.....Revision UMST-00A
5.4-8.....Revision UMST-00A
5.4-9.....Revision UMST-00A
5.4-10.....Revision UMST-00A
5.4-11.....Revision UMST-00A
5.4-12.....Revision UMST-00A
5.4-13.....Revision UMST-00A
5.4-14.....Revision UMST-00A
5.4-15.....Revision UMST-00A
5.4-16.....Revision UMST-00A
5.4-17.....Revision UMST-00A
5.4-18.....Revision UMST-00A
5.4-19.....Revision UMST-00A
5.4-20.....Revision UMST-00A
5.4-21.....Revision UMST-00A
5.4-22.....Revision UMST-00A
5.4-23.....Revision UMST-00A
5.4-24.....Revision UMST-00A
5.4-25.....Revision UMST-00A
5.4-26.....Revision UMST-00A
5.5-1.....Revision UMST-00A
5.5.1-1.....Revision UMST-01C

List of Effective Pages (Continued)

5.5.1-2.....Revision UMST-00A
5.5.1-3.....Revision UMST-00A
5.5.1-4.....Revision UMST-00A
5.5.1-5.....Revision UMST-00A
5.5.1-6.....Revision UMST-00A
5.5.1-7.....Revision UMST-00A
5.5.1-8.....Revision UMST-00A
5.5.1-9.....Revision UMST-00A
5.5.1-10.....Revision UMST-00A
5.5.1-11.....Revision UMST-00A
5.5.1-12.....Revision UMST-01C
5.5.1-13.....Revision UMST-01C
5.5.1-14.....Revision UMST-01C
5.5.1-15.....Revision UMST-01C
5.5.1-16.....Revision UMST-01C
5.5.1-17.....Revision UMST-01C
5.5.1-18.....Revision UMST-01C
5.5.1-19.....Revision UMST-01C
5.5.1-20.....Revision UMST-01C
5.5.1-21.....Revision UMST-01C
5.5.1-22.....Revision UMST-01C
5.5.1-23.....Revision UMST-01C
5.5.1-24.....Revision UMST-01C
5.5.1-25.....Revision UMST-01C
5.5.1-26.....Revision UMST-01C
5.5.1-27.....Revision UMST-01C
5.5.1-28.....Revision UMST-01C
5.5.1-29.....Revision UMST-01C
5.5.1-30.....Revision UMST-01C
5.5.1-31.....Revision UMST-01C
5.5.1-32.....Revision UMST-01C
5.5.1-33.....Revision UMST-01C
5.5.1-34.....Revision UMST-01C
5.5.1-35.....Revision UMST-01C
5.5.1-36.....Revision UMST-01C
5.5.1-37.....Revision UMST-01C
5.5.1-38.....Revision UMST-01C
5.5.1-39.....Revision UMST-01C
5.5.1-40.....Revision UMST-01C
5.5.1-41.....Revision UMST-01C
5.5.1-42.....Revision UMST-01C
5.5.2-1.....Revision UMST-99A
5.5.2-2.....Revision UMST-99A
5.5.2-3.....Revision UMST-99A
5.5.3-1.....Revision UMST-00A
5.5.3-2.....Revision UMST-00A
5.5.3-3.....Revision UMST-00A
5.5.3-4.....Revision UMST-00A
5.5.3-5.....Revision UMST-00A
5.5.3-6.....Revision UMST-00A
5.5.3-7.....Revision UMST-00A
5.5.3-8.....Revision UMST-00A
5.5.3-9.....Revision UMST-00A
5.5.3-10.....Revision UMST-00A
5.5.3-11.....Revision UMST-00A
5.5.3-12.....Revision UMST-00A
5.5.3-13.....Revision UMST-00A
5.5.3-14.....Revision UMST-00A
5.5.3-15.....Revision UMST-00A
5.5.3-16.....Revision UMST-00A
5.5.3-17.....Revision UMST-00A
5.5.3-18.....Revision UMST-00A
5.5.3-19.....Revision UMST-00A
5.5.3-20.....Revision UMST-00A
5.5.3-21.....Revision UMST-00A
5.5.3-22.....Revision UMST-00A

List of Effective Pages (Continued)

5.5.3-23.....Revision UMST-00A
5.5.3-24.....Revision UMST-00A
5.5.3-25.....Revision UMST-00A
5.5.3-26.....Revision UMST-00A
5.5.3-27.....Revision UMST-00A
5.5.3-28.....Revision UMST-00A
5.5.3-29.....Revision UMST-00A
5.5.3-30.....Revision UMST-00A
5.5.3-31.....Revision UMST-00A
5.5.3-32.....Revision UMST-00A
5.5.3-33.....Revision UMST-00A
5.5.3-34.....Revision UMST-00A
5.5.3-35.....Revision UMST-00A
5.5.3-36.....Revision UMST-00A
5.5.3-37.....Revision UMST-00A
5.5.3-38.....Revision UMST-00A
5.5.3-39.....Revision UMST-00A
5.5.3-40.....Revision UMST-00A
5.5.3-41.....Revision UMST-00A
5.5.3-42.....Revision UMST-00A
5.5.3-43.....Revision UMST-00A
5.5.3-44.....Revision UMST-00A
5.5.3-45.....Revision UMST-00A
5.5.3-46.....Revision UMST-00A
5.5.3-47.....Revision UMST-00A
5.5.3-48.....Revision UMST-00A
5.5.3-49.....Revision UMST-00A
5.5.3-50.....Revision UMST-00A
5.6-1.....Revision UMST-99A
5.6-2.....Revision UMST-99A

Chapter 6

6-i .....Revision UMST-00A
6-ii .....Revision UMST-00A
6-iii .....Revision UMST-00A
6-iv .....Revision UMST-01C
6-v.....Revision UMST-01C
6-vi .....Revision UMST-00A
6-vii .....Revision UMST-01C
6-viii .....Revision UMST-01C
6.1-1.....Revision UMST-00A
6.1-2.....Revision UMST-00A
6.1-3.....Revision UMST-00A
6.2-1.....Revision UMST-00A
6.2-2.....Revision UMST-01C
6.2-3.....Revision UMST-99A
6.2-4.....Revision UMST-00A
6.3-1.....Revision UMST-00A
6.3-2.....Revision UMST-00A
6.3-3.....Revision UMST-00A
6.3-4.....Revision UMST-00A
6.3-5.....Revision UMST-00A
6.3-6.....Revision UMST-00A
6.3-7.....Revision UMST-99A
6.3-8.....Revision 0
6.3-9.....Revision 0
6.3-10.....Revision 0
6.3-11.....Revision 0
6.3-12.....Revision 0
6.3-13.....Revision 0
6.3-14.....Revision 0
6.4-1.....Revision 0
6.4-2.....Revision 0

List of Effective Pages (Continued)

6.4-3.....Revision 0
6.4-4.....Revision 0
6.4-5.....Revision 0
6.4-6.....Revision 0
6.4-7.....Revision UMST-99A
6.4-8.....Revision UMST-99A
6.4-9.....Revision UMST-99A
6.4-10.....Revision UMST-99A
6.4-11.....Revision UMST-99A
6.4-12.....Revision UMST-99A
6.4-13.....Revision UMST-01A
6.4-14.....Revision UMST-00A
6.4-15.....Revision UMST-00A
6.4-16.....Revision UMST-99A
6.4-17.....Revision UMST-99A
6.4-18.....Revision UMST-00A
6.4-19.....Revision UMST-01A
6.4-20.....Revision UMST-00A
6.4-21.....Revision UMST-00A
6.4-22.....Revision UMST-00A
6.4-23.....Revision UMST-00A
6.4-24.....Revision UMST-01C
6.4-25.....Revision UMST-00A
6.4-26.....Revision UMST-00A
6.4-27.....Revision UMST-00A
6.4-28.....Revision UMST-00A
6.4-29.....Revision UMST-00A
6.4-30.....Revision UMST-00A
6.4-31.....Revision UMST-00A
6.4-32.....Revision UMST-00A
6.4-33.....Revision UMST-00A
6.4-34.....Revision UMST-00A
6.5-1.....Revision 0
6.5-2.....Revision 0
6.5-3.....Revision 0
6.5-4.....Revision 0
6.5-5.....Revision 0
6.5-6.....Revision UMST-99A
6.5-7.....Revision UMST-99A
6.5-8.....Revision UMST-99A
6.5-9.....Revision UMST-00A
6.5-10.....Revision UMST-01C
6.5-11.....Revision UMST-00A
6.5-12.....Revision UMST-00A
6.5-13.....Revision UMST-00A
6.5-14.....Revision UMST-00A
6.5-15.....Revision UMST-00A
6.5-16.....Revision UMST-00A
6.5-17.....Revision UMST-00A
6.5-18.....Revision UMST-00A
6.5-19.....Revision UMST-00A
6.5-20.....Revision UMST-00A
6.5-21.....Revision UMST-00A
6.5-22.....Revision UMST-00A
6.5-23.....Revision UMST-00A
6.5-24.....Revision UMST-00A
6.5-25.....Revision UMST-00A
6.5-26.....Revision UMST-00A
6.5-27.....Revision UMST-00A
6.5-28.....Revision UMST-00A
6.5-29.....Revision UMST-00A
6.5-30.....Revision UMST-00A
6.5-31.....Revision UMST-00A
6.5-32.....Revision UMST-00A
6.5-33.....Revision UMST-01C
6.5-34.....Revision UMST-01C

List of Effective Pages (Continued)

6.5-35.....Revision UMST-00A
6.5-36.....Revision UMST-00A
6.5-37.....Revision UMST-00A
6.5-38.....Revision UMST-00A
6.5-39.....Revision UMST-00A
6.5-40.....Revision UMST-00A
6.5-41.....Revision UMST-00A
6.5-42.....Revision UMST-00A
6.5-43.....Revision UMST-00A
6.5-44.....Revision UMST-00A
6.6-1.....Revision UMST-00A
6.6.1-1.....Revision UMST-01C
6.6.1-2.....Revision UMST-00A
6.6.1-3.....Revision UMST-00A
6.6.1-4.....Revision UMST-01C
6.6.1-5.....Revision UMST-01C
6.6.1-6.....Revision UMST-01C
6.6.1-7.....Revision UMST-01C
6.6.1-8.....Revision UMST-01C
6.6.1-9.....Revision UMST-01C
6.6.1-10.....Revision UMST-01C
6.6.1-11.....Revision UMST-01C
6.6.1-12.....Revision UMST-01C
6.6.1-13.....Revision UMST-01C
6.6.1-14.....Revision UMST-01C
6.6.1-15.....Revision UMST-01C
6.6.1-16.....Revision UMST-01C
6.6.1-17.....Revision UMST-01C
6.6.1-18.....Revision UMST-01C
6.6.1-19.....Revision UMST-01C
6.6.1-20.....Revision UMST-01C
6.6.1-21.....Revision UMST-01C
6.6.1-22.....Revision UMST-01C
6.6.1-23.....Revision UMST-01C
6.6.2-1.....Revision UMST-00A
6.6.2-2.....Revision UMST-99A
6.6.2-3.....Revision UMST-00A
6.6.2-4.....Revision UMST-00A
6.6.2-5.....Revision UMST-00A
6.6.2-6.....Revision UMST-00A
6.6.2-7.....Revision UMST-00A
6.6.2-8.....Revision UMST-00A
6.6.2-9.....Revision UMST-00A
6.6.2-10.....Revision UMST-00A
6.6.2-11.....Revision UMST-00A
6.6.2-12.....Revision UMST-00A
6.6.2-13.....Revision UMST-00A
6.6.2-14.....Revision UMST-00A
6.6.2-15.....Revision UMST-00A
6.6.2-16.....Revision UMST-00A
6.6.2-17.....Revision UMST-00A
6.6.2-18.....Revision UMST-00A
6.6.2-19.....Revision UMST-00A
6.6.2-20.....Revision UMST-00A
6.6.2-21.....Revision UMST-00A
6.6.2-22.....Revision UMST-00A
6.6.2-23.....Revision UMST-00A
6.6.2-24.....Revision UMST-00A
6.6.2-25.....Revision UMST-00A
6.6.2-26.....Revision UMST-00A
6.6.2-27.....Revision UMST-00A
6.6.2-28.....Revision UMST-00A
6.6.2-29.....Revision UMST-00A
6.6.2-30.....Revision UMST-00A
6.6.2-31.....Revision UMST-00A
6.6.2-32.....Revision UMST-00A

List of Effective Pages (Continued)

6.6.2-33.....Revision UMST-00A
6.6.2-34.....Revision UMST-00A
6.6.2-35.....Revision UMST-00A
6.6.2-36.....Revision UMST-00A
6.6.2-37.....Revision UMST-00A
6.6.2-38.....Revision UMST-00A
6.6.2-39.....Revision UMST-00A
6.6.2-40.....Revision UMST-00A
6.6.2-41.....Revision UMST-00A
6.6.2-42.....Revision UMST-00A
6.6.2-43.....Revision UMST-00A
6.6.2-44.....Revision UMST-00A
6.6.2-45.....Revision UMST-00A
6.6.2-46.....Revision UMST-00A
6.6.2-47.....Revision UMST-00A
6.6.2-48.....Revision UMST-00A
6.6.2-49.....Revision UMST-00A
6.6.2-50.....Revision UMST-00A
6.6.2-51.....Revision UMST-00A
6.6.2-52.....Revision UMST-00A
6.6.2-53.....Revision UMST-00A
6.6.2-54.....Revision UMST-00A
6.6.2-55.....Revision UMST-00A
6.6.2-56.....Revision UMST-00A
6.6.2-57.....Revision UMST-00A
6.6.2-58.....Revision UMST-00A
6.6.2-59.....Revision UMST-00A
6.6.2-60.....Revision UMST-00A
6.6.2-61.....Revision UMST-00A
6.6.2-62.....Revision UMST-00A
6.6.2-63.....Revision UMST-00A
6.6.2-64.....Revision UMST-00A
6.6.2-65.....Revision UMST-00A
6.6.2-66.....Revision UMST-00A
6.6.2-67.....Revision UMST-00A
6.6.2-68.....Revision UMST-00A
6.6.2-69.....Revision UMST-00A
6.6.2-70.....Revision UMST-00A
6.6.2-71.....Revision UMST-00A
6.6.2-72.....Revision UMST-00A
6.6.2-73.....Revision UMST-00A
6.6.2-74.....Revision UMST-00A
6.6.2-75.....Revision UMST-00A
6.6.2-76.....Revision UMST-00A
6.6.2-77.....Revision UMST-00A
6.6.2-78.....Revision UMST-00A
6.6.2-79.....Revision UMST-00A
6.6.2-80.....Revision UMST-00A
6.6.2-81.....Revision UMST-00A
6.6.2-82.....Revision UMST-00A
6.6.2-83.....Revision UMST-00A
6.6.2-84.....Revision UMST-00A
6.6.2-85.....Revision UMST-00A
6.6.2-86.....Revision UMST-00A
6.6.2-87.....Revision UMST-00A
6.6.2-88.....Revision UMST-00A
6.6.2-89.....Revision UMST-00A
6.6.2-90.....Revision UMST-00A
6.6.2-91.....Revision UMST-00A
6.6.2-92.....Revision UMST-00A
6.6.2-93.....Revision UMST-00A
6.6.2-94.....Revision UMST-00A
6.6.3-1.....Revision UMST-00A
6.6.3-2.....Revision UMST-00A
6.6.3-3.....Revision UMST-00A
6.6.3-4.....Revision UMST-00A

List of Effective Pages (Continued)

6.6.3-5.....Revision UMST-00A
6.6.3-6.....Revision UMST-00A
6.6.3-7.....Revision UMST-00A
6.6.3-8.....Revision UMST-00A
6.6.3-9.....Revision UMST-00A
6.6.3-10.....Revision UMST-00A
6.6.3-11.....Revision UMST-00A
6.6.3-12.....Revision UMST-00A
6.6.3-13.....Revision UMST-00A
6.6.3-14.....Revision UMST-00A
6.6.3-15.....Revision UMST-00A
6.6.3-16.....Revision UMST-00A
6.6.3-17.....Revision UMST-00A
6.6.3-18.....Revision UMST-00A
6.6.3-19.....Revision UMST-00A
6.6.3-20.....Revision UMST-00A
6.6.3-21.....Revision UMST-00A
6.6.3-22.....Revision UMST-00A
6.6.3-23.....Revision UMST-00A
6.6.3-24.....Revision UMST-00A
6.6.3-25.....Revision UMST-00A
6.6.3-26.....Revision UMST-00A
6.6.3-27.....Revision UMST-00A
6.6.3-28.....Revision UMST-00A
6.6.3-29.....Revision UMST-00A
6.6.3-30.....Revision UMST-00A
6.6.3-31.....Revision UMST-00A
6.6.3-32.....Revision UMST-00A
6.6.3-33.....Revision UMST-00A
6.6.3-34.....Revision UMST-00A
6.7-1.....Revision UMST-99A
6.7-2.....Revision UMST-00A

Chapter 7

7-i .....Revision UMST-00A
7-ii .....Revision UMST-00A
7-1.....Revision UMST-00A
7-2.....Revision UMST-00A
7-3.....Revision UMST-00A
7.1-1.....Revision UMST-00A
7.1-2.....Revision UMST-00A
7.1-3.....Revision UMST-00A
7.1-4.....Revision UMST-00A
7.1-5.....Revision UMST-00A
7.1-6.....Revision UMST-00A
7.1-7.....Revision UMST-00A
7.2-1.....Revision UMST-00A
7.2-2.....Revision UMST-00A
7.3-1.....Revision UMST-00A
7.3-2.....Revision UMST-00A
7.3-3.....Revision UMST-00A
7.3-4.....Revision UMST-00A
7.4-1.....Revision UMST-00A
7.5-1.....Revision UMST-00A
7.5-2.....Revision UMST-00A
7.5-3.....Revision UMST-00A
7.5-4.....Revision UMST-00A
7.5-5.....Revision UMST-00A
7.5-6.....Revision UMST-01C
7.5-7.....Revision UMST-00A
7.5-8.....Revision UMST-00A
7.5-9.....Revision UMST-00A
7.5-10.....Revision UMST-00A
7.5-11.....Revision UMST-00A
7.5-12.....Revision UMST-00A

List of Effective Pages (Continued)

7.6-1.....Revision UMST-99A

Chapter 8

8-i .....Revision UMST-00A
8-ii .....Revision UMST-00A
8-iii .....Revision UMST-00A
8-1.....Revision UMST-00A
8.1-1.....Revision UMST-00A
8.1-2.....Revision 0
8.1-3.....Revision UMST-00A
8.1-4.....Revision UMST-00A
8.1-5.....Revision UMST-00A
8.1-6.....Revision UMST-00A
8.1-7.....Revision UMST-00A
8.1-8.....Revision UMST-00A
8.1-9.....Revision UMST-00A
8.1-10.....Revision UMST-00A
8.1-11.....Revision UMST-00A
8.1-12.....Revision UMST-00A
8.1-13.....Revision UMST-00A
8.1-14.....Revision UMST-00A
8.1-15.....Revision UMST-00A
8.2-1.....Revision UMST-00A
8.2-2.....Revision UMST-00A
8.2-3.....Revision UMST-00A
8.2-4.....Revision UMST-00A
8.2-5.....Revision UMST-00A
8.3-1.....Revision UMST-00A
8.3-2.....Revision UMST-00A
8.3-3.....Revision 0
8.3-4.....Revision UMST-00A
8.3-5.....Revision 0
8.3-6.....Revision 0
8.3-7.....Revision 0
8.3-8.....Revision 0

THIS PAGE INTENTIONALLY LEFT BLANK

Master Table of Contents (Continued)

2.7.12 Cask Inner Shell Buckling Analysis 2.7-201
2.7.12.1 Analysis Methodology 2.7-201
2.7.12.2 Analysis Results 2.7-202
2.7.12.3 Detailed Code Case N-284-1 Buckling Evaluation 2.7-202

2.8 Special Form 2.8-1

2.9 Fuel Rod Buckling Evaluation 2.9-1
2.9.1 UMS® Design Basis Fuel Buckling Evaluation 2.9.1-1
2.9.1.1 Design Basis PWR Fuel Rod Mode Shapes and Buckling Evaluation 2.9.1-2
2.9.1.2 Design Basis BWR Fuel Rod Mode Shapes and Buckling Evaluation 2.9.1-3
2.9.2 Buckling Evaluation for Maine Yankee Site Specific Fuel 2.9.2-1
2.9.2.1 Buckling Evaluation for Maine Yankee High Burnup Fuel 2.9.2-1
2.9.2.2 Buckling Evaluation for Maine Yankee High Burnup Fuel with Mechanical Damage 2.9.2-4

2.10 Appendices 2.10-1
2.10.1 Computer Program Descriptions 2.10.1-1
2.10.1.1 ANSYS 2.10.1-1
2.10.1.2 LS-DYNA 2.10.1-2
2.10.2 Finite Element Model - Universal Transport Cask 2.10.2-1
2.10.2.1 Load Application and Boundary Conditions 2.10.2-5
2.10.2.2 Post-Processing of Results 2.10.2-13
2.10.3 Confirmatory Testing Program – UMS® Impact Limiters and Attachments 2.10.3-1
2.10.3.1 Confirmatory Testing Program Results Summary 2.10.3-1
2.10.3.2 Acceptance Criteria for Model Performance 2.10.3-3

Master Table of Contents (Continued)

2.10.3.3 30-Foot Top End Drop and 30-Foot Top Corner Drop Tests Performed at ORNL 2.10.3-4
2.10.3.4 30-Foot Side Drop Test Performed at SNL 2.10.3-19
2.10.3.5 Evaluation of a 30-Foot Oblique Drop 2.10.3-26
2.10.3.6 Scale Model Drawings 2.10.3-26
2.10.3.7 LS-DYNA Analyses of the UMS® Quarter-Scale Model 2.10.3-27

2.10.4 Dynamic Load Factor (DLF) Evaluation for PWR and BWR Support Disks 2.10.4-1
2.10.4.1 1-Foot End Drop Analysis 2.10.4-1
2.10.4.2 Side Drop Analysis 2.10.4-7

2.11 Site Specific Contents Structural Evaluations 2.11-1
2.11.1 Site Specific Spent Fuel 2.11-1
2.11.1.1 Maine Yankee Site Specific Spent Fuel 2.11.1-1
2.11.2 Site Specific Greater Than Class C Waste 2.11.2-1
2.11.2.1 Maine Yankee Greater Than Class C Waste 2.11.2-1

2.12 References 2.12-1

3.0 THERMAL EVALUATION 3.1-1

3.1 Discussion 3.1-1

3.2 Summary of Thermal Properties of Materials 3.2-1
3.2.1 Conductive Properties 3.2-1
3.2.2 Radiative Properties 3.2-1
3.2.2.1 Governing Radiation Principle 3.2-1
3.2.2.2 Radiation from Cask Surface 3.2-2
3.2.2.3 Radiation Across Gaps Within the Cask 3.2-3
3.2.2.4 Radiation from the Top of the Canister 3.2-4
3.2.3 Convective Properties 3.2-4

Master Table of Contents (Continued)

5.5 Appendices 5.5-1
5.5.1 Site Specific Contents Shielding Evaluations 5.5.1-1
5.5.1.1 Maine Yankee Site Specific Spent Fuel 5.5.1-1
5.5.1.2 Maine Yankee Site Specific GTCC Waste 5.5.1-36
5.5.2 Dose Response Factors 5.5.2-1
5.5.3 Sample Input Files 5.5.3-1
5.5.3.1 SAS2H Input 5.5.3-1
5.5.3.2 Sample Shielding Model Files 5.5.3-4

5.6 References 5.6-1

6.0 CRITICALITY EVALUATION 6.1-1

6.1 Discussion and Results 6.1-1

6.2 Package Fuel Loading 6.2-1

6.3 Criticality Model Specification 6.3-1
6.3.1 Calculational Methodology 6.3-1
6.3.2 Basket Model Assumptions 6.3-2
6.3.3 Description of Calculational Models 6.3-4
6.3.4 Package Regional Densities 6.3-6
6.3.4.1 Fuel Region 6.3-6
6.3.4.2 Cask Material 6.3-7
6.3.4.3 Water Reflector Densities 6.3-8

6.4 Criticality Calculation 6.4-1
6.4.1 Calculation or Experimental Method 6.4-1
6.4.1.1 Determination of Fuel Arrays for Criticality Analysis 6.4-1
6.4.1.2 Most Reactive Fuel Assembly Determination 6.4-2
6.4.1.3 Universal Transport Cask Criticality Analysis 6.4-5

Master Table of Contents (Continued)

6.4.2 Fuel Loading Optimization 6.4-12
6.4.3 Criticality Results 6.4-13
6.4.3.1 Summary of Maximum Criticality Values 6.4-13
6.4.3.2 Criticality Results for PWR 6.4-14
6.4.3.3 Criticality Results for BWR 6.4-15
6.4.4 Fuel Assembly Lattice Dimension Variations 6.4-16
6.4.5 Evaluation of Transport Cask End Impact 6.4-18
6.4.6 Regulatory Compliance 6.4-20

6.5 Critical Benchmark Experiments 6.5-1
6.5.1 Benchmark Experiments and Applicability 6.5-3
6.5.1.1 Description of Experiments 6.5-3
6.5.1.2 Applicability of Experiments 6.5-3
6.5.2 Results of Benchmark Calculations 6.5-4
6.5.3 Trends 6.5-5
6.5.4 Comparison of NAC Method to NUREG/CR-6361 ..... 6.5-6
6.5.5 MONK Validation in Accordance with NUREG/CR-6361 ..... 6.5-10

6.6 Appendices 6.6-1
6.6.1 Criticality Evaluation for Site Specific Contents 6.6.1-1
6.6.1.1 Criticality Evaluation for Maine Yankee Site Specific Spent Fuel 6.6.1-1
6.6.2 CSAS Inputs and Outputs 6.6.2-1
6.6.3 MONK8a Input and Output Files 6.6.3-1

6.7 References 6.7-1

7.0 OPERATING PROCEDURES 7-1

7.1 Receiving Universal Transport Cask and Loading Transportable Storage Canister into Universal Transport Cask 7.1-1
7.1.1 Receiving Inspection 7.1-1
7.1.2 Preparing the Universal Transport Cask for Dry Loading 7.1-2

3.6 Thermal Evaluation for Site Specific Contents

3.6.1 Maine Yankee Site Specific Contents

The standard spent fuel assembly for the Maine Yankee site is the Combustion Engineering (CE) 14x14 fuel assembly. Fuel of the same design has also been supplied by Westinghouse and by Exxon. The standard 14x14 fuel assembly is included in the population of the design basis PWR fuel assemblies for the UMS Transport System (See Table 1.2.5). The maximum decay heat for the Maine Yankee fuel is limited to the design basis heat load for the PWR fuels (20 kW total, or 0.83 kW per assembly). This heat load is bounded by the thermal evaluations in Sections 3.4 and 3.5 for the normal conditions of transport and hypothetical accident conditions, respectively.

The Maine Yankee site specific fuels and GTCC waste are described in Sections 1.3.1.1.1 and 1.3.1.1.2, respectively.

The thermal evaluations of the Maine Yankee site specific fuels and the GTCC waste are provided in Sections 3.6.1.1 and 3.6.1.2, respectively.

3.6.1.1 Spent Fuel

The Maine Yankee site specific fuels included in this evaluation are:

1. Consolidated fuel rod lattices consisting of a 17x17 lattice fabricated with 17x17 grids, 4 stainless steel support rods and stainless steel end fittings. One of these lattices contains 283 fuel rods and 2 vacancies. The other contains 172 fuel rods, with the remaining locations either empty or containing stainless steel dummy rods.
2. Standard fuel assemblies with a Control Element Assembly (CEA) inserted in each one.
3. Standard fuel assemblies that have been repaired by removing damaged fuel rods and replacing them with stainless steel dummy rods, solid zirconium rods, or 1.95 wt % enriched fuel rods.
4. Standard fuel assemblies that have had the burnable poison rods removed and replaced with hollow Zircaloy tubes.

5. Standard fuel assemblies with in-core instrument thimble assemblies stored in the center guide tube.
6. Standard fuel assemblies that are designed with variable enrichment (radial) and axial blankets.
7. Standard fuel assemblies that have fuel rods removed.
8. Damaged fuel assemblies.
9. Fuel assemblies with inserted start-up sources and other non-fuel items.

The thermal evaluations of these site specific fuels are provided below. The maximum heat load per assembly is limited to the design basis heat load (0.83 kW) for all Maine Yankee site specific fuels listed in the foregoing.

1. Consolidated Fuel

There are two (2) consolidated fuel lattices (pseudo assemblies). The maximum decay heat of each consolidated fuel assembly is 0.279 kW. The heat load of the consolidated fuel lattice with 283 fuel rods is bounded by the design basis PWR fuel assembly, since its heat load is only one-third (0.279/0.83) of the design basis heat load.

The second consolidated fuel lattice has 172 fuel rods with 76 stainless steel dummy rods at the outer periphery of the lattice. Due to the presence of the stainless steel rods, the effective thermal conductivities of this assembly may be slightly lower than those of the standard CE 14x14 fuel assembly. While the stainless steel rods provide better conductance in the axial direction, the radiation heat transfer is less effective at the surface of stainless steel rods, as compared to the standard fuel rods. The radiation is a function of surface emissivity and the emissivity for stainless steel (0.36) is less than one-half of that for Zircaloy (0.75). A parametric study is performed to demonstrate that the thermal performance of the UMS® PWR basket loading configuration consisting of 23 standard CE 14x14 fuel assemblies and the consolidated fuel lattice with stainless rods is bounded by that of the configuration consisting of 24 standard CE 14x14 fuel assemblies. Two finite element models are used in the study: a two-dimensional fuel assembly model and a three-dimensional periodic canister internal model.

The two-dimensional model is used to determine the effective thermal conductivities of the consolidated fuel lattice with stainless steel rods. Considering the symmetry of the consolidated

8. Damaged Fuel Assemblies

Damaged fuel assemblies are standard fuel assemblies with fuel rods that have known or suspected cladding defects greater than hairline cracks or pinhole leaks. Each damaged fuel assembly will be placed in a Maine Yankee fuel can. The primary function of the fuel can is to confine fuel material within the can and to facilitate handling and retrievability. The Maine Yankee fuel can is shown in Drawings 412-501 and 412-502. The placement of the loaded fuel cans is restricted by operating procedures and/or Technical Specifications to loading into the four fuel tube positions at the periphery of the fuel basket as shown in Figure 3.6.1.1-4. The heat load for each damaged fuel assembly is limited to the design basis heat load of 0.833 kW (20 kW/24).

A steady-state thermal analysis is performed using the three-dimensional cask model described in Section 3.4.1.1.1 simulating 100% failure of the damaged fuel rods held in the Maine Yankee fuel can. The canister is assumed to contain twenty (20) design basis PWR fuel assemblies and damaged fuel assemblies in fuel cans in each of the four corner positions.

A debris compaction length of 104 inches is considered in the analysis based on the volume of fuel rods and a 50% compaction of the debris. Additionally, this 104-inch debris region is assumed to be located at the center of the active fuel region of the design basis PWR fuel assemblies, as shown in Figure 3.6.1.1-4. The entire heat load for a single fuel assembly (i.e., 0.833 kW) is considered to be concentrated in the debris region. The effective thermal conductivities for the design basis PWR fuel assembly (Section 3.4.1.1.2) are used for the debris region. This is conservative, since the debris (100% failed rods) is expected to have a higher density (better conduction) and more surface area (better radiation) than an intact fuel assembly. In addition, the thermal conductivity of helium is used for the remainder of the active fuel length. Boundary conditions corresponding to normal transport are used at the outer surface of the cask (see Section 3.4.1.1.1). The results of the steady-state thermal analysis for 100% fuel rod, fuel cladding and guide tube failure are:

Description	Maximum Temperature (°F)			
	Fuel Cladding	Damaged Fuel	Support Disk	Heat Transfer Disk
Configuration with damaged fuel loaded in four basket corner locations	682	633	618	614
Design basis PWR fuel	673	N/A	608	605
Allowable	716	N/A	650	700

As shown in the previous table, the maximum temperatures for the fuel cladding, damaged fuel assembly, support disks, and heat transfer disks for the configuration with damaged fuel loaded in four (4) basket corner locations are within the allowable temperature range. Additionally, the maximum temperature of the support disk remains bounded by that used in the structural analyses of the fuel basket (Table 3.4-1, Canister Gas: Air).

9. Fuel Assemblies with Inserted Start-up Sources and Other Non-Fuel Items

Five Control Element Assembly (CEA) fingertips and a 24-inch ICI segment may be placed into the guide tubes of a fuel assembly. In addition, four used start-up neutron sources and one unirradiated source will each be loaded into separate fuel assemblies. With the CEA fingertips and the neutron sources inserted into the guide tubes of the fuel assemblies, the effective conductivity in the axial direction of the fuel assembly is increased because solid material replaces helium in the guide tubes. The change in the effective conductivity in the transverse direction of the fuel assembly is negligible, since the non-fuel items are inside of the guide tubes. Note that the total heat load of the fuel assembly, including the small amount of extra heat generated by the CEA fingertips (0.4 watts) and the four irradiated neutron sources (15.4 watts, total), remains below the design basis heat load. Therefore, the thermal performance of the fuel assemblies with CEA fingertips and neutron sources inserted is bounded by that of the standard fuel assemblies.

Table of Contents

5.0 SHIELDING EVALUATION 5-1

5.1 Discussion and Results 5.1-1
5.1.1 Fuel Assembly Classification 5.1-2
5.1.1.1 PWR Fuel Assembly Classes 5.1-2
5.1.1.2 BWR Fuel Assembly Classes 5.1-3
5.1.2 Codes Employed 5.1-3
5.1.3 Results of Analysis 5.1-4
5.1.3.1 Normal Conditions of Transport 5.1-5
5.1.3.2 Hypothetical Accident Conditions 5.1-6

5.2 Source Specification 5.2-1
5.2.1 Gamma Source 5.2-1
5.2.2 Neutron Source 5.2-2
5.2.3 PWR Fuel Assembly Descriptions 5.2-2
5.2.4 BWR Fuel Assembly Descriptions 5.2-4
5.2.5 Design Basis Fuel Assemblies 5.2-5
5.2.6 Axial Source Profile 5.2-6
5.2.6.1 Axial Burnup Profile 5.2-6
5.2.6.2 Axial Source Profiles 5.2-6

5.3 Model Specification 5.3-1
5.3.1 One-Dimensional Models 5.3-1
5.3.1.1 One-Dimensional Radial Model 5.3-1
5.3.1.2 One-Dimensional Top Axial Model 5.3-2
5.3.1.3 One-Dimensional Bottom Axial Model 5.3-3
5.3.2 Three-Dimensional Shielding Models 5.3-3
5.3.2.1 Geometric Models 5.3-4
5.3.2.2 Biasing Models 5.3-6
5.3.2.3 Detector Descriptions 5.3-6
5.3.2.4 Accident Conditions 5.3-7
5.3.2.5 Neutron Shield Heat Transfer Fin Model 5.3-7
5.3.3 Material Compositions 5.3-8

Table of Contents (Continued)

5.4 Shielding Evaluation 5.4-1
5.4.1 Computer Code Description 5.4-1
5.4.2 Three-Dimensional Shielding Calculations 5.4-2
5.4.2.1 Normal Conditions of Transport 5.4-2
5.4.2.2 Bounding Analysis of Class 3 Canister 5.4-3
5.4.2.3 Accident Conditions 5.4-4

5.4.3 Loading Table Analysis 5.4-4
5.4.3.1 Methodology 5.4-5
5.4.3.2 Limiting Decay Heat and Dose Rate Values 5.4-7
5.4.3.3 Cool Time Determination 5.4-8
5.4.3.4 Results 5.4-9

5.5 Appendices 5.5-1
5.5.1 Site Specific Contents Shielding Evaluations 5.5.1-1
5.5.1.1 Maine Yankee Site Specific Spent Fuel 5.5.1-1
5.5.1.2 Maine Yankee Site Specific GTCC Waste 5.5.1-36
5.5.2 Dose Response Factors 5.5.2-1
5.5.3 Sample Input Files 5.5.3-1
5.5.3.1 SAS2H Input 5.5.3-1
5.5.3.2 Sample Shielding Model Files 5.5.3-4

5.6 References 5.6-1

List of Figures

Figure 5.1-1 Location of Maximum Dose Rates for Intact Fuel in Normal Conditions of Transport 5.1-7
Figure 5.1-2 Location of Maximum Dose Rates for Intact Fuel in Hypothetical Accident Conditions 5.1-8
Figure 5.2-1 Enveloping Axial Burnup Profile for PWR Design Basis Fuel 5.2-8
Figure 5.2-2 Enveloping Axial Burnup Profile for BWR Design Basis Fuel 5.2-8
Figure 5.2-3 PWR Photon and Neutron Axial Source Profiles 5.2-9
Figure 5.2-4 BWR Photon and Neutron Axial Source Profiles 5.2-9
Figure 5.3-1 Illustration of SAS4 Axial Surface Detector Partitioning 5.3-10
Figure 5.3-2 Illustration of SAS4 Radial Surface Detector Partitioning 5.3-10
Figure 5.3-3 One-Dimensional Radial Shielding Regions 5.3-11
Figure 5.3-4 Equivalent Homogenized Cylindrical Source: PWR (Dimensions in cm) 5.3-12
Figure 5.3-5 Equivalent Homogenized Cylindrical Source: BWR (Dimensions in cm) 5.3-13
Figure 5.3-6 Design Basis PWR (WE 17×17) Fuel Assembly Source Region Elevations 5.3-14
Figure 5.3-7 Design Basis BWR (GE 9×9-2) Fuel Assembly Source Region Elevations 5.3-15
Figure 5.3-8 One-Dimensional Top Axial Model: BW 15×15 Fuel Assembly (Dimensions in cm) 5.3-16
Figure 5.3-9 One-Dimensional Bottom Axial Model: BW 15×15 Fuel Assembly (Dimensions in cm) 5.3-16
Figure 5.3-10 Transport Cask Bottom Model – PWR Design Basis (Dimensions in cm) 5.3-17
Figure 5.3-11 Transport Cask Bottom Model – BWR Design Basis (Dimensions in cm) 5.3-18
Figure 5.3-12 Transport Cask Top Model – PWR Design Basis (Dimensions in cm) 5.3-19
Figure 5.3-13 Transport Cask Top Model – BWR Design Basis (Dimensions in cm) 5.3-20
Figure 5.3-14 PICTURE Representation of PWR Top Model – Normal Conditions – Showing Trunnion Recesses and Lid Vent 5.3-21
Figure 5.3-15 PICTURE Representation of PWR Bottom Model – Normal Conditions – Slice Through Lower Rotation Pockets 5.3-22
Figure 5.3-16 Radial Lead Slump Model (Dimensions in Inches) 5.3-23

List of Figures (Continued)

Figure 5.3-17 PICTURE Representation of PWR Top Model – Accident Conditions ... 5.3-24
Figure 5.3-18 PICTURE Representation of BWR Fuel Region and Heat Transfer Fin Models at Fuel Axial Midplane ... 5.3-25
Figure 5.4-1 PWR Total Dose Rate – Side – Normal Conditions ... 5.4-11
Figure 5.4-2 PWR Total Dose Rate – Top – Normal Conditions ... 5.4-11
Figure 5.4-3 PWR Total Dose Rate – Bottom – Normal Conditions ... 5.4-12
Figure 5.4-4 BWR Total Dose Rate – Side – Normal Conditions ... 5.4-12
Figure 5.4-5 BWR Total Dose Rate – Azimuthal Profile at Rotation Pocket Elevation – Normal Conditions ... 5.4-13
Figure 5.4-6 BWR Total Dose Rate – Top – Normal Conditions ... 5.4-13
Figure 5.4-7 BWR Total Dose Rate – Bottom – Normal Conditions ... 5.4-14
Figure 5.4-8 Effect of Heat Transfer Fins on Cask Surface Fuel Neutron and Gamma Dose Rates [mrem/hr] ... 5.4-14
Figure 5.4-9 PWR Canister with No Spacer Assembly - Side Total Dose Rate Profile (Lower Half) ... 5.4-15

Figure 5.5.1.1-1 SAS2H Model Input File – CE 14x14 ... 5.5.1-17

List of Tables

Table 5.1-1 PWR Maximum Total Dose Rate Summary for Intact Fuel – Normal Conditions 5.1-9
Table 5.1-2 PWR Maximum Total Dose Rate Summary for Intact Fuel – Accident Conditions 5.1-9
Table 5.1-3 BWR Maximum Total Dose Rate Summary for Intact Fuel – Normal Conditions 5.1-10
Table 5.1-4 BWR Maximum Total Dose Rate Summary for Intact Fuel – Accident Conditions 5.1-10

Table 5.2-1 Description of Fuel Assembly Types 5.2-10
Table 5.2-2 Representative PWR Fuel Assembly Physical Characteristics 5.2-11
Table 5.2-3 Representative PWR Fuel Assembly Hardware Data Per Assembly 5.2-12
Table 5.2-4 Nuclear and Thermal Parameters of PWR Fuel Assemblies with 3.7 wt % ^{235}U Enrichment, 45,000 MWD/MTU Burnup, 10 Years Cooling Time 5.2-13
Table 5.2-5 PWR Fuel Assembly Activated Hardware Comparison [γ/s], 10 Year Cooling Time 5.2-13
Table 5.2-6 Representative BWR Fuel Physical Characteristics 5.2-14
Table 5.2-7 Representative BWR Fuel Assembly Hardware Data 5.2-14
Table 5.2-8 Nuclear and Thermal Parameters of BWR Fuel with 3.25 wt % ^{235}U Enrichment, 40,000 MWD/MTU Burnup and 10 Years Cooling Time 5.2-15
Table 5.2-9 BWR Fuel Assembly Activated Hardware Comparison [γ/s] at 40,000 MWD/MTU Burnup, 10 Year Cooled 5.2-15
Table 5.2-10 One-Dimensional Dose Rate Results Relative to PWR Design Basis 5.2-16
Table 5.2-11 One-Dimensional Dose Rate Results Relative to BWR Design Basis 5.2-17
Table 5.2-12 Design Basis PWR 10 Year Fuel Neutron Source Spectrum 5.2-18

List of Tables (Continued)

Table 5.2-13 Design Basis PWR 10 Year Fuel Photon Spectrum 5.2-19
Table 5.2-14 Design Basis PWR 10 Year Hardware Photon Spectrum 5.2-20
Table 5.2-15 Design Basis BWR 10 Year Fuel Neutron Source Spectrum 5.2-21
Table 5.2-16 Design Basis BWR 10 Year Fuel Photon Spectrum 5.2-22
Table 5.2-17 Design Basis BWR 10 Year Hardware Photon Spectrum 5.2-23
Table 5.2-18 Source Rate Versus Burnup Fit Parameters 5.2-24
Table 5.2-19 Scale Factors Applied to Neutron Source Rate at Average Burnup 5.2-24
Table 5.2-20 PWR Axial Source Profile 5.2-25
Table 5.2-21 BWR Axial Source Rate Profile 5.2-26
Table 5.3-1 Radial Shield Regions Employed in One-Dimensional Model 5.3-26
Table 5.3-2 Universal Transport Cask One-Dimensional Model Axial Dimensions ... 5.3-27
Table 5.3-3 Source Region Summary for PWR Three-Dimensional Model 5.3-28
Table 5.3-4 Source Region Summary for BWR Three-Dimensional Model 5.3-28
Table 5.3-5 PWR Top Model Radial Detector Description – Normal Conditions 5.3-29
Table 5.3-6 PWR Top Model Axial Detector Description – Normal Conditions 5.3-29
Table 5.3-7 PWR Bottom Model Radial Detector Description – Normal Conditions . 5.3-30
Table 5.3-8 PWR Bottom Model Axial Detector Description – Normal Conditions ... 5.3-30
Table 5.3-9 PWR Top Model Radial Detector Description – Accident Conditions 5.3-31
Table 5.3-10 PWR Top Model Axial Detector Description – Accident Conditions 5.3-31
Table 5.3-11 PWR Bottom Model Radial Detector Description – Accident Conditions 5.3-31
Table 5.3-12 PWR Bottom Model Axial Detector Description – Accident Conditions 5.3-31
Table 5.3-13 Homogenized Fuel Region Isotopic Composition [atom/b-cm] 5.3-32
Table 5.3-14 Isotopic Compositions of PWR Fuel Assembly Non-Fuel Source Regions [atom/b-cm] 5.3-32
Table 5.3-15 Isotopic Compositions of BWR Fuel Assembly Non-Fuel Source Regions [atom/b-cm] 5.3-33
Table 5.3-16 Isotopic Compositions of PWR Canister Annular Region Materials (One-Dimensional Analysis Only) [atom/b-cm] 5.3-33
Table 5.3-17 Isotopic Compositions of BWR Canister Annular Region Materials (One-Dimensional Analysis Only) [atom/b-cm] 5.3-34

List of Tables (Continued)

Table 5.3-18 Isotopic Composition of Additional Shielding Materials [atom/b-cm] 5.3-34
Table 5.3-19 Isotopic Composition of Additional Shielding Materials [atom/b-cm] 5.3-35
Table 5.4-1 SAS4 Runs Performed for Each Source Region 5.4-16
Table 5.4-2 PWR Surface Average Dose Rates – Top Model – Radial Detectors – Normal Conditions 5.4-16
Table 5.4-3 PWR Surface Average Dose Rates – Top Model – Axial Detectors – Normal Conditions 5.4-17
Table 5.4-4 PWR Maximum Subdetector Dose Rates – Top Model – Radial Detectors – Normal Conditions 5.4-17
Table 5.4-5 PWR Maximum Subdetector Dose Rates – Bottom Model – Radial Detectors – Normal Conditions 5.4-17
Table 5.4-6 PWR Maximum Subdetector Dose Rates – Top Model – Axial Detectors – Normal Conditions 5.4-18
Table 5.4-7 PWR Maximum Subdetector Dose Rates – Bottom Model – Axial Detectors – Normal Conditions 5.4-18
Table 5.4-8 BWR Maximum Subdetector Dose Rates – Top Model – Radial Detectors – Normal Conditions 5.4-19
Table 5.4-9 BWR Maximum Subdetector Dose Rates – Top Model – Axial Detectors – Normal Conditions 5.4-19
Table 5.4-10 BWR Maximum Subdetector Dose Rates – Bottom Model – Radial Detectors – Normal Conditions 5.4-20
Table 5.4-11 BWR Maximum Subdetector Dose Rates – Bottom Model – Axial Detectors – Normal Conditions 5.4-20
Table 5.4-12 PWR Surface Average Dose Rates – Top Model – Radial Detectors – Accident Conditions 5.4-21
Table 5.4-13 PWR Maximum Subdetector Dose Rates – Top Model – Radial Detectors – Accident Conditions 5.4-21
Table 5.4-14 PWR Maximum Subdetector Dose Rates – Bottom Model – Radial Detectors – Accident Conditions 5.4-21
Table 5.4-15 PWR Maximum Subdetector Dose Rates – Top Model – Axial Detectors – Accident Conditions 5.4-22

List of Tables (Continued)

Table 5.4-16 PWR Maximum Subdetector Dose Rates – Bottom Model – Axial Detectors – Accident Conditions 5.4-22
Table 5.4-17 BWR Maximum Subdetector Dose Rates – Top Model – Radial Detectors – Accident Conditions 5.4-22
Table 5.4-18 BWR Maximum Subdetector Dose Rates – Bottom Model – Radial Detectors – Accident Conditions 5.4-23
Table 5.4-19 BWR Maximum Subdetector Dose Rates – Top Model – Axial Detectors – Accident Conditions 5.4-23
Table 5.4-20 BWR Maximum Subdetector Dose Rates – Bottom Model – Axial Detectors – Accident Conditions 5.4-23

Table 5.4-21 Loading Table for PWR Fuel 5.4-24
Table 5.4-22 Loading Table for BWR Fuel 5.4-25
Table 5.4-23 Results of Verification Study for Normal Conditions 5.4-26
Table 5.4-24 Results of Verification Study for Accident Conditions 5.4-26
Table 5.5.1.1-1 CEA Exposure History by Group – Maine Yankee 5.5.1-18
Table 5.5.1.1-2 CE14x14 CEA Hardware Spectra – 5, 10, 15, and 20 Years Cool Time – Maine Yankee 5.5.1-19
Table 5.5.1.1-3 Maine Yankee ICI Thimble Exposure History and Total Source Rate by Group 5.5.1-20
Table 5.5.1.1-4 Maine Yankee Core Exposure History by Cycle of Operation 5.5.1-21
Table 5.5.1.1-5 Maine Yankee Fuel Assemblies with Stainless Steel Replacement Rods (SSR) Showing Cycles of Operation and Burnup Received 5.5.1-22
Table 5.5.1.1-6 Contents of Maine Yankee Consolidated Fuel Lattices CN-1 and CN-10 ..... 5.5.1-22
Table 5.5.1.1-7 Maine Yankee CE14x14 Homogenized Fuel Region Isotopic Composition 5.5.1-23
Table 5.5.1.1-8 Isotopic Compositions of Maine Yankee CE14x14 Fuel Assembly Non-Fuel Source Regions 5.5.1-23

List of Tables (Continued)

Table 5.5.1.1-9 Isotopic Compositions of Maine Yankee CE14x14 Canister Annular Region Materials (One-Dimensional Analysis Only) 5.5.1-24
Table 5.5.1.1-10 Loading Table for Maine Yankee CE14x14 Fuel with No Non-Fuel Material – Required Cool Time in Years Before Assembly is Acceptable 5.5.1-24

Table 5.5.1.1-11 Three-Dimensional Shielding Analysis Results for Various Maine Yankee CEA Configurations Establishing One-Dimensional Dose Rate Limits for Loading Table Analysis 5.5.1-25
Table 5.5.1.1-12 Loading Table for Maine Yankee CE14x14 Fuel Containing CEA Cooled to Indicated Time 5.5.1-26
Table 5.5.1.1-13 Design Basis Maine Yankee CEA Source Rate at Each Cool Time Analyzed 5.5.1-27
Table 5.5.1.1-14 Establishment of Dose Rate Limit for Maine Yankee ICI Thimble Analysis 5.5.1-27
Table 5.5.1.1-15 Loading Table for Maine Yankee CE14x14 Fuel Containing ICI Thimble 5.5.1-27
Table 5.5.1.1-16 Required Cool Time for Maine Yankee Fuel Assemblies with Activated Stainless Steel Replacement Rods 5.5.1-28
Table 5.5.1.1-17 Maine Yankee Consolidated Fuel Model Parameters 5.5.1-28
Table 5.5.1.1-18 Maine Yankee Source Rate Analysis for CN-10 Consolidated Fuel Lattice 5.5.1-28
Table 5.5.1.1-19 Loading Table for Maine Yankee CE 14x14 Damaged Fuel 5.5.1-29
Table 5.5.1.1-20 Additional Maine Yankee Non-Fuel Hardware Characterization – Non-Neutron Sources 5.5.1-29
Table 5.5.1.1-21 Additional Maine Yankee Non-Fuel Hardware Characterization – Neutron Sources 5.5.1-29
Table 5.5.1.1-22 Pu-Be Assy Hardware Spectra (Cycles 1-13) – 9-Year Cool Time from 1/1/1997 ..... 5.5.1-30
Table 5.5.1.1-23 Additional Maine Yankee Non-Fuel Hardware – Hardware Assembly Spectra (Class 2 Canister) – 10-Year Cool Time for 1/1/1997 ..... 5.5.1-31

List of Tables (Continued)

Table 5.5.1.1-24 Additional Maine Yankee Non-Fuel Hardware – Source Assembly Spectra – 10-Year Cool Time from 1/1/1997 ..... 5.5.1-32
Table 5.5.1.1-25 Additional Maine Yankee Non-Fuel Hardware – Hardware Assembly Dose Rates (Class 2) – 10-Year Cool Time from 1/1/1997 ..... 5.5.1-33
Table 5.5.1.1-26 Additional Maine Yankee Non-Fuel Hardware – Transport Cask Source Assembly Surface Dose Rates – Normal Conditions – 2m + Railcar Dose – 10-Year Cool Time from 1/1/1997 ..... 5.5.1-34
Table 5.5.1.1-27 Additional Maine Yankee Non-Fuel Hardware – Transport Cask Source Assembly Surface Dose Rates – Accident Conditions – 1m Dose – 10-Year Cool Time from 1/1/1997 ..... 5.5.1-35
Table 5.5.1.2-1 Design Basis GTCC Source Term 5.5.1-41
Table 5.5.1.2-2 Design Basis GTCC Gamma Source Spectra 5.5.1-41
Table 5.5.1.2-3 Design Basis GTCC Source Strength 5.5.1-42
Table 5.5.1.2-4 GTCC Waste Dose Rate Results – Normal Conditions of Transport 5.5.1-42
Table 5.5.1.2-5 GTCC Waste Dose Rate Results – Accident Conditions 5.5.1-42
Table 5.5.2-1 Neutron Dose Response Factors 5.5.2-2
Table 5.5.2-2 Photon Dose Response Factors 5.5.2-3

5.0 SHIELDING EVALUATION

The Universal Transport Cask meets the 10 CFR 71 [1] requirements for transportation dose rate limits. The optimized multiwall design provides an efficient shielding arrangement for the transportation of 24 PWR or 56 BWR spent fuel assemblies. This chapter describes the shielding design and the analysis used to establish bounding radiological dose rates for the transport of various PWR and BWR fuels.

The shielding design criteria for the Universal Transport Cask are in accordance with the requirements established in 10 CFR Parts 71.47 and 71.51 for normal conditions of transport and hypothetical accident conditions. The 10 CFR 71.47 requirements for the transport of spent fuel under normal conditions of transport for consignments in exclusive use include the following:

- The dose rate on the surface of the package must not exceed 1000 mrem/hr.
- The dose rate on a vertical plane at the lateral surfaces of the railcar must not exceed 200 mrem/hr.
- The dose rate on a vertical plane two meters from the lateral surfaces of the railcar must not exceed 10 mrem/hr.
- The dose rate in any normally occupied positions of the railcar must not exceed 2 mrem/hr.

The 10 CFR 71.51 requirements state that the dose rate under hypothetical accident conditions must not exceed 1,000 mrem/hr at 1 meter from the surface of the cask. A summary description of the modeling methodology and dose rate results is provided in Section 5.1.

The shielding analysis is performed on the basis of design basis fuel descriptions for both PWR and BWR fuel. The design basis PWR fuel is a Westinghouse 17×17 assembly with a burnup of 45,000 MWD/MTU, an initial enrichment of 3.7 wt % ^{235}U, and a 10-year cooling time. The design basis BWR fuel is a GE 9×9 assembly design with a burnup of 40,000 MWD/MTU, an initial enrichment of 3.25 wt % ^{235}U, and a 10-year cooling time. A detailed description of the source term specification is provided in Section 5.2.

In the Universal Transport Cask design, the spent fuel assemblies are surrounded by a multiwalled arrangement of shielding materials. However, structural design requirements lead to cask extremity regions, such as rotation pockets, in which shield materials are reduced or

penetrated. Detailed analytical treatment of these shield transition regions is required to assess the radiological consequences of the design. Section 5.3 describes the three-dimensional shielding models employed in this analysis.

Dose rate results are obtained for both normal conditions of transport and hypothetical accident conditions. Under accident conditions, the cask is analyzed for the simultaneous effects of complete loss of radial neutron shielding including loss of the outer neutron shield shell; loss of impact limiters; and combined radial and axial lead slumps resulting from postulated cask side and end drops. Analytical details and dose rate results are given in Section 5.4. Under all postulated conditions, the fully loaded cask is shown to meet regulatory radiological limits.

The design basis fuel descriptions characterize Universal Transport Cask dose and heat generation rates at nominal conditions of burnup and initial enrichment for a particular PWR and BWR fuel type. In order to extend the results to other fuel types and various combinations of initial enrichment and burnup, a detailed analysis is conducted that determines, for any given fuel type, enrichment, and burnup combination, the cool time required for radiation dose and heat generation rates to fall below the design basis values. The analysis explicitly models the source term for the various fuel combinations based on SAS2H results, and the dose rate evaluation is made on the basis of computed one-dimensional dose rates which explicitly consider the effects of radiation spectrum and cask shielding properties rather than a simple source rate comparison.

For clarity, the various fuel assembly types considered are classified according to array size, with the results for the most limiting fuel type within each array size taken as the minimum required cool time for all assemblies within that size. The result of the analysis is a fuel assembly loading table showing the required cool time for any combination of fuel array size, initial enrichment, and burnup. Results are summarized in Section 5.1.3.

An analysis is performed for fuel at various combinations of burnup and initial enrichment to determine the required cool time for the fuel to fall below the design basis dose and decay heat levels. The bounding cool time is determined considering the cask normal and accident condition dose rates and total decay in the cask. This analysis is presented in Section 5.4.3.

Site specific fuel and GTCC waste is evaluated in Section 5.5.1.

The source specifications for the design basis fuel are discussed in Section 5.2.

5.1.1.2 BWR Fuel Assembly Classes

On the basis of similarity of length, the BWR fuel assemblies to be transported in the Universal Transport Cask are compiled into two classes (Class 4 corresponds to BWR/2–3 assemblies and Class 5 corresponds to BWR/4–6 assemblies). Of these assemblies, the following are chosen as candidate design basis assemblies for the cask shielding analysis on the basis of their computed radiation source terms:

- GE 7×7 BWR/2–3 version GE-2b (Class 4)
- GE 8×8–2 BWR/2–3 version GE-5 (Class 4)
- GE 8×8–4 BWR/2–3 version GE-8 (Class 4)
- GE 7×7 BWR/4–6 version GE-2 (Class 5)
- GE 8×8–2 BWR/4–6 version GE-5 (Class 5)
- GE 8×8–4 BWR/4–6 version GE-10 (Class 5)
- GE 9×9–2 BWR/4–6 version GE-11 (Class 5)

These assemblies constitute the candidate design basis BWR fuel assemblies for the cask shielding analysis. One-dimensional shielding calculations performed for each assembly identify a single assembly type that is selected as the design basis assembly for subsequent detailed three-dimensional shielding analysis. The candidate BWR fuel assemblies are analyzed on the basis of an initial enrichment of 3.25 wt % ^{235}U, a burnup of 40,000 MWD/MTU, and a cooling time of 10 years.

5.1.2 Codes Employed

The SCALE 4.3PC [3] code system is used in the analysis of the Universal Transport Cask. Source terms are generated by using the SAS2H [4] sequence as described in Section 5.2. One-dimensional radial and axial SAS1 [5] analyses are performed in order to identify design basis PWR and BWR fuel types. With these design basis source descriptions, a detailed three-dimensional analysis is performed by using the SAS4 [2] Monte Carlo

shielding analysis sequence. Modifications to SAS4 permit computation of dose rate profiles along surface detectors. These changes are further described in Section 5.4.1.

The 27 group neutron, 18 group gamma, coupled cross section library (27N-18COUPLE) derived from ENDF/B-IV [6] data is used in all shielding evaluations. Source terms include fuel neutron, fuel gamma, and gamma contributions from activated hardware. The effects of subcritical neutron multiplication and secondary gamma production due to neutron capture are included in the analysis. Dose rate evaluations include the effect of axial fuel burnup variation on fuel neutron and gamma source terms as described in Section 5.2.6.

5.1.3 Results of Analysis

The calculated normal transport and hypothetical accident condition dose rates are discussed in the following sections. The cask surface dose rates calculated at the fuel midplane include (1) neutrons and gammas originating from the fuel; (2) neutrons resulting from subcritical multiplication; (3) secondary gammas resulting from neutron capture in the neutron shield; and (4) gammas from activated materials in the grid spacers, end-fittings, and plenum springs.

The results of the intact fuel shielding analysis demonstrate that computed dose rates remain below 200 mrem/hr at all accessible locations on the surface of the cask. Computed dose rates slightly above 200 mrem/hr occur in the narrow, inaccessible gap between the neutron shield and the lower impact limiter in the BWR case and in an analysis of the PWR case with no spacer employed. Computed dose rates above 200 mrem/hr also occur at the cask surface between the top impact limiter and the neutron shell in the damaged fuel evaluation. Dose rates for this condition are below 450 mrem/hr on the cask surface and are below 100 mrem/hr at the personnel barrier. The dose rates remain below 10 mrem/hr at all locations 2 m from the edge of the railcar (any point 2 m from the vertical planes projected from the outer edges of the conveyance), 2 m above or below the Transport Cask, and 2 m from the axial surfaces of the impact limiters.

In addition, the hypothetical accident conditions do not result in a dose rate that exceeds the accident condition dose rate limit of 1000 mrem/hr at 1 m from the cask surface. Therefore, the Universal Transport Cask satisfies the regulatory criteria of 10 CFR 71.47 and paragraph 469 of IAEA Safety Series No. 6 under normal conditions of transport; and 10 CFR 71.51(a) and paragraph 542 of IAEA Safety Series No. 6 for hypothetical accident conditions.

In the tabulated results, computed dose rates are reported along with the relative uncertainty associated with each computed value expressed as a percentage. The relative uncertainty corresponds to plus or minus one standard deviation in the quoted value.

5.1.3.1 Normal Conditions of Transport

The maximum radial and axial dose rates for intact fuel calculated for the PWR and BWR casks under normal conditions of transport are shown in Table 5.1-1 and Table 5.1-3, respectively. The locations of the maximum dose rates in normal conditions of transport relative to the cask body and transporter are shown in Figure 5.1-1. The tables present the maximum computed dose rates and corresponding relative uncertainties on radial and axial surfaces outside the cask. Dose rates indicated at the personnel barrier correspond to the maximum values computed on a cylindrical surface extending between the top and bottom impact limiters and surrounding the cask at a radius of 53.5 in. In the radial case, dose rates indicated at the "2 m position" correspond to a position 2 m from the edge of a 124 in. wide standard railcar. For axial results, this position corresponds to a dose location 2 m from the top or bottom impact limiter surface.

For the PWR cask, the maximum normal conditions intact fuel surface dose rate is 167.2 (±1.8%) mrem/hr, occurring on the surface of the upper forging at the upper trunnion recess. (Values in parentheses following a dose rate result indicate the relative uncertainty in the value.) At the surface of the personnel barrier, the dose rate is much less than 200 mrem/hr with a maximum computed dose rate of 46.6 (±1.6%) mrem/hr. In addition, the 10 mrem/hr criterion is met at all locations 2 m from the railcar, 2 m above or below the cask, and 2 m from the axial surfaces of the impact limiters. Axial shifting of damaged fuel material increases the calculated dose rate on the upper forging and personnel barrier (at the elevation of the forging). Dose rates remain below 450 mrem/hr at the cask surface and 100 mrem/hr at the personnel barrier.

For the BWR cask, the maximum normal conditions surface dose rate is 84.8 (±2.0%) mrem/hr, occurring on the surface of the lower rotation pocket. The dose rate at the outer shell surface in the inaccessible 1.25-in. wide gap between the neutron shield shell and lower impact limiter, is computed to be 225.6 (±3.5%) mrem/hr. However, this dose rate is not considered significant due to the inaccessibility of the location. Furthermore, the dose rate at the gap opening is well below 200 mrem/hr as demonstrated in Section 5.4.2.2. All other cask surface dose rates are less than 200 mrem/hr. At the personnel barrier, the maximum dose rate is much less than 200 mrem/hr, with a maximum computed dose rate of 40.4 (±1.5%) mrem/hr. The 10 mrem/hr criterion is met at all locations 2 m from the railcar and from the axial surfaces of the impact limiters.

5.1.3.2 Hypothetical Accident Conditions

Table 5.1-2 and Table 5.1-4 provide accident dose rates that could occur in the event of the loss of the neutron shield, shield shell, and impact limiters in the PWR and BWR casks, respectively. The location of the maximum hypothetical accident dose rates relative to the transport cask body are shown in Figure 5.1-2. An accident involving the complete loss of the impact limiters or neutron shielding is not credible for the Universal Transport Cask, although some of the neutron shielding capability may be lost as a result of a fire. Nonetheless, the shielding analysis conservatively assumes a complete loss of radial neutron shielding. In addition, axial and radial lead slumps resulting from postulated cask side and end drop accidents are modeled in the accident condition analysis.

In the event of a cask end drop, the lead gamma shielding could slump and fill the annular gap (if one exists) created by the cooling of the lead after fabrication. This accident could create a 3.05 in. gap at the top of the lead annulus. The major radiation concern in this event is the "shine through" of the activated end-fittings. If the cask is subjected to a side drop, the lead gamma shielding could slump and create a void on the upper side of the cask. An evaluation of this side drop accident shows that the lead may sag at the opposite side by a maximum 0.91 in.

The dose rates presented here and in more detail in Section 5.4 show that neither the loss of the neutron shielding nor the lead slump conditions will result in a dose rate that exceeds the hypothetical accident dose rate limit of 1000 mrem/hr at 1 m from the surface of the cask.

Figure 5.1-1 Location of Maximum Dose Rates for Intact Fuel in Normal Conditions of Transport

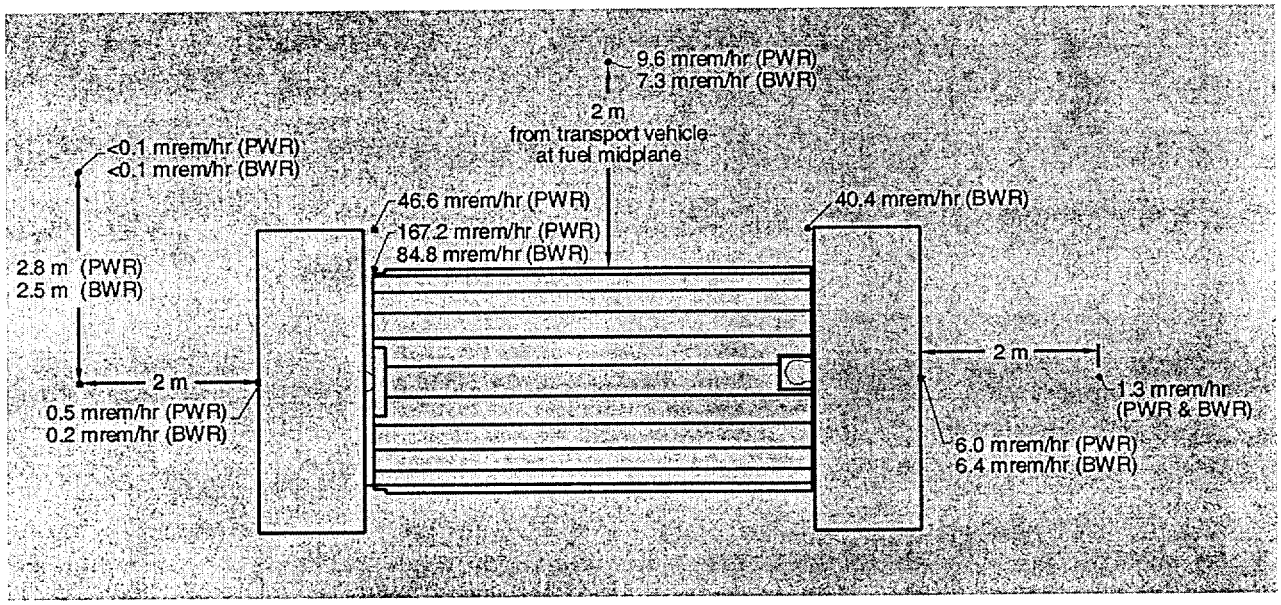

Figure 5.1-2 Location of Maximum Dose Rates for Intact Fuel in Hypothetical Accident Conditions

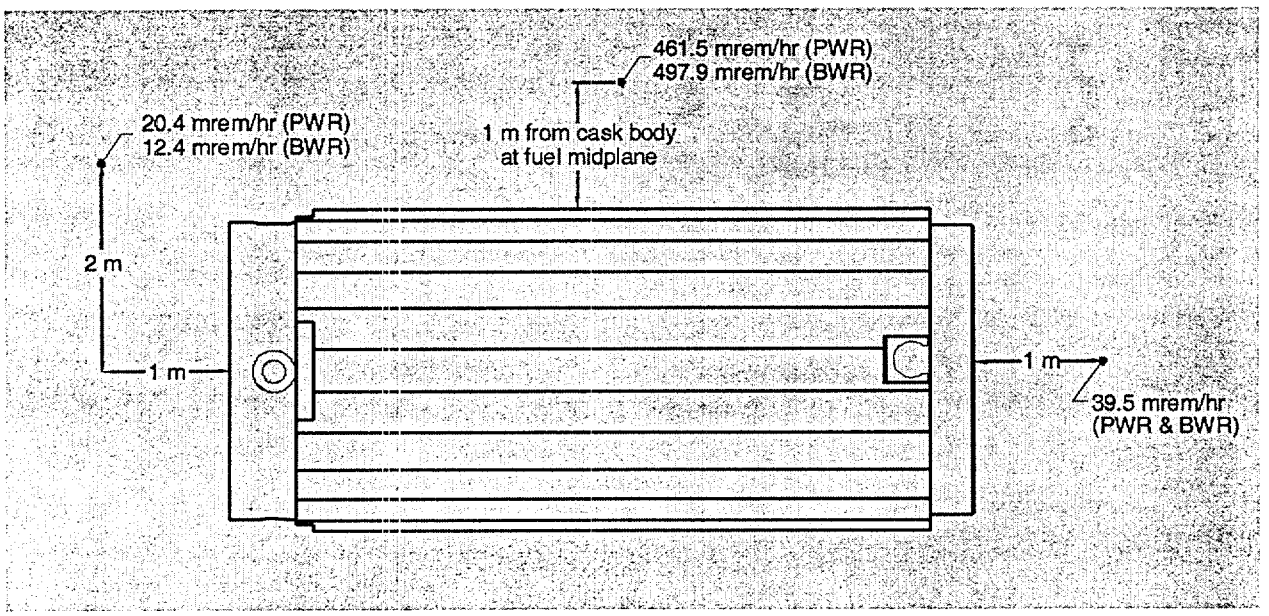

Table 5.1-1 PWR Maximum Total Dose Rate Summary for Intact Fuel – Normal Conditions

Location	Dose Type	Radial		Top Axial		Bottom Axial	
Surface	Gamma	66.2	(0.6%)	0.5	(2.0%)	6.0	(0.4%)
	Neutron	101.1	(2.9%)	<0.1	(1.4%)	<0.1	(1.7%)
	Total	167.2	(1.8%)	0.5	(1.9%)	6.0	(0.4%)
Personnel Barrier	Gamma	23.5	(0.5%)	-		-	
	Neutron	23.2	(3.1%)	-		-	
	Total	46.6	(1.6%)	-		-	
2 m Position	Gamma	6.4	(0.3%)	<0.1	(3.5%)	1.3	(1.0%)
	Neutron	3.2	(0.9%)	<0.1	(14.9%)	<0.1	(3.2%)
	Total	9.6	(0.4%)	<0.1	(11.4%)	1.3	(1.0%)

Table 5.1-2 PWR Maximum Total Dose Rate Summary for Intact Fuel – Accident Conditions

Location	Dose Type	Radial		Top Axial		Bottom Axial	
1 m Position	Gamma	44.8	(0.5%)	<0.1	(8.6%)	28.7	(0.4%)
	Neutron	416.7	(0.2%)	20.3	(2.9%)	10.9	(0.6%)
	Total	461.5	(0.2%)	20.4	(2.8%)	39.5	(0.4%)

Table 5.1-3 BWR Maximum Total Dose Rate Summary for Intact Fuel – Normal Conditions

Location	Dose Type	Radial		Top Axial		Bottom Axial	
Surface	Gamma	50.4	(1.1%)	0.2	(2.8%)	6.4	(0.4%)
	Neutron	34.5	(4.6%)	<0.1	(1.6%)	<0.1	(2.0%)
	Total	84.8 [1]	(2.0%)	0.2	(2.7%)	6.4	(0.4%)
Personnel Barrier	Gamma	20.7	(0.5%)	-		-	
	Neutron	19.8	(3.0%)	-		-	
	Total	40.4	(1.5%)	-		-	
2 m Position	Gamma	4.0	(0.4%)	<0.1	(3.9%)	1.3	(1.0%)
	Neutron	3.4	(0.8%)	<0.1	(24.1%)	<0.1	(4.3%)
	Total	7.3	(0.4%)	<0.1	(15.3%)	1.3	(1.0%)

[1] Dose rate at forging surface inside gap between lower limiter and shield shell is 225.6 (3.5%)

Table 5.1-4 BWR Maximum Total Dose Rate Summary for Intact Fuel – Accident Conditions

Location	Dose Type	Radial		Top Axial		Bottom Axial	
1 m Position	Gamma	25.3	(0.8%)	<0.1	(8.9%)	30.8	(0.4%)
	Neutron	472.7	(0.2%)	12.3	(3.9%)	8.7	(0.7%)
	Total	497.9	(0.2%)	12.4	(3.9%)	39.5	(0.4%)

5.5.1 Site Specific Contents Shielding Evaluations

This section describes fuel assembly characteristics and configurations, or waste configurations, which are unique to specific reactor sites. These site specific content configurations result from conditions that occurred during reactor operations, participation in research and development programs, testing programs intended to improve reactor operations, and from decommissioning activities.

Site specific fuel assembly configurations are either shown to be bounded by the analysis of the standard design basis fuel assembly configuration of the same type (PWR or BWR), or are shown to be acceptable contents by specific evaluation of the configuration.

5.5.1.1 Maine Yankee Site Specific Spent Fuel

This analysis considers both assembly fuel sources and sources from activated non-fuel material such as control element assemblies (CEA), in-core instrument (ICI) thimbles, and fuel assemblies containing activated stainless steel replacement (SSR) rods and other non-fuel material, including start-up neutron sources. It also considers the consolidated fuel present in the Maine Yankee spent fuel inventory.

The Maine Yankee spent fuel inventory also contains fuel assemblies with hollow zirconium rods, removed fuel rods, axial blankets, poison rods, variable radial enrichment, and low enriched substitute rods. These components do not result in additional sources to be considered in shielding evaluations and are, therefore, enveloped by the standard fuel assembly evaluation. For shielding considerations of the variably enriched rods the planar-average enrichment is employed in determining minimum cool times.

5.5.1.1.1 Fuel Source Term Description

Maine Yankee utilized 14x14 array size fuel based on designs provided by Combustion Engineering, Westinghouse, and Exxon Nuclear. The previously analyzed Combustion Engineering CE14x14 Standard fuel design is selected as the design basis for this analysis because its potential Uranium loading is the highest of the three vendor fuel types, based on a 0.3765-inch nominal fuel pellet diameter, a 137 inch active fuel length, and a 95% theoretical fuel density. This results in a fuel mass of 0.4307 MTU. This exceeds the maximum reported Maine Yankee fuel mass of 0.397 MTU, and therefore, produces bounding source terms. The

SAS2H model of the CE14x14 assembly at a nominal burnup of 45,000 MWD and initial enrichment of 3.7 wt.% based on data provided in Table 1-2-4 is shown in Figure 5.5.1.1-1.

Source terms for various combinations of burnup and initial enrichment are computed by adjusting the SAS2H BURN parameter to model the desired burnup and specifying the initial enrichment in the Material Information Processor input for UO_2.

5.5.1.1.1.1 Control Element Assemblies (CEA)

For the CEA evaluation, the assumptions are:

1. The irradiated portion of the CEA assembly is limited to the CEA tips, as during normal operation, the elements are retracted from the core and only the tips are subject to significant neutron flux.
2. The CEA tips are defined as that portion present in the "Gas Plenum" neutron source region in the Characteristics Database (CDB) [9].
3. Material subject to activation in the CEA tips is limited to stainless steel Inconel, and the AgInCd absorber material present in the lower eight inches of the CEA.
4. All stainless steel and Inconel material is assumed to have a concentration of 1.2 g/kg ^{59}Co. The CDB indicates that a total of 2.495 kg/CEA of this material is present in the Gas Plenum region of the core during operation.
5. The mass of AgInCd present in each CEA tip is 2.767 kg/CEA [9]. The AgInCd material is modeled as 80 wt.% Ag, 15.35 wt. % In, and 5.35 wt. % Cd. Note that the composition sums to a value greater than 100%, but this only means that conservatively more mass is represented than is actually present.
6. The irradiated CEA material is assumed to be present in the bottom eight inches of the active fuel region when inserted in the assembly.
7. The decay heat generated in the most limiting CEA at a 5-year cool time is 2.16 W/kg of stainless steel or Inconel and 3.11 W/kg of AgInCd. For a cask fully loaded with fuel assemblies containing design basis CEAs, the additional heat generation due to the CEAs amounts to: [(2.16 W/kg SS or Inconel)(2.495 kg/CEA) + (3.11 W/kg AgInCd)(2.767 kg/CEA)](24 CEA/cask) = 336 W/cask.
   This value is conservatively rounded up to 350 W. Although longer cool times are considered in this analysis for the fuel source terms, this decay heat generation rate is conservatively used for all longer CEA cool times.

source term. Hence, no adjustment to the one-dimensional dose rate limits is required as in previous analyses involving added non-fuel sources. The results of the cool time analysis for each assembly are shown in Table 5.5.1.1-16.

5.5.1.1.4.4 Consolidated Fuel

There are two consolidated fuel lattices intended for shipment in the Universal Transport Cask. The lattices house fuel rods taken from assemblies as shown in Table 5.5.1.1-6. The consolidated fuel rods have decayed for over twenty years and do not represent a significant shielding issue.

A limiting cool time analysis is conducted by identifying a fuel assembly description analyzed in the loading table analysis which bounds the parameters of the fuel rods in the consolidated fuel lattices. The parameters of those fuel rods are shown in Table 5.5.1.1-17. The CE14x14 fuel at 30,000 MWD/MTU and 1.9 wt % enrichment represents a bounding assembly type since it has a significantly higher burnup and a lower enrichment than the original assemblies. This fuel requires six years cool time before it can be loaded in the transport cask as shown in Table 5.5.1.1-10. The consolidated fuel has been cooled for at least 24 years. For container CN-1 lattice, one can immediately conclude that dose rates are bounded by the limiting fuel.

However, the CN-10 lattice contains significantly more fuel rods than an intact assembly. Neglecting the mitigating effects of additional self-shielding, this configuration is addressed by comparing the radiation source strength of the limiting fuel at six and 24 years cool time. Conservatively assuming that all fuel rods present in CN-10 are at the limiting conditions of 30,000 MWD/MTU and 1.9 wt %, the ratio of the source rate in the CN-10 to the source rate in the limiting fuel assembly is shown to be less than one for each source type in Table 5.5.1.1-18. For each source type, the ratio is computed as:

Ratio = (Num Rods in CN-10)(Source Rate at 24 Yr) / (Num Rods in F/A)(Source Rate at 6 Yr)

Hence, CN-10 is also bounded by the limiting case and the consolidated fuel is eligible for shipment in the transport cask as of January 1, 2001.

5.5.1.1.4.5 Damaged Fuel

To provide minimum cool times for Maine Yankee damaged fuel inserted in Maine Yankee fuel cans in the four corner locations of the basket, an analysis is performed that determines, for any given enrichment and burnup combination, the minimum cool time required for dose rates to fall below the design basis values for these locations. The analysis models the source term for combinations of enrichment, burnup, and cool time based on SAS2H results. The dose rate evaluation is made on the basis of computed three-dimensional dose rates that explicitly consider the effects of radiation spectrum and cask shielding properties. The analysis considers the migration of damaged fuel from the active fuel region into the upper end-fitting and upper plenum assembly regions.

5.5.1.1.4.5.1 Damaged Fuel Loading Table Analysis

The loading table analysis extends the applicability of the initial 10-year-cooled, 45,000 MWD/MTU PWR design basis shielding evaluation by providing minimum cool times for 30,000 to 50,000 MWD/MTU burned fuel assemblies in increments of 5,000 MWD/MTU. In addition to the burnup range, the loading table evaluation includes minimum initial enrichment limits ranging from 1.9 to 3.7 wt % ^{235}U in 0.2 wt % ^{235}U increments.

A complete set of source spectra for the design basis Maine Yankee CE 14x14 fuel assembly is computed using the SAS2H code at various initial enrichment, burnup, and cool times representative of the fuel inventory intended for shipment. Next, the damaged fuel material descriptions are computed for the upper end-fitting and upper plenum assembly regions. The volume of void space in each region is calculated and is then assumed completely filled with UO_2. Thus, 56% of the assembly fuel mass is assumed to migrate into the upper assembly region with no reduction in fuel modeled over the active fuel length.

With the damaged fuel defined, gamma and neutron source spectra for the four corner basket locations are constructed based on the mass of UO_2 in each fuel assembly region for seven sources: active fuel gamma; active fuel neutron; active fuel hardware; upper end-fitting gamma; upper end-fitting neutron; upper plenum gamma; and upper plenum neutron.

Because of the migration of the fuel out of the active fuel region, the one-dimensional dose response approach outlined in Section 5.4.3.1 cannot be used. Therefore, a three-dimensional

dose response methodology is used to generate the large number of dose rates required. Thus, seven sets of three-dimensional response cases are run to generate the groupwise contribution to dose rates at the dose rate locations of interest.

For each enrichment, burnup, cool time, and source region, the product of the normalized source spectrum and the response spectrum is multiplied by the total source to calculate the dose rates at the detector locations of interest. The dose rates from all sources are then summed. With the dose rates calculated for each possible combination, the exclusive use dose limits are used in conjunction with the four corner location results of the design basis PWR fuel to compute required cool times.

The SCALE computer code system is used to evaluate radiation source terms and to perform three-dimensional shielding calculations. Source terms are evaluated using the SAS2H code, which provides a simplified interface to the ORIGEN-S code, including burnup-dependent cross-section processing. The SAS4 code sequence is used to determine three-dimensional dose rate response functions. All SCALE analyses are conducted using the SCALE 27N18G group library.

SAS2H runs are executed for the CE 14x14 assembly at the following combinations of burnup, initial enrichment, and cool time:

Burnup:	30, 35, 40, 45, 50 MWD/MTU
Enrichment:	1.9, 2.1, 2.3, 2.5, 2.7, 2.9, 3.1, 3.3, 3.5, 3.7 wt % ^{235}U
Cool Time:	5, 6, 7, 8, 9, 10, 12, 14, 16, 18, 20, 22, 24, 26, 28, 30, 35, 40 years

Final cool times are established by interpolating between results calculated for each cool time listed above. This interpolation procedure is conservative due to the exponentially decreasing behavior of radiation source rates with time. The maximum cool time (that is, the cool time that ensures the dose rate limit is met) is always rounded up to the next whole year.

The various combinations of enrichment and burnup shown above define a discrete mesh of possible combinations. When considering the required cool time for a particular assembly, the actual enrichment of the assembly should be rounded down to the next lower analyzed value, and the assembly burnup should be rounded up to the next higher analyzed value in order to ensure that a conservative value is obtained from the loading table.

5.5.1.1.4.5.2 Establishment of Limiting Values

Normal condition dose rate limits are established using the SAS4 code by computing the contribution of the sources in the four corner basket locations to the total dose rate for the design basis PWR fuel. The SAS4 geometric models are described in Section 5.3.2. The dose rate limits are established based on the difference between the total design basis Westinghouse 17 x 17 fuel dose rate and the Westinghouse 17 x 17 fuel four corner dose rate contribution and the exclusive use dose rate limits. The limiting detector location for maximum cool times is at a distance 2m from the edge of a 124-inch wide railcar (357.48 cm from the cask centerline) for the exclusive use surface dose rate limit of 1000 mrem/hr. The resulting three-dimensional dose rate limit for damaged fuel in the four corner basket locations is 2.65 mrem/hr at the limiting detector location.

5.5.1.1.4.5.3 Damaged Fuel Cool Time Determination

The strategy used to determine the limiting cool times for a given initial enrichment and burnup combination is:

1. Determine dose rate values at each cool time step.
2. Interpolate in the resulting collection of data to find the minimum cool time required to meet the limiting dose rate (total of 10 mrem/hr at 2m from the edge of the railcar).

The minimum cool times required to meet the dose rate limit are rounded up to the next whole year. The results of the Maine Yankee damaged fuel loading table analysis are shown in Table 5.5.1.1-19.

5.5.1.1.4.6 Additional Non-Fuel and Neutron Source Material

Additional non-fuel material consists of:

1. Three plutonium-beryllium (Pu-Be) neutron sources, two irradiated and one unirradiated.
2. Two antimony-beryllium (Sb-Be) neutron sources, both irradiated.
3. Control element assembly (CEA) fingertips.
4. ICI string segment.

The five neutron sources will be inserted into the center guide tubes of five different assemblies and loaded into Class 1 canisters. These five assemblies must be loaded in five different canisters. The CEA fingertips and ICI string segment may be inserted into the guide tubes of one fuel assembly, but the assembly must be loaded into a Class 2 canister to accommodate a flow mixer to plug the guide tubes holding the non-fuel components.

The characterization of the additional non-fuel hardware is provided in Tables 5.5.1.1-20 and 5.5.1.1-21. The data is divided into two separate categories:

1. Non-neutron producing radiation sources – this category includes the CEA fingertips, ICI string segment, and the Sb-Be neutron sources (the neutron production rate of these is negligible).
2. Neutron producing radiation sources – this category includes the two irradiated and one unirradiated Pu-Be neutron sources.

The masses of ^{238}Pu and ^{239}Pu given for the unirradiated Pu-Be source are used in conjunction with the delivery date of May 1972 to generate source terms.

The neutron sources have an additional source component due to the irradiation of the stainless steel rod encasing the source. The quantity of irradiated steel is taken as 10 lbs (4.54 kg).

From the waste characterization, it is apparent that the Sb-Be sources already include the contribution of irradiated stainless steel. Therefore, only the Pu-Be irradiated stainless steel requires activation. The hardware source spectra for the irradiated Pu-Be sources are based on the Maine Yankee exposure history shown in Table 5.5.1.1-4. The combined Pu-Be assembly hardware irradiation for Cycles 1-13 is shown in Table 5.5.1.1-22 at a cool time of nine years from 1/1/1997.

The waste characterizations given in Table 5.5.1.1-20 and 5.5.1.1-21 are used to generate source terms using ORIGEN-S [8]. For the non-neutron producing sources, the total curie content is assigned to ^{60}Co to provide bounding source terms. Also, only one Sb-Be spectrum is produced, based on the higher curie content source. For the neutron-producing sources, the given curie contents are used for the irradiated sources, whereas the plutonium masses are used for the unirradiated Pu-Be source.

Based on the loading plan, there are two areas of application of both spectra and dose rates. The CEA fingertips and ICI string segment may be loaded into one assembly. Therefore, the gamma spectra of these items are summed and only one gamma spectrum is used to calculate the dose rates due to this loaded assembly. Each of the five neutron sources will be loaded into different fuel assemblies, and the spectra are presented accordingly. The single assembly spectra are presented in Table 5.5.1.1-23 and the neutron source assembly spectra are presented in Table 5.5.1.1-24.

Dose rates are calculated by simply groupwise multiplying the spectra and CE14x14 dose rate response functions and adjusting by a factor of 24/(10E+10 x 5.6193E+06) to remove the volume component and the calculation scaling factor. Dose rates are presented in Tables 5.5.1.1-25 through 5.5.1.1-27 and show the minimal dose rate contribution due to the inclusion of the additional non-fuel material.

Figure 5.5.1.1-1 SAS2H Model Input File – CE 14x14

```
=SAS2H      PARM=(HALT03,SKIPSHIPDATA)
CE 14X14 3.7 W/O U235, 45000 MWD/MTU 12.0-22.0 YEAR COOLING
27GROUPNDF4 LATTICECELL
UO2         1 0.950 900 92235 3.7 92238 96.3 END
ZIRCALLOY   2 1.0 620 END
H2O         3 DEN=0.725 1.0 580 END
ARBM-BORMOD 0.725 1 1 0 0 5000 100 3 550.0E-6 580 END
END COMP
SQUAREPITCH 1.4732 0.9563 1 3 1.1176 2 0.9754 0 END
NPIN=176 FUEL=347.98 NCYC=3 NLIB=1 PRIN=6 LIGH=5
INPL=1 NUMH=20 NUMI=0 ORTU=0.5588 SRTU=0.49285 END
POWER=13.065 BURN=463.5350 DOWN=60.0 END
POWER=13.065 BURN=463.5350 DOWN=60.0 END
POWER=13.065 BURN=463.5350 DOWN=1461.00 END
FE 0.672 CR 0.190 NI 0.115 MN 0.020 CO 0.0012
END
```

Table 5.5.1.1-1 CEA Exposure History by Group – Maine Yankee

CEA Group	First Cycle	Last Cycle	Maximum Exposure (MWD/MTU)	Number of Cycles	Exposure Per Cycle (MWD/MTU)	Cool Time as of 1/1/2001 (y)
A1-A8	7	15	60239	9	6693	4
B1-B5	9	15	48909	7	6987	4
C1-C11, C13-C15	10	15	44315	6	7386	4
D1-D15	11	15	35283	5	7057	4
E1-E17, GN, *78, 101, 102, 138-153	12	15	29367	4	7342	4
F1,F2	13	15	18663	3	6221	4
4A	12	12	9786	1	9786	8
C12	10	12	24309	3	8103	8
NA	1	11	75444	11	6859	10
1-69	1	8	53258	8	6657	15

The asterisk is added to CEA 78* to distinguish it from the original CEA 78.

Table 5.5.1.1-2 CE14x14 CEA Hardware Spectra – 5, 10, 15 and 20 Years Cool Time – Maine Yankee

Group	5 year (γ / sec)	10 year (γ / sec)	15 year (γ / sec)	20 year (γ / sec)
1	0.0000E+00	0.0000E+00	0.0000E+00	0.0000E+00
2	0.0000E+00	0.0000E+00	0.0000E+00	0.0000E+00
3	0.0000E+00	0.0000E+00	0.0000E+00	0.0000E+00
4	0.0000E+00	0.0000E+00	0.0000E+00	0.0000E+00
5	1.3479E-04	4.4697E-06	1.4822E-07	4.9154E-09
6	7.1467E+06	2.6384E+06	1.3598E+06	7.0431E+05
7	4.0337E+09	1.6979E+09	8.7691E+08	4.5422E+08
8	3.7246E+10	2.3434E+08	1.4804E+06	1.5188E+04
9	1.8642E+14	7.1649E+13	3.6955E+13	1.9142E+13
10	4.8840E+14	2.5265E+14	1.3086E+14	6.7790E+13
11	1.3804E+14	9.4554E+11	4.7779E+10	3.7897E+10
12	1.1469E+15	9.3808E+14	9.1172E+14	8.8714E+14
13	4.3885E+14	4.2316E+14	4.1174E+14	4.0065E+14
14	9.1526E+11	5.5505E+11	5.2913E+11	5.0949E+11
15	1.2039E+12	8.4093E+11	8.0140E+11	7.6939E+11
16	3.8479E+12	2.9855E+12	2.7489E+12	2.5803E+12
17	5.1828E+13	4.4134E+13	4.2118E+13	4.0659E+13
18	3.4899E+14	2.7741E+14	2.6393E+14	2.5520E+14
SS Source Rate	6.3886E+14	3.2951E+14	1.7066E+14	8.8413E+13
AgInCd Source Rate	2.1666E+15	1.6829E+15	1.6308E+15	1.5861E+15
Total Source Rate	2.8055E+15	2.0124E+15	1.8014E+15	1.6745E+15
SFA[1]	5.6110E+15	4.0249E+15	3.6029E+15	3.3490E+15

1. SAS4 file input value.

Table 5.5.1.1-3 Maine Yankee ICI Thimble Exposure History and Total Source Rate by Group

Group	Quantity	Cycles Exposed	Number of Cycles	Total Source [γ/sec]
A	41	1, 1A, 2	3	9.1881E+11
B	1	1	1	2.3775E+11
C	2	1, 1A	2	3.6244E+11
D	1	1A, 2	2	6.8106E+11
E	3	2	1	5.5637E+11
F	15	3 thru 11, 13	10	1.1695E+13
G	12	3 thru 11, 14	10	1.2126E+13
H	12	3 thru 11, 15	10	1.1454E+13
I	3	3 thru 9,14,15	9	1.1309E+13
J	2	10 thru 15	6	1.4940E+13
K	1	10 thru 12	3	6.1296E+12
L	25	12 thru 15	4	1.1491E+13
M	17	12	1	2.6801E+12
N	3	13 thru 15	3	8.8105E+12

Table 5.5.1.1-4 Maine Yankee Core Exposure History by Cycle of Operation

Cycle	Discharge Date	Cycle Burnup [MWD/MTU]	Core Average Enrichment [wt %]
1	6/29/74	10367	2.44
1A	5/2/75	4492	2.30
2	4/9/77	17365	2.45
3	7/14/78	11105	2.59
4	1/11/80	10500	2.84
5	5/8/81	10799	2.98
6	9/24/82	11585	3.01
7	3/31/84	12483	3.10
8	8/17/85	12504	3.20
9	3/28/87	14424	3.29
10	10/15/88	12675	3.36
11	4/7/90	13786	3.50
12	2/14/92	15364	3.62
13	7/30/93	13668	3.68
14	1/14/95	13075	3.75
15	12/6/96	7859	3.76

Table 5.5.1.1-5 Maine Yankee Fuel Assemblies with Stainless Steel Replacement Rods (SSR) Showing Cycles of Operation and Burnup Received

Assembly Number	1st Cycle	2nd Cycle	3rd Cycle	1st Cycle Burnup[1]	2nd Cycle Burnup[1]	3rd Cycle Burnup[1]	Number SSR
N420	9	10	11	16,428	13,467	11,893	3
N842	9	10	–	18,420	13,885	0	1
N868	9	10	11	18,622	13,386	4,919	1
R032	12	13	14	16,464	15,386	12,168	1
R439	12	13	14	20,371	14,779	11,685	1
R444	12	13	14	20,371	14,779	11,685	4
U01	15	–	–	7,339	0	0	1
U05	15	–	–	7,339	0	0	1
U16	15	–	–	10,598	0	0	1
U37	15	–	–	9,005	0	0	1
U51	15	–	–	8,288	0	0	1
U60	15	–	–	8,288	0	0	5

1. MWD/MTU

Table 5.5.1.1-6 Contents of Maine Yankee Consolidated Fuel Lattices CN-1 and CN-10

C.F. Lattice	Original Fuel Assembly	Number Rods	Actual Burnup [MWD/MTU]	Initial Enrichment [wt %]
CN-1	EF0039	172	5150	1.929
CN-10	EF0045	176	17150	1.953
	EF0046	107	17150	1.953

Table 5.5.1.1-7 Maine Yankee CE14x14 Homogenized Fuel Region Isotopic Composition

Isotope	CE14x14 [atom/b-cm]
ALUMINUM	2.05114E-03
BORON-10	1.90898E-04
BORON-11	7.68387E-04
CARBON-12	2.39821E-04
CHROMIUM(SS304)	7.19369E-04
IRON(SS304)	2.4501E-03
MANGANESE	7.16674E-05
NICKEL(SS304)	3.18674E-04
OXYGEN-16	8.72597E-03
URANIUM-234	2.39964E-07
URANIUM-235	3.14135E-05
URANIUM-238	4.33133E-03
ZIRCALOY	3.06324E-03

Table 5.5.1.1-8 Isotopic Compositions of Maine Yankee CE14x14 Fuel Assembly Non-Fuel Source Regions

Isotope	Upper Plenum [atom/b-cm]	Upper End Fitting [atom/b-cm]	Lower End Fitting [atom/b-cm]
CHROMIUM(SS304)	1.59190E-03	1.89910E-03	3.08125E-03
MANGANESE	1.58594E-04	1.89199E-04	3.06971E-04
IRON(SS304)	5.42166E-03	6.46791E-03	1.04941E-02
NICKEL(SS304)	7.05196E-04	8.41284E-04	1.36497E-03
ZIRCALOY	3.22036E-03	[redacted]	[redacted]

Table 5.5.1.1-9 Isotopic Compositions of Maine Yankee CE14x14 Canister Annular Region Materials (One-Dimensional Analysis Only)

Isotope	Fuel Annulus [atom/b-cm]	Upper Plenum Annulus [atom/b-cm]	Upper End Fitting Annulus [atom/b-cm]	Lower End Fitting Annulus [atom/b-cm]
ALUMINUM	5.96817E-03	[redacted]	[redacted]	[redacted]
CHROMIUM(SS304)	1.77895E-03	9.31065E-04	2.53529E-03	4.13797E-03
MANGANESE	1.77228E-04	9.27577E-05	2.52579E-04	4.12247E-04
IRON(SS304)	6.05870E-03	3.1710E-03	8.63463E-03	1.40930E-02
NICKEL(SS304)	7.88057E-04	4.12453E-04	1.12311E-03	1.83308E-03

Table 5.5.1.1-10 Loading Table for Maine Yankee CE14x14 Fuel with No Non-Fuel Material – Required Cool Time in Years Before Assembly is Acceptable

Loading Table for CE14x14 Fuel with No Non-Standard Fuel Material					
Enrichment	Burnup (B) [GWD/MTU]				
[wt %]	B ≤ 30	30 ≤ B < 35	35 ≤ B < 40	40 ≤ B < 45	45 ≤ B < 50
1.9 ≤ E < 2.1	6 years	8 years	11 years	18 years	27 years
2.1 ≤ E < 2.3	6 years	7 years	10 years	15 years	24 years
2.3 ≤ E < 2.5	6 years	7 years	9 years	14 years	22 years
2.5 ≤ E < 2.7	6 years	7 years	9 years	12 years	19 years
2.7 ≤ E < 2.9	6 years	6 years	8 years	11 years	17 years
2.9 ≤ E < 3.1	5 years	6 years	8 years	10 years	15 years
3.1 ≤ E < 3.3	5 years	6 years	7 years	10 years	15 years
3.3 ≤ E < 3.5	5 years	6 years	7 years	9 years	15 years
3.5 ≤ E < 3.7	5 years	6 years	7 years	9 years	14 years
3.7 ≤ E ≤ 4.2	5 years	6 years	7 years	9 years	14 years

Table 5.5.1.1-11 Three-Dimensional Shielding Analysis Results for Various Maine Yankee CEA Configurations Establishing One-Dimensional Dose Rate Limits for Loading Table Analysis

CEA Cool Time [y]	Dose Rate [mrem/hr]	FSD [%]	Ratio [%]	Limit [mrem/hr]
Class 1 Result	7.70	0.72	-	6.71
No CEA	7.92	0.63	97.2%	6.53
5y	9.41	0.55	81.9%	5.49
10y	8.53	0.59	90.3%	6.06
15y	8.22	0.60	93.6%	6.28
20y	8.08	0.61	95.3%	6.39

Table 5.5.1.1-12 Loading Table for Maine Yankee CE14x14 Fuel Containing CEA Cooled to Indicated Time

Loading Table for CE14x14 Fuel - Minimum Required Cool Time in Years

Burnup	30 GWD/MTU	Minimum Cool Time [y] for				
Enrichment	No CEA (Class 1)	No CEA (Class 2)	5 Yr CEA	10 Yr CEA	15 Yr CEA	20 Yr CEA
1.9	6	6	7	6	6	6
2.1	6	6	7	6	6	6
2.3	6	6	6	6	6	6
2.5	6	6	6	6	6	6
2.7	6	6	6	6	6	6
2.9	5	6	6	6	6	6
3.1	5	5	6	6	6	5
3.3	5	5	6	6	5	5
3.5	5	5	6	5	5	5
3.7	5	5	6	5	5	5
Burnup	35 GWD/MTU	Minimum Cool Time [y] for				
Enrichment	No CEA (Class 1)	No CEA (Class 2)	5 Yr CEA	10 Yr CEA	15 Yr CEA	20 Yr CEA
1.9	8	8	9	8	8	8
2.1	7	7	9	8	8	8
2.3	7	7	8	7	7	7
2.5	7	7	8	7	7	7
2.7	6	7	7	7	7	7
2.9	6	6	7	7	6	6
3.1	6	6	7	6	6	6
3.3	6	6	7	6	6	6
3.5	6	6	6	6	6	6
3.7	6	6	6	6	6	6
Burnup	40 GWD/MTU	Minimum Cool Time [y] for				
Enrichment	No CEA (Class 1)	No CEA (Class 2)	5 Yr CEA	10 Yr CEA	15 Yr CEA	20 Yr CEA
1.9	11	12	14	13	12	12
2.1	10	10	13	11	11	11
2.3	9	9	12	10	10	10
2.5	9	9	10	9	9	9
2.7	8	8	10	9	8	8
2.9	8	8	9	8	8	8
3.1	7	7	8	8	8	8
3.3	7	7	8	7	7	7
3.5	7	7	8	7	7	7
3.7	7	7	7	7	7	7
Burnup	45 GWD/MTU	Minimum Cool Time [y] for				
Enrichment	No CEA (Class 1)	No CEA (Class 2)	5 Yr CEA	10 Yr CEA	15 Yr CEA	20 Yr CEA
1.9	18	18	21	19	18	18
2.1	15	16	19	17	17	16
2.3	14	14	18	16	15	15
2.5	12	13	16	14	14	13
2.7	11	12	14	13	12	12
2.9	10	11	13	12	11	11
3.1	10	10	12	11	10	10
3.3	9	9	11	10	10	10
3.5	9	9	10	10	10	10
3.7	9	9	10	10	10	10
Burnup	50 GWD/MTU	Minimum Cool Time [y] for				
Enrichment	No CEA (Class 1)	No CEA (Class 2)	5 Yr CEA	10 Yr CEA	15 Yr CEA	20 Yr CEA
1.9	27	27	29	27	27	27
2.1	24	24	27	25	24	24
2.3	22	22	25	23	22	22
2.5	19	19	23	21	20	20
2.7	17	17	21	19	18	18
2.9	15	16	19	18	18	18
3.1	15	15	18	17	17	17
3.3	15	15	17	17	17	17
3.5	14	14	15	15	15	15
3.7	14	14	15	15	15	15

Table 5.5.1.1-13 Design Basis Maine Yankee CEA Source Rate at Each Cool Time Analyzed

CEA Cool Time [y]	Source Strength [γ/sec/CEA]
5	1.1690E+14
10	8.3851E+13
15	7.5060E+13
20	6.9771E+13

Table 5.5.1.1-14 Establishment of Dose Rate Limit for Maine Yankee ICI Thimble Analysis

Case	Bottom		Top	
	Rate (mrem/hr)	FSD (%)	Rate (mrem/hr)	FSD (%)
No ICI	8.50	0.7	9.78	0.8
4 Yr Cooled ICI	8.50	0.7	9.87	0.8
Delta			-0.08	
Original Limit			6.71	
Adjusted Limit			6.63	

Table 5.5.1.1-15 Loading Table for Maine Yankee CE14x14 Fuel Containing ICI Thimble

Enrichment [wt %]	Burnup [GWD/MTU]				
	30	35	40	45	50
1.9	6 years	8 years	11 years	18 years	27 years
2.1	6 years	7 years	10 years	16 years	24 years
2.3	6 years	7 years	9 years	14 years	22 years
2.5	6 years	7 years	9 years	13 years	19 years
2.7	6 years	6 years	8 years	11 years	17 years
2.9	5 years	6 years	8 years	10 years	15 years
3.1	5 years	6 years	7 years	10 years	15 years
3.3	5 years	6 years	7 years	9 years	15 years
3.5	5 years	6 years	7 years	9 years	14 years
3.7	5 years	6 years	7 years	9 years	14 years

Table 5.5.1.1-16 Required Cool Time for Maine Yankee Fuel Assemblies with Activated Stainless Steel Replacement Rods

Assy Number	Burnup [GWD/MTU]	Enrichment [wt %]	SSR Source [g/s/assy]	Cool Time [y]	Earliest Load Date
N420	45	3.3	2.1602E+13	10	Jan 2001
N842	35	3.3	3.1396E+12	6	Jan 2001
N868	40	3.3	5.2444E+12	7	Jan 2001
R032	45	3.5	1.4550E+13	9	Jan 2005
R439	50	3.5	1.3998E+13	14	Jan 2010
R444	50	3.5	5.5993E+13	19	Jan 2015

Table 5.5.1.1-17 Maine Yankee Consolidated Fuel Model Parameters

			Actual		Modeled		Required	Cool Time
		No.	Burnup	Enrichment	Burnup	Enrichment	Cool Time	1/1/01
Lattice	Assy	Rods	[MWD/MTU]	[wt %]	[MWD/MTU]	[wt %]	[y]	[y]
CN-1	EF0039	172	5150	1.929	30000	1.9	6	26
CN-10	EF0045	176	17150	1.953	30000	1.9	6	24
	EF0046	107	17150	1.953	30000	1.9	6	24

Table 5.5.1.1-18 Maine Yankee Source Rate Analysis for CN-10 Consolidated Fuel Lattice

Cool Time [y]	No. Rods Present	Decay Heat [kW/cask]	Fuel Neutron [n/s/assy]	Fuel Gamma [g/sec/assy]	Fuel Hardware [g/sec/assy]
6	176	13.9	1.63E+08	3.16E+15	9.28E+12
24	283	7.42	8.41E+07	1.28E+15	8.67E+11
Src Ratio 24/6		0.86	0.83	0.65	0.15

Table 5.5.1.1-19 Loading Table for Maine Yankee CE 14x14 Damaged Fuel

Enrichment [wt % ^{235}U]	Burnup [MWD/MTU]				
	30,000	35,000	40,000	45,000	50,000
1.9	7 years	11 years	19 years	28 years	37 years
2.1	6 years	9 years	16 years	26 years	34 years
2.3	6 years	8 years	14 years	23 years	32 years
2.5	6 years	8 years	12 years	21 years	30 years
2.7	6 years	7 years	11 years	19 years	27 years
2.9	6 years	7 years	10 years	17 years	25 years
3.1	5 years	7 years	9 years	15 years	23 years
3.3	5 years	6 years	8 years	13 years	21 years
3.5	5 years	6 years	8 years	12 years	19 years
3.7	5 years	6 years	7 years	11 years	17 years

Table 5.5.1.1-20 Additional Maine Yankee Non-Fuel Hardware Characterization – Non-Neutron Sources

Item	Waste Volume [ft^3]	Total Curies	^{60}Co Curies
Sb-Be Source 1H1	0.020	4.15E+02	2.22E+02
Sb-Be Source 6H4	0.020	4.32E+02	2.31E+02
CEA Fingertips	0.100	1.06E+02	8.90E+01
ICI String Segment	0.007	2.82E+01	1.76E+01

Table 5.5.1.1-21 Additional Maine Yankee Non-Fuel Hardware Characterization – Neutron Sources

Item	^{238}Pu Grams	^{238}Pu Curies	^{239}Pu Grams	^{239}Pu Curies
Pu-Be Unirradiated Source	1.16	[illegible]	0.24	[illegible]
Pu-Be Irradiated Sources	1.16	5.10E-02	0.24	5.88E-05

Table 5.5.1.1-22 Pu-Be Assy Hardware Spectra (Cycles 1-13) – 9-Year Cool Time from 1/1/1997

Group	Pu-Be SS Hw [g/sec]
1	0.0000E+00
2	0.0000E+00
3	0.0000E+00
4	0.0000E+00
5	1.6598E-15
6	2.1099E+05
7	1.3607E+08
8	5.5885E-09
9	5.7338E+12
10	2.0304E+13
11	1.3362E+09
12	2.3989E+07
13	6.9076E+07
14	1.0929E+09
15	8.3300E+08
16	1.6776E+10
17	6.9545E+10
18	3.5629E+11
TOTAL	4.9691E+12

Table 5.5.1.1-23 Additional Maine Yankee Non-Fuel Hardware – Hardware Assembly Spectra (Class 2 Canister) – 10-Year Cool Time from 1/1/1997

Group	ICI String [g/sec]	CEA Fingertips [g/sec]	Total Gamma [g/sec]
1	0.0000E+00	0.0000E+00	0.0000E+00
2	0.0000E+00	0.0000E+00	0.0000E+00
3	0.0000E+00	0.0000E+00	0.0000E+00
4	0.0000E+00	0.0000E+00	0.0000E+00
5	0.0000E+00	0.0000E+00	0.0000E+00
6	7.7679E+03	2.9198E+04	3.6966E+04
7	5.0096E+06	1.8830E+07	2.3840E+07
8	0.0000E+00	0.0000E+00	0.0000E+00
9	2.1109E+11	7.9347E+11	1.0046E+12
10	7.4750E+11	2.8098E+12	3.5573E+12
11	3.3302E+07	1.2518E+08	1.5848E+08
12	8.8318E+05	3.3197E+06	4.2029E+06
13	2.5431E+06	9.5592E+06	1.2102E+07
14	4.0238E+07	1.5125E+08	1.9149E+08
15	3.0668E+07	1.1528E+08	1.4595E+08
16	6.1764E+08	2.3216E+09	2.9392E+09
17	2.5600E+09	9.6228E+09	1.2183E+10
18	1.2840E+10	4.8265E+10	6.1105E+10
Total	9.7472E+11	3.6639E+12	4.6386E+12

Table 5.5.1.1-24 Additional Maine Yankee Non-Fuel Hardware – Source Assembly Spectra – 10-Year Cool Time from 1/1/1997

	Sb-Be Source	Pu-Be Unirradiated Source		Pu-Be Irradiated Source			
Group	Gamma [g/sec]	Gamma [g/sec]	Neutron [n/sec]	Gamma [g/sec]	Hw Gamma [g/sec]	Total Gamma [g/sec]	Neutron [n/sec]
1	0.0000E+00	1.7724E+00	4.5780E+01	5.6750E-03	0.0000E+00	5.6750E-03	1.4660E-01
2	0.0000E+00	8.6878E+00	3.0620E+03	2.7817E-02	0.0000E+00	2.7817E-02	9.8050E+00
3	0.0000E+00	4.6818E+01	7.7810E+03	1.4991E-01	0.0000E+00	1.4991E-01	2.4920E+01
4	0.0000E+00	1.2370E+02	2.2600E+03	3.9608E-01	0.0000E+00	3.9608E-01	7.2370E+00
5	0.0000E+00	3.9121E+02	1.5280E+03	1.2526E+00	1.6598E-15	1.2526E+00	4.8930E+00
6	1.1900E+05	4.5986E+02	7.9540E+02	1.4722E+00	2.1099E+05	2.1099E+05	2.5470E+00
7	7.6742E+07	8.3349E+02	1.4320E+02	2.6552E+00	1.3607E+08	1.3607E+08	4.5850E-01
8	0.0000E+00	1.4479E+03	-	4.6003E+00	5.5885E-09	4.6003E+00	-
9	3.2338E+12	6.7259E+00	-	1.0044E-04	5.7338E+12	5.7338E+12	-
10	1.1451E+13	8.6431E+03	-	2.7632E+01	2.0304E+13	2.0304E+13	-
11	5.1015E+08	3.7894E+04	-	1.2132E+02	1.3362E+09	1.3362E+09	-
12	1.3530E+07	2.9010E+05	-	9.2911E+02	2.3989E+07	2.3990E+07	-
13	3.8958E+07	8.7568E+03	-	3.4472E+01	6.9076E+07	6.9076E+07	-
14	6.1641E+08	2.6912E+04	-	1.0610E+02	1.0929E+09	1.0929E+09	-
15	4.6980E+08	2.4539E+04	-	8.1311E+01	8.3300E+08	8.3300E+08	-
16	9.4617E+09	1.9698E+07	-	6.3049E+04	1.6776E+10	1.6776E+10	-
17	3.9217E+10	2.7826E+07	-	8.9027E+04	6.9545E+10	6.9545E+10	-
18	1.9670E+11	2.9816E+10	-	9.5465E+07	3.5629E+11	3.5639E+11	-
Total	1.4932E+13	2.9864E+10	1.562E+04	9.5618E+07	2.6484E+13	2.6484E+13	5.001E+01

Table 5.5.1.1-25 Additional Maine Yankee Non-Fuel Hardware – Hardware Assembly Dose Rates (Class 2) – 10-Year Cool Time from 1/1/1997

Group	Normal – Railcar + 2m Dose Gamma Dose [mrem/hr]	Accident - 1m Dose Gamma Dose [mrem/hr]
1	0.00E+00	0.00E+00
2	0.00E+00	0.00E+00
3	0.00E+00	0.00E+00
4	0.00E+00	0.00E+00
5	0.00E+00	0.00E+00
6	7.43E-09	3.42E-08
7	2.39E-06	1.18E-05
8	0.00E+00	0.00E+00
9	1.18E-02	6.91E-02
10	6.70E-03	4.38E-02
11	2.01E-08	1.52E-07
12	2.44E-11	2.08E-10
13	1.28E-13	1.31E-12
14	1.30E-18	1.72E-17
15	1.21E-34	1.99E-33
16	0.00E+00	0.00E+00
17	0.00E+00	0.00E+00
18	0.00E+00	0.00E+00
Total	1.85E-02	1.13E-01

Table 5.5.1.1-26 Additional Maine Yankee Non-Fuel Hardware – Transport Cask Source Assembly Surface Dose Rates – Normal Conditions – 2m + Railcar Dose – 10-Year Cool Time from 1/1/1997

	Sb-Be Source Dose	Pu-Be Unirradiated Source Dose		Pu-Be Irradiated Source Dose	
Group	Gamma [mrem/hr]	Gamma [mrem/hr]	Neutron [mrem/hr]	Gamma [mrem/hr]	Neutron [mrem/hr]
1	0.00E+00	1.16E-12	1.12E-07	3.71E-15	3.59E-10
2	0.00E+00	6.35E-12	4.09E-06	2.03E-14	1.31E-08
3	0.00E+00	3.16E-11	9.39E-06	1.01E-13	3.01E-08
4	0.00E+00	6.62E-11	1.93E-06	2.12E-13	6.20E-09
5	0.00E+00	1.43E-10	1.04E-06	4.57E-13	3.33E-09
6	2.39E-08	9.25E-11	4.13E-07	4.24E-08	1.32E-09
7	7.69E-06	8.35E-11	3.55E-08	1.36E-05	1.14E-10
8	0.00E+00	5.46E-11		1.73E-13	
9	3.80E-02	7.90E-14		6.73E-02	
10	2.16E-02	1.63E-11		3.83E-02	
11	6.49E-08	4.82E-12		1.70E-07	
12	7.84E-11	1.68E-12		1.39E-10	
13	4.13E-13	9.28E-17		7.32E-13	
14	4.17E-18	1.82E-22		7.39E-18	
15	3.90E-34	2.04E-38		6.91E-34	
16	0.00E+00	0.00E+00		0.00E+00	
17	0.00E+00	0.00E+00		0.00E+00	
18	0.00E+00	0.00E+00		0.00E+00	
Total	5.96E-02	5.01E-10	1.70E-05	1.06E-01	5.45E-08

Table 5.5.1.1-27 Additional Maine Yankee Non-Fuel Hardware – Transport Cask Source Assembly Surface Dose Rates – Accident Conditions – 1m Dose – 10-Year Cool Time from 1/1/1997

	Sb-Be Source Dose	Pu-Be Unirradiated Source Dose		Pu-Be Irradiated Source Dose	
Group	Gamma [mrem/hr]	Gamma [mrem/hr]	Neutron [mrem/hr]	Gamma [mrem/hr]	Neutron [mrem/hr]
1	0.00E+00	4.04E-12	7.22E-06	1.29E-14	2.31E-08
2	0.00E+00	2.27E-11	3.80E-04	7.28E-14	1.22E-06
3	0.00E+00	1.18E-10	9.62E-04	3.79E-13	3.08E-06
4	0.00E+00	2.63E-10	2.43E-04	8.42E-13	7.78E-07
5	0.00E+00	6.06E-10	1.46E-04	1.94E-12	4.67E-07
6	1.10E-07	4.25E-10	6.96E-05	1.95E-07	2.23E-07
7	3.79E-05	4.12E-10	5.61E-06	6.73E-05	1.80E-08
8	0.00E+00	2.94E-10		9.33E-13	
9	2.22E-01	4.63E-13		3.94E-01	
10	1.41E-01	1.06E-10		2.50E-01	
11	4.89E-07	3.64E-11		1.28E-06	
12	6.70E-10	1.44E-11		1.19E-09	
13	4.23E-12	9.50E-16		7.49E-12	
14	5.52E-17	2.41E-21		9.79E-17	
15	6.41E-33	3.35E-37		1.14E-32	
16	0.00E+00	0.00E+00		0.00E+00	
17	0.00E+00	0.00E+00		0.00E+00	
18	0.00E+00	0.00E+00		0.00E+00	
Total	3.63E-01	2.30E-09	1.81E-03	6.44E-01	5.81E-06

5.5.1.2 Maine Yankee Site Specific GTCC Waste

Source terms, decay heat, and dose rates are calculated for the Maine Yankee Greater Than Class C (GTCC) waste to be transported in the Universal Transport Cask. The calculations are performed by first determining the gamma source spectra and decay heat from the GTCC isotopics, then using the gamma source information to calculate radial and axial dose rates. The results of these calculations show that the dose rates produced by the GTCC waste are bounded by the dose rates previously calculated for the design basis spent fuel, as presented in Section 5.1.3. Detailed results for the Maine Yankee GTCC waste are presented in Section 5.5.1.2.4.

5.5.1.2.1 GTCC Waste Transport Configuration

The GTCC waste basket is described in Section 1.3.1.1.2. The GTCC waste material is loaded into a cylindrical shell that is 3 inches thick. The cavity is divided into two loading sections using an insert that is placed into the GTCC basket after loading the bottom section. Each of the two sections may contain up to 10,000 pounds of waste, for a total of 20,000 pounds per canister.

5.5.1.2.2 GTCC Waste Source Term

The radionuclide inventories presented in Table 5.5.1.2-1 are utilized to develop the bounding source spectra and decay heat. These bounding radionuclide inventories are developed from information provided by the utility of all significant isotopes in the activated metal to be transported. The decay heat resulting from this source term is 4,490 watts.

The gamma source spectra presented in Table 5.5.1.2-2 is produced from the radionuclide inventory presented in Table 5.5.1.2-1. This information is used to derive the total gamma source strength which is utilized along with the homogenized source volume to calculate the uniformly distributed source strength per unit volume, as shown in Table 5.5.1.2-3.

The source volume information presented in Table 5.5.1.2-3 is based on the cylindrical region of the basket and the 77-inch (195.58 cm) length of each of the two GTCC canister loading cavities. These dimensions are used to determine the volumetric source strength and homogenized material densities that are used as input in the SAS1 sequence of the SCALE 4.3 computer code package to calculate external dose rates.

5.5.1.2.3 GTCC Waste Shielding Models

The radial and top axial models for the transport cask are described in the following sections. The relevant dimensions of the GTCC basket/canister within the transport cask are taken from the drawings presented in Section 1.3.4.

5.5.1.2.3.1 Radial Models

The 1-D radial models consist of a series of infinitely long concentric cylinders representing a cross section taken at a point along the length of the GTCC source cavity region of the GTCC basket/canister. The nested cylindrical regions consist of the following regions and cumulative thicknesses:

1.	Homogenized waste source region	61.900 cm
2.	GTCC basket stainless steel shield	7.620 cm
3.	Basket support disks	13.690 cm
4.	Canister stainless steel shell	1.588 cm
5.	Gap	0.698 cm
6.	Transport cask stainless steel inner shell	5.080 cm
7.	Transport cask lead gamma shielding	6.871 cm
8.	Transport cask lead gap	0.114 cm
9.	Transport cask stainless steel outer shell	6.985 cm
10.	Transport cask NS-4-FR neutron shielding	11.430 cm
11.	Transport cask stainless steel neutron shield shell	0.635 cm

The SAS1 input is generated using these regions, and specifying a buckling height of 391.16 cm, which is equal to the two 77-inch (195.58 cm) loading cavity heights within the GTCC basket.

5.5.1.2.3.2 Top Axial Models

The 1-D SAS1 top axial models consist of a series of infinite slabs representing the GTCC waste, canister and cask materials. Both the normal and accident conditions models are symmetric about the bottom of the top source region, assuming that the bottom region source does not penetrate the 3-inch separator plate and top source region sufficiently to contribute to the dose rate at the top of the cask. The slabs modeled for the top axial normal condition models are:

1.	Homogenized waste source region	195.580 cm
2.	Basket stainless steel top lid	3.810 cm
3.	Canister stainless steel shield lid	17.780 cm
4.	Canister stainless steel structural lid	7.620 cm
5.	Transport Cask stainless steel lid	16.510 cm
6.	Impact Limiter stainless steel inner shell	0.635 cm
7.	Impact Limiter redwood	75.565 cm
8.	Impact Limiter balsa wood	3.810 cm
9.	Impact Limiter stainless steel outer shell	0.635 cm

The SAS1 input is generated using these regions, and specifying a buckling diameter of 170.4 cm, which is equal to the diameter of the canister. This buckling is conservative, as the value is larger than the actual source diameter of approximately 124 cm.

5.5.1.2.3.3 Bottom Axial Models

Like the 1-D top axial models, the 1-D bottom axial models represent the canister and cask materials as a series of infinite slabs. Both the normal and accident conditions models are symmetric about the top of the bottom source region, assuming that the top region source does not penetrate the 3-inch separator plate and bottom source region sufficiently to contribute to the dose rate at the bottom of the cask. The slabs modeled for the bottom axial normal condition models are:

1.	Homogenized waste source region	195.580 cm
2.	Basket stainless steel bottom plate	7.620 cm
3.	Canister stainless steel bottom	4.445 cm
4.	Transport cask spacer (modeled as void)	42.545 cm
5.	Transport cask stainless steel inner bottom plate	10.795 cm
6.	Transport cask NS-4-FR neutron shielding	2.540 cm
7.	Transport cask stainless steel outer bottom plate	12.700 cm
8.	Impact Limiter stainless steel inner shell	0.635 cm
9.	Impact Limiter redwood	75.565 cm
10.	Impact Limiter balsa wood	3.810 cm
11.	Impact Limiter stainless steel outer shell	0.635 cm

The SAS1 input is generated using these regions, and specifying a buckling diameter of 170.4 cm, which is equal to the diameter of the canister. This buckling is conservative, as the value is larger than the actual source diameter of approximately 124 cm.

5.5.1.2.4 GTCC Waste Dose Rate Results

The models described in the previous sections were analyzed using the SAS1 1-D code. The resulting dose rates were multiplied by a 20% peaking factor to provide additional conservatism to the results. This conservative factor accounts for potential non-uniformity in the radionuclide distribution within the GTCC waste material and for potential shifting of the waste material during transport.

The Transport Cask containing Maine Yankee GTCC waste produces external dose rates below those calculated for the design basis PWR fuel loading. This ensures that the GTCC waste will meet all 10CFR71 normal and accident shielding requirements. During normal operation 10 CFR 71.47 requires the package surface dose rate be less than 200 mrem/hr and the dose rate two meters from the transportation vehicle not exceed 10 mrem/hr, including the conservative peaking factor.

As presented in Table 5.5.1.2-4, the highest calculated normal condition package surface dose rate is 33 mrem/hr, which occurs on the radial surface. Likewise, the highest package dose rate at 2 meters from the surface is 9.24 mrem/hr.

During accident conditions, 10 CFR 71.51 limits the dose rate to 1000 mrem/hr at 1 meter from the package surface. The maximum dose rate at 1 meter from the radial surface, as shown in Table 5.5.1.2-5, considering the combined accident of a loss of neutron shielding and lead slump, is 204 mrem/hr.

Table 5.5.1.2-1 Design Basis GTCC Source Term

Radionuclide	Curie Inventory
H-3	3.00E+02 Ci
C-14	1.50E+02 Ci
MN-54	3.50E+02 Ci
FE-55	2.00E+05 Ci
CO-58	1.00E+01 Ci
CO-60	2.90E+05 Ci
NI-59	8.20E+02 Ci
NI-63	9.00E+04 Ci
NB-94	1.00E+01 Ci
TC-99	1.00E+01 Ci
Total	5.82E+05 Ci

Table 5.5.1.2-2 Design Basis GTCC Gamma Source Spectra

Energy Range			Gamma/sec	MeV/sec	Normalized Gamma/sec
8.00E+00	to	1.00E+01	0.00E+00	0.00E+00	0.00E+00
6.50E+00	to	8.00E+00	0.00E+00	0.00E+00	0.00E+00
5.00E+00	to	6.50E+00	0.00E+00	0.00E+00	0.00E+00
4.00E+00	to	5.00E+00	0.00E+00	0.00E+00	0.00E+00
3.00E+00	to	4.00E+00	0.00E+00	0.00E+00	0.00E+00
2.50E+00	to	3.00E+00	1.76E+08	4.84E+08	7.96E-09
2.00E+00	to	2.50E+00	1.13E+11	2.55E+11	5.14E-06
1.66E+00	to	2.00E+00	1.75E+09	3.20E+09	7.92E-08
1.33E+00	to	1.66E+00	4.78E+15	7.15E+15	2.16E-01
1.00E+00	to	1.33E+00	1.69E+16	1.97E+16	7.66E-01
8.00E-01	to	1.00E+00	1.35E+13	1.21E+13	6.09E-04
6.00E-01	to	8.00E-01	3.92E+11	2.74E+11	1.77E-05
4.00E-01	to	6.00E-01	1.71E+11	8.57E+10	7.76E-06
3.00E-01	to	4.00E-01	9.12E+11	3.19E+11	4.13E-05
2.00E-01	to	3.00E-01	6.96E+11	1.74E+11	3.15E-05
1.00E-01	to	2.00E-01	1.40E+13	2.10E+12	6.33E-04
5.00E-02	to	1.00E-01	5.80E+13	4.35E+12	2.63E-03
1.00E-02	to	5.00E-02	2.95E+14	8.84E+12	1.33E-02
TOTALS			2.21E+16	2.69E+16	1.00E+00

Table 5.5.1.2-3 Design Basis GTCC Source Strength

Parameter	Value
Total Source Strength	2.21E+16 gamma/sec
Equivalent Source Radius	61.9 cm
Equivalent Source Length	391.16 cm
Equivalent Source Volume	4.709E+06 cc
Weight Volume Fraction	2.438E-01
Volumetric Source	4.69E+09 gamma/sec/cc

Table 5.5.1.2-4 GTCC Waste Dose Rate Results – Normal Conditions of Transport

Location	Surface	2 Meters from Surface
Radial	32.66 mr/hr	9.24 mr/hr
Top Axial	0.21 mr/hr	0.06 mr/hr
Bottom Axial	3.11 mr/hr	0.91 mr/hr

Table 5.5.1.2-5 GTCC Waste Dose Rate Results – Accident Conditions

Location	1 Meter from Surface
Radial	203.94 mr/hr
Top Axial	1.18 mr/hr
Bottom Axial	23.51 mr/hr

List of Figures

Figure 6.3-1 Universal Transport Cask KENO-Va PWR Basket Cell Model 6.3-9

Figure 6.3-2 Universal Transport Cask KENO-Va BWR Basket Cell Model 6.3-10

Figure 6.3-3 Universal Transport Cask PWR KENO-Va Cask Model 6.3-11

Figure 6.3-4 Universal Transport Cask BWR KENO-Va Cask Model 6.3-12

Figure 6.3-5 PWR Basket Criticality Control Design 6.3-13

Figure 6.3-6 BWR Basket Criticality Control Design 6.3-14

Figure 6.4-1 Visage Slice – Hypothetical Shifting of PWR Fuel 6.4-22

Figure 6.4-2 Visage Slice – Hypothetical Shifting of BWR Fuel 6.4-23

Figure 6.5-1 KENO-Va Validation - 27 Group Library Results: Frequency Distribution of k_{eff} Values 6.5-11

Figure 6.5-2 KENO-Va Validation - 27 Group Library Results: k_{eff} versus Enrichment 6.5-12

Figure 6.5-3 KENO-Va Validation - 27 Group Library Results: k_{eff} versus Rod Pitch 6.5-13

Figure 6.5-4 KENO-Va Validation - 27 Group Library Results: k_{eff} versus H/U Volume Ratio 6.5-14

Figure 6.5-5 KENO-Va Validation - 27 Group Library Results: k_{eff} versus Average Group of Fission 6.5-15

Figure 6.5-6 KENO-Va Validation - 27 Group Library Results: k_{eff} versus ^{10}B Loading for Flux Trap Criticals 6.5-16

Figure 6.5-7 KENO-Va Validation - 27 Group Library Results: k_{eff} versus Flux Trap Critical Gap Thickness 6.5-17

List of Figures (Continued)

Figure 6.5-8 USLSTATS Output for Fuel Enrichment Study 6.5-18

Figure 6.5-9 MONK8A – JEF 2.2 Library Validation Statistics - k_{eff} versus Fuel Enrichment 6.5-20

Figure 6.5-10 MONK8A – JEF 2.2 Library - k_{eff} versus Rod Pitch 6.5-21

Figure 6.5-11 MONK8A – JEF 2.2 Library - k_{eff} versus H/U (fissile) Atom Ratio 6.5-22

Figure 6.5-12 MONK8A – JEF 2.2 Library - k_{eff} versus ^{10}B Loading 6.5-23

Figure 6.5-13 MONK8A – JEF 2.2 Library – keff versus Mean Neutron Log(E) Causing Fission 6.5-24

Figure 6.5-14 MONK8A – JEF 2.2 Library - k_{eff} versus Cluster Gap Thickness 6.5-25

Figure 6.5-15 MONK8A – JEF 2.2 Library – k_{eff} versus Fuel Pellet Outside Diameter 6.5-26

Figure 6.5-16 MONK8A – JEF 2.2 Library - k_{eff} versus Fuel Rod Outside Diameter 6.5-27

Figure 6.5-17 USLSTATS Output – k_{eff} versus Gap Thickness 6.5-28

Figure 6.6.1.1-1 24 Removed Fuel Rods – Diamond Shaped Geometry, Maine Yankee Site Specific Fuel 6.6.1-12

Figure 6.6.1.1-2 Consolidated Fuel Geometry, 113 Empty Fuel Rod Positions, Maine Yankee Site Specific Fuel 6.6.1-13

Figure 6.6.2-1 CSAS Input & Output for Normal Conditions Criticality Analysis: PWR Fuel 6.6.2-2

List of Figures (Continued)

Figure 6.6.2-2 CSAS Input & Output for Accident Conditions Criticality Analysis: PWR Fuel 6.6.2-25

Figure 6.6.2-3 CSAS Input & Output for Normal Conditions Criticality Analysis: BWR Fuel 6.6.2-49

Figure 6.6.2-4 CSAS Input & Output for Accident Conditions Criticality Analysis: BWR Fuel 6.6.2-74

Figure 6.6.3-1 MONK8a Input File - UMS Transport Cask PWR Top End Impact 6.6.3-2

Figure 6.6.3-2 MONK8a Output Summary – UMS Transport Cask PWR Top End Impact 6.6.3-11

Figure 6.6.3-3 MONK8a Input File –UMS Transport Cask BWR Top End Impact 6.6.3-17

Figure 6.6.3-4 MONK8a Output Summary – UMS Transport Cask BWR Top End Impact 6.6.3-29

List of Tables

Table 6.1-1 Summary of Criticality Analysis Results 6.1-3

Table 6.2-1 PWR Fuel Assembly Characteristics (Zirc-4 Clad) 6.2-2

Table 6.2-2 BWR Fuel Assembly Characteristics (Zirc-2 Clad) 6.2-3

Table 6.2-3 UMS Transport Cask Top End Impact Bounding Fuel Dimensions 6.2-4

Table 6.4-1 k_{eff} for Most Reactive PWR Fuel Assembly Determination (1.0-in. Web) 6.4-24

Table 6.4-2 k_{eff} for Highest Reactivity Assemblies in 1.5 in. Web (Dry Gap) 6.4-24

Table 6.4-3 k_{eff} for Most Reactive BWR Fuel Assembly Determination 6.4-25

Table 6.4-4 PWR Fuel Tube in Basket KENO-Va Results for Geometric Tolerances and Mechanical Perturbations 6.4-26

Table 6.4-5 PWR Basket in Cask KENO-Va Results for Geometric Tolerances and Tube Movement 6.4-26

Table 6.4-6 BWR Basket in Cask KENO-Va Results for Geometric Tolerances and Mechanical Perturbations 6.4-27

Table 6.4-7 PWR Single Cask Analysis Criticality Results 6.4-28

Table 6.4-8 PWR Cask Array Analysis Criticality Results - Normal Condition - Dry Interior 6.4-28

Table 6.4-9 PWR Cask Array Analysis Criticality Results - Accident Condition - Wet Interior 6.4-29

Table 6.4-10 PWR Cask Array Analysis Criticality Results—Mist Exterior 6.4-29

Table 6.4-11 BWR Single Cask Analysis Criticality Results 6.4-30

Table 6.4-12 BWR Cask Array Analysis Criticality Results - Normal Condition - Dry Interior 6.4-30

Table 6.4-13 BWR Cask Array Analysis Criticality Results - Accident Condition - Wet Interior 6.4-31

Table 6.4-14 BWR Cask Array Analysis Criticality Results—Mist Exterior 6.4-31

List of Tables (Continued)

Table 6.4-15 BWR Cask Array Analysis Criticality Results – Variable Exterior 6.4-32

Table 6.4-16 Heterogeneous vs. Homogeneous Enrichment Analysis Results (GE) 6.4-32

Table 6.4-17 PWR Lattice Parameter Study Criticality Analysis Results 6.4-33

Table 6.4-18 BWR Lattice Parameter Study Criticality Analysis Results 6.4-34

Table 6.5-1 KENO-Va and 27-Group Library Validation Statistics 6.5-30

Table 6.5-2 Scale 4.3 Correlation Coefficient for Linear Curve-Fit of Critical Benchmarks 6.5-33

Table 6.5-3 Scale 4.3 Range of Correlated Parameters of Most Reactive Configurations 6.5-33

Table 6.5-4 MONK8A Range of Correlated Parameters for Design Basis Fuel 6.5-34

Table 6.5-5 MONK8A – Correlation Coefficient for Linear Curve-Fit of Critical Benchmarks 6.5-34

Table 6.5-6 MONK8A – JEF 2.2 Library Validation Statistics 6.5-35

Table 6.6.1.1-1 Maine Yankee Standard Fuel Characteristics 6.6.1-14

Table 6.6.1.1-2 Maine Yankee Most Reactive Fuel Dimensions 6.6.1-14

Table 6.6.1.1-3 Maine Yankee Pellet Diameter Study 6.6.1-15

Table 6.6.1.1-4 Maine Yankee Annular Fuel Results 6.6.1-15

Table 6.6.1.1-5 Maine Yankee Removed Fuel Rod Results with Small Pellet Diameter 6.6.1-16

Table 6.6.1.1-6 Maine Yankee Removed Fuel Rod Results with Maximum Pellet Diameter 6.6.1-17

List of Tables (Continued)

Table 6.6.1.1-7 Maine Yankee Fuel Rods in Guide Tubes Results 6.6.1-18

Table 6.6.1.1-8 Maine Yankee Consolidated Fuel Empty Fuel Rod Position Results 6.6.1-19

Table 6.6.1.1-9 Fuel Can Infinite Height Model Results of Fuel – Water Mixture Between Rods 6.6.1-20

Table 6.6.1.1-10 Fuel Can Finite Model Results of Fuel – Water Mixture Outside BORAL Coverage 6.6.1-21

Table 6.6.1.1-11 Fuel Can Finite Model Results of Replacing All Rods with Fuel – Water Mixture 6.6.1-22

Table 6.6.1.1-12 Infinite Height Analysis of Maine Yankee Start-up Sources 6.6.1-23

6.2 Package Fuel Loading

The Universal Transport Cask is designed to transport one of five Transportable Storage Canisters of different lengths. Each canister is specifically designed to accommodate one of three classes of PWR fuel assemblies or one of two classes of BWR fuel assemblies. The classification of the fuel assemblies is based primarily on fuel assembly length and cross section. The classes of major fuel assemblies to be transported in the cask and their characteristics are shown in Tables 6.2-1 (PWR) and 6.2-2 (BWR). Limiting fuel axial dimensions for each class are provided in Table 6.2-3.

Table 6.2-1 PWR Fuel Assembly Characteristics (Zirc-4 Clad)

Fuel Class	Vendor	Array	Version	Max MTU	No of Fuel Rods	Pitch (in)	Rod Dia. (in)	Clad Thick (in)	Pellet Dia (in)	Active Length (in)
1	CE	14 x 14	Std.	0.4037	176	0.5800	0.440	0.0280	0.3765	137.0
1	CE	14 x 14	Ft Cal.	0.3772	176	0.5800	0.440	0.0280	0.3765	128.0
1	CE	15 x 15	Palis.	0.4317	216	0.5500	0.418	0.0260	0.3580	132.0
1	CE	16 x 16	Lucie 2	0.4025	236	0.5060	0.382	0.0230	0.3255	136.7
1	Ex/ANF	14 x 14	WE	0.3689	179	0.5560	0.424	0.0300	0.3505	142.0
1	Ex/ANF	14 x 14	CE	0.3814	176	0.5800	0.440	0.0310	0.3700	134.0
1	Ex/ANF	14 x 14	Praire Isl.	0.3741	179	0.5560	0.417	0.0300	0.3505	144.0
1	Ex/ANF	15 x 15	WE	0.4410	204	0.5630	0.424	0.0300	0.3565	144.0
1	Ex/ANF	15 x 15	Palis	0.4310	216	0.5500	0.417	0.0300	0.3580	131.8
1	Ex/ANF	17 x 17	WE	0.4123	264	0.4960	0.360	0.0250	0.3030	144.0
1	WE	14 x 14	Std/ZCA	0.4144	179	0.5560	0.422	0.0225	0.3674	145.2
1	WE	14 x 14	OFA	0.3612	179	0.5560	0.400	0.0243	0.3444	144.0
1	WE	14 x 14	Std/ZCB	0.4144	179	0.5560	0.422	0.0225	0.3674	145.2
1	WE	14 x 14	CE Model	0.4115	176	0.5800	0.440	0.0260	0.3805	136.7
1	WE	15 x 15	Std	0.4646	204	0.5630	0.422	0.0242	0.3659	144.0
1	WE	15 x 15	Std/ZC	0.4646	204	0.5630	0.422	0.0242	0.3659	144.0
1	WE	15 x 15	OFA	0.4646	204	0.5630	0.422	0.0242	0.3659	144.0
1	WE	17 x 17	Std	0.4671	264	0.4960	0.374	0.0225	0.3225	144.0
1	WE	17 x 17	OFA	0.4282	264	0.4960	0.360	0.0225	0.3088	144.0
1	WE	17 x 17	Vant 5	0.4282	264	0.4960	0.360	0.0225	0.3088	144.0
2	B&W	15 x 15	Mark B	0.4807	208	0.5680	0.430	0.0265	0.3686	144.0
2	B&W	15 x 15	Mark BZ	0.4807	208	0.5680	0.430	0.0265	0.3686	144.0
2	B&W	17 x 17	Mark C	0.4658	264	0.5020	0.379	0.0240	0.3232	143.0
3	CE	16 x 16	Sono 2&3	0.4417	236	0.5060	0.382	0.0230	0.3255	150.0
3	CE	16 x 16	ANO2	0.4417	236	0.5060	0.382	0.0230	0.3255	150.0
3	CE	16 x 16	SYS80	0.4417	236	0.5060	0.382	0.0230	0.3255	150.0

Figure 6.4-2 Visage Slice - Hypothetical Shifting of BWR Fuel

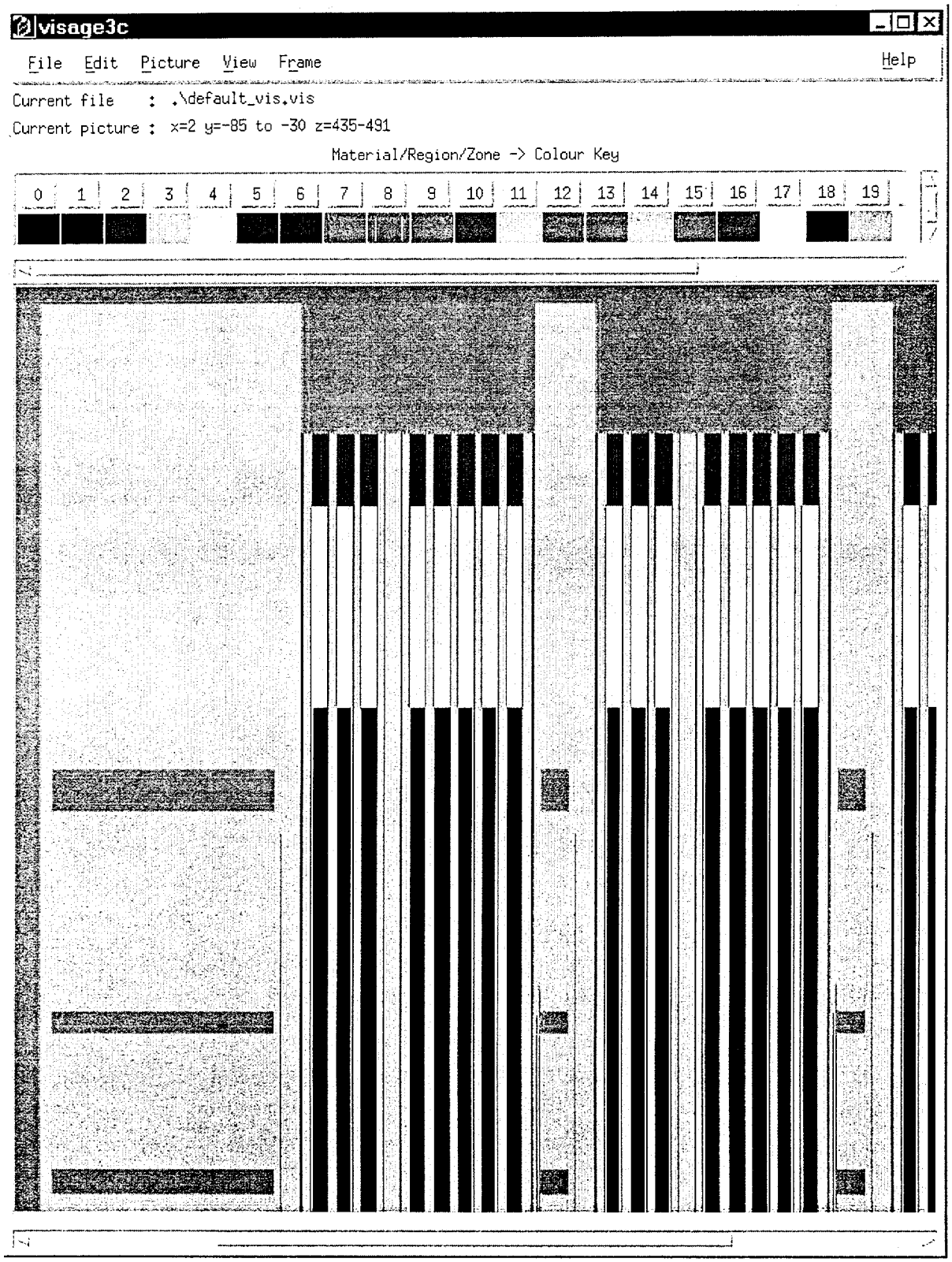

Table 6.4-1 k_{eff} for Most Reactive PWR Fuel Assembly Determination (1.0-in. Web)

Assembly Type	Dry Gap		Wet Gap		Δk_{eff} Wet - Dry
	k_{eff}	σ	k_{eff}	σ	
B&W 15x15 Mark B4	0.9613	0.0011	0.9692	0.0012	0.0079
B&W 17x17 Mark C	0.9621	0.0012	0.9705	0.0011	0.0084
CE 14x14	0.9295	0.0013	0.9381	0.0011	0.0085
CE 16x16 SYS 80	0.9348	0.0012	0.9442	0.0012	0.0095
West 14x14	0.9177	0.0013	0.9264	0.0012	0.0086
West 14x14 OFA	0.9238	0.0012	0.9326	0.0012	0.0088
West 15x15	0.9662	0.0011	0.9712	0.0012	0.0050
West 17x17	0.9596	0.0012	0.9673	0.0012	0.0077
West 17x17 OFA	0.9656	0.0013	0.9727	0.0012	0.0070
Ex/ANF 14x14 CE	0.9309	0.0012	0.9362	0.0011	0.0053
Ex/ANF 14x14 WE	0.9065	0.0012	0.9176	0.0011	0.0111
Ex/ANF 15x15 WE	0.9559	0.0012	0.9634	0.0013	0.0074
Ex/ANF 17x17 WE	0.9631	0.0012	0.9704	0.0012	0.0073

Table 6.4-2 k_{eff} for Highest Reactivity Assemblies in 1.5-in. Web (Dry Gap)

Assembly Type	k_{eff}	σ
B&W 15x15 Mark B4	0.9119	0.0011
B&W 17x17 Mark C	0.9141	0.0011
West 15x15	0.9147	0.0013
West 17x17	0.9116	0.0012
West 17x17 OFA	0.9196	0.0012
Ex/ANF 17x17 WE	0.9172	0.0011

NUREG/CR-6361. However, if no strong correlation can be determined, then a constant bias adjustment can be made. This is typically done with a one-side tolerance factor that guarantees 95% confidence in the uncertainty in the bias. This is the approach taken in the UMS criticality analysis.

Both NUREG/CR-6361 and the NAC evaluation perform regression analysis on key system parameters. For all of the major system parameters, the evaluation found no strong correlation. This is based on the observation that the correlation coefficients are all much less than ± 1. Thus a constant bias with a 95/95 confidence factor is applied to the system k_{eff}. NAC's statistical analysis of the k_{eff} results produced a bias of 0.0052 and a 95/95 uncertainty of 0.0087. Adding the two together and subtracting from 0.95 yields an effective constant USL of 0.9361.

To assure compliance with NUREG/CR-6361, an upper safety limit is generated using USLSTATS and is compared to the constant NAC bias and bias uncertainty used in Section 6.5.2.

To evaluate the relative importance of the trend analysis to the upper safety limits, correlation coefficients are required for all independent parameters. Table 6.5-2 contains the correlation coefficient, R, for each linear fit of k_{eff} versus experimental parameter (data is extracted from Figure 6.5-2 through Figure 6.5-7 by taking the square root of the R^2 value). Based on the highest correlation coefficient and the method presented in NUREG/CR-6361, a USL is established based on the variation of k_{eff} with enrichment. Note that even the enrichment function shows a low statistical correlation coefficient (an $|R|$ equal or near 1 would indicate a good fit). The output generated by USLSTATS is shown in Figure 6.5-8.

The NAC applied USL of 0.9361 bounds the calculated upper safety limits for all enrichment values above 3.0 wt % ^{235}U. Since the maximum reactivities in the UMS are calculated at enrichments well above this level, the existing bias bounds the NUREG calculated USL. The most reactive UMS configuration is the PWR basket configuration with Westinghouse 17x17 OFA fuel assemblies. The parameters of the most reactive fuel configuration for the UMS design basis fuel and for the Maine Yankee fuel are presented in Table 6.5-3. This table also compares the most reactive fuel parameters to the minimum and maximum benchmark values to demonstrate the applicability of the critical benchmarks.

6.5.5 MONK Validation in Accordance with NUREG/CR-6361

NUREG/CR-6361, "Criticality Benchmark Guide for Light-Water-Reactor Fuel in Transportation and Storage Packages" (NUREG), provides a guide to LWR criticality benchmark calculations and the determination of bias and subcritical limits in critical safety evaluations. Section 6.5.4 presents the implementation of the NUREG in subcritical limit evaluations for the UMS® Transport Cask. This section implements the ULSTATS method of the NUREG for MONK8A application with JEF 2.2 point energy libraries in LWR transport and storage applications.

AEA Technologies has performed an extensive benchmarking of MONK8A. Critical benchmarks relevant to LWR fuel evaluations were extracted from the total benchmark set and listed in Table 6.5-6. The range of the parameters to be benchmarked is summarized in Table 6.5-4. Trending in k_{eff} was evaluated for the following independent variables: enrichment, rod pitch, fuel pellet diameter, fuel rod diameter, H/U ratio, average neutron group causing fission, ^{10}B loading for flux trap cases, and flux trap gap thickness. The data is plotted in Figures 6.5-9 through 6.5-16.

To evaluate the relative importance of the trend analysis to the upper safety limits, correlation coefficients are required for all independent parameters. Table 6.5-5 contains the correlation coefficient, R, for each linear fit of k_{eff} versus experimental parameter (data is extracted from Figure 6.5-9 through Figure 6.5-16 by taking the square root of the R^2 value). Based on the highest correlation coefficient and the method presented in NUREG/CR-6361, a USL is established based on the variation of k_{eff} with flux trap thickness. Note that even the flux trap function shows a low statistical correlation coefficient (an |R| equal or near 1 would indicate a good fit). The output generated by USLSTATS is shown in Figure 6.5-17.

The NAC applied USL is 0.9425, and bounds the calculated upper safety limits for the typical flux trap spacing found in multi-purpose casks. The range of the correlated parameters of the most reactive design basis fuel is included in Table 6.5-4 to show that the most reactive configuration is within the range of applicability of the validation.

Table 6.5-2 Scale 4.3 Correlation Coefficient for Linear Curve-Fit of Critical Benchmarks

Correlation Studied	Correlation Coefficient (R)
k_{eff} versus enrichment	0.361
k_{eff} versus rod pitch	0.328
k_{eff} versus H/U volume ratio	0.246
k_{eff} versus ^{10}B loading	0.069
k_{eff} versus average group causing fission	0.133
k_{eff} versus flux gap thickness	0.137

Table 6.5-3 Scale 4.3 Range of Correlated Parameters of Most Reactive Configurations

Parameter	Benchmark Minimum Value	Benchmark Maximum Value	UMS Design Basis PWR Fuel Most Reactive Configuration	Maine Yankee Fuel Most Reactive Configuration
Enrichment (wt. % ^{235}U)	2.35	4.74	4.2	4.2
Rod pitch (cm)	1.26	2.54	1.26	1.50
H/U volume ratio	1.6	11.5	1.9	2.6
^{10}B areal density (g/cm^2)	0.00	0.45	0.025	0.025
Average energy group causing fission	21.7	24.2	22.3	22.5
Flux gap thickness (cm)	0.64	5.16	2.2 to 3.8	2.22 to 3.8

Table 6.5-4 MONK8A Range of Correlated Parameters for Design Basis Fuel

Parameter	Benchmark Minimum Value	Benchmark Maximum Value	Design Basis (WE 17x17 OFA)
Enrichment (wt % ^{235}U)	2.35	7.00	4.20
Rod pitch (cm)	1.26	2.54	1.26
H/U (fissile) atomic ratio	97.08	453.84	111.31
^{10}B loading (g/cm^2)	0.000	0.072	0.025
Log energy causing fission	7.31E-08	3.33E-07	2.39E-07
Cluster gap thickness (cm)	0.0	11.92	2.22-3.81
Fuel diameter (cm)	0.743	1.265	0.7844
Clad diameter (cm)	0.8324	1.4150	0.9144

Table 6.5-5 MONK8A – Correlation Coefficient for Linear Curve-Fit of Critical Benchmarks

Correlation Studied	Correlation Coefficient (R)
k_{eff} versus enrichment	0.390
k_{eff} versus rod pitch	0.140
k_{eff} versus H/U (fissile) atomic ratio	0.369
k_{eff} versus ^{10}B loading	0.273
k_{eff} versus log energy causing fission	0.127
k_{eff} versus cluster gap thickness	0.532
k_{eff} versus fuel diameter	0.236
k_{eff} versus clad diameter	0.185

6.6.1 Criticality Evaluation for Site Specific Contents

This section presents the criticality evaluation for the fuel assembly types or configurations that are unique to specific reactor sites. Site specific spent fuel content configurations result from conditions that occurred during reactor operations, participation in research and development programs, testing programs intended to improve reactor operations, and from decommissioning activities.

Site specific fuel assembly configurations are either shown to be bounded by the analysis of the standard design basis fuel assembly configuration of the same type (PWR or BWR), or are shown to be acceptable contents by specific evaluation of the configuration.

6.6.1.1 Criticality Evaluation for Maine Yankee Site Specific Spent Fuel

Loading the transport cask with the standard CE 14x14 fuel assembly is shown in Section 6.4 to be less reactive than loading the cask with the most reactive Westinghouse 17x17 OFA criticality design basis spent fuel. This analysis addresses variations in fuel assembly dimensions, variable enrichment axial zoning patterns, annular axial fuel blankets, removed fuel rods or empty rod positions, fuel rods placed in guide tubes, fuel assemblies with an inserted start-up source, or other non-fuel items or components, consolidated fuel assemblies, damaged fuel and fuel debris. These configurations are not included in the standard fuel analysis, but are present in the site fuel inventory that must be transported.

6.6.1.1.1 Maine Yankee Fuel Criticality Model

The criticality evaluations of the Maine Yankee fuel inventory require the basket cell and basket in cask models described in Sections 6.3 and 6.4. The basket cell model is principally employed in the most reactive dimension evaluation for the Maine Yankee intact fuel types. The basket cell model represents an infinite array of fuel tubes separated by one-inch flux traps and neglects the radial neutron leakage of the basket. This will result in k_{eff} values greater than 0.95. The basket cell model is, therefore, only used to determine relative reactivities of the various physical dimensions of the Maine Yankee fuel inventory, not to establish maximum k_s values for the basket loaded with Maine Yankee fuel assemblies. The basket in cask model is used for the evaluation of the remaining fuel configurations. The basket criticality model uses the nominal basket configuration with full moderation under accident conditions, where accident conditions implying the loss of fuel cladding integrity and flooding of the pellet to cladding gap in all fuel rods. The analyses presented are performed using the UMS® transport cask shield geometry.

Transport Cask Model

The infinite array geometry is used only to determine the most reactive dimensions. The most reactive lattice dimensions determined by the basket cell model are incorporated into the basket in cask model. The Universal Transport Cask geometry is evaluated using the nominal basket configuration with full moderation. The transport cask accident event is modeled assuming that the fuel clad gap is flooded, the basket is flooded and the neutron shield material is replaced with water. Evaluating 24 hybrid 14x14 fuel assemblies with the most reactive pellet diameter for the accident condition produces a $k_{eff} + 2\sigma$ of 0.91014. This is less reactive than the accident condition for the transport cask loaded with the Westinghouse 17 x 17 OFA assemblies ($k_{eff} + 2\sigma$ of 0.9210). Therefore, the Westinghouse 17 x 17 OFA fuel criticality evaluation is bounding.

6.6.1.1.2 Maine Yankee Intact Spent Fuel

The evaluation of the intact Maine Yankee spent fuel inventory demonstrates that under all conditions the maximum reactivity of the UMS® basket loaded with Maine Yankee fuel assemblies is bounded by the Westinghouse 17 x 17 OFA evaluation presented in Section 6.4. The intact fuel assembly evaluation includes the determination of maximum reactivity dimensions of the Maine Yankee fuel assemblies, and the reactivity effects of variably enriched assemblies, annular axial end blankets, removed rods, fuel in guide tubes, and consolidated fuel assemblies. Where necessary, loading restrictions are applied to limit the number and location of the basket payload evaluated.

Fuel Assembly Lattice Dimensional Variations

Maine Yankee 14x14 PWR fuel has been provided by Combustion Engineering, Exxon/ANF and Westinghouse. The range of fuel assembly dimensions evaluated for Maine Yankee are shown in Table 6.6.1.1-1.

Most Reactive Fuel Dimensions

Bounding fuel assembly dimensions are determined using the guidelines set in Section 6.4.4 and are reported in Table 6.6.1.1-2. The dimensional perturbations that can increase the reactivity of any undermoderated array of fuel assemblies in a flooded system (including flooding the fuel-clad gap) are:

- Decreasing the clad outside diameter (OD)
- Increasing the clad inside diameter (ID) (i.e., increasing the gap)
- Decreasing the pellet diameter
- Decreasing the guide tube thickness

To conservatively model the clad thickness of the Maine Yankee standard fuel, the outside diameter of the clad is iteratively decreased until the clad thickness reaches the minimum. The pellet diameter is studied separately to determine which diameter maximizes the reactivity of the assembly. This study is performed using an infinite array of hybrid 14x14 fuel assemblies. These hybrid assemblies have the combination of most reactive dimensional parameters listed in Table 6.6.1.1-2 and are used in the evaluation of site specific fuel configurations. The pellet diameter is modeled first at the maximum diameter, and then it is iteratively decreased until a peak reactivity (H/U ratio) is reached. The results of this study are reported in Table 6.6.1.1-3. The maximum reactivity occurs at a pellet diameter of 0.3527 inches. This pellet diameter, which produces the most reactive system, is conservatively used in the analyses of an assembly with 176 fuel rods.

The reactivity of an infinite array of basket unit cells containing infinitely tall, hybrid 14x14 fuel assemblies and a flooded fuel-clad gap is $k_{eff} + 2\sigma = 0.96268$. This is less reactive than the same array of Westinghouse 17x17 OFA assemblies ($k_{eff} + 2\sigma = 0.9751$ from Table 6.4-1). Therefore, the design basis Westinghouse 17x17 OFA fuel criticality analysis is bounding. The conservatism obtained by decreasing the pellet diameter below that of the reported Maine Yankee fuel pellet diameter results in a Δk_{eff} of 0.00247.

6.6.1.1.3 Variably Enriched Fuel Assemblies

Two batches of fuel used at Maine Yankee contain variably enriched fuel rods. Fuel rod enrichments of one batch are 4.21 wt % ^{235}U and 3.5 wt % ^{235}U. The maximum planar average enrichment of this batch is 3.99 wt % ^{235}U. In the other batch, the fuel rod enrichments are 4.0 wt % ^{235}U and 3.4 wt % ^{235}U. The maximum planar average enrichment of this batch is 3.92 wt % ^{235}U. Loading 24 variably enriched fuel assemblies having both a maximum fuel rod enrichment of 4.21 wt % ^{235}U and a maximum planar average enrichment of 3.99 wt % ^{235}U results in a $k_{eff} + 2\sigma$ of 0.89940. Using a planar fuel rod enrichment of 4.2 wt % ^{235}U results in a $k_{eff} + 2\sigma$ of 0.91014. Therefore, all of the fuel rods are conservatively modeled as if enriched to 4.2 wt % ^{235}U for the remaining Maine Yankee analyses.

6.6.1.1.4 Assemblies with Annular Axial End Blankets

One batch of variably enriched fuel also incorporates 2.6 wt% ^{235}U axial end blankets with annular fuel pellets. The top and bottom 5% of the active fuel length of each fuel rod in this batch contains annular fuel pellets having an inner diameter of 0.183 inches. This geometry is discretely modeled as approximately 5% annular fuel, 90% solid fuel and then 5% annular fuel, with all fuel materials enriched to 4.2 wt % ^{235}U. The diameter of all pellets is modeled first as the most reactive pellet diameter. The accident case model is used for this evaluation, which includes flooding the cladding annulus. The periodic boundary conditions remain, which keeps the conservatism of the infinite fuel height.

Use of the smaller pellet diameter is not considered to be conservative when evaluating the annular fuel pellets. The smaller pellet diameter is the most reactive under the assumption that the fuel pellet is solid, not an annulus. Flooding the annulus in the axial end blankets provides additional moderator to the fuel lattice. Therefore, the diameter of the annular pellets is also modeled as the maximum pellet diameter of 0.3800 inches to regain a small portion of the fuel that is missing. The 0.3800-inch diameter is applied only to the annular pellets, while the smaller diameter of the solid pellets remains. The results of this study are reported in Table 6.6.1.1-4.

As shown in the table, the most reactive annular fuel model for the axial annular fuel end blankets results in a slightly more reactive system than the hybrid fuel accident evaluation. However, this annular condition is less reactive than the accident evaluation including Westinghouse 17x17 OFA assemblies. Therefore, the Westinghouse 17x17 OFA fuel criticality evaluation is bounding.

6.6.1.1.5 Assemblies with Removed Fuel Rods

Some of the Maine Yankee fuel assemblies have had fuel rods removed from the 14 x 14 lattice or have had poison rods replaced by hollow Zircaloy rods. The exact number and location of removed rods and hollow rods differs from one assembly to another. To determine a bounding reactivity for these assemblies, an analysis changing the location and the number of removed rods is performed. The removed rod analysis bounds that of the hollow rod analysis, since the Zircaloy tubes displace moderator in the under moderated assembly lattice. For each case, all 24 assemblies are centered in the fuel tubes and have the same number and location of removed fuel rods. Various patterns of removed fuel rod locations are analyzed when the number of removed

fuel rods is small enough to allow a different and possibly more reactive geometry. As the number of removed fuel rods increases, the number of possible highly reactive locations for these removed rods decreases. As described in Section 6.6.1.1.2, the fuel pellet diameter of every fuel rod is modeled first using the most reactive pellet diameter (0.3527 inches), and then as the maximum pellet diameter (0.380 inches).

The results of these analyses, which determine the most reactive number and geometry of removed rods for any Maine Yankee assembly, are presented in Tables 6.6.1.1-5 and 6.6.1.1-6. Table 6.6.1.1-5 contains the results based on a 0.3527-inch fuel pellet. All of the removed fuel rod cases using the smaller pellet diameter show cask reactivity levels lower than those of Westinghouse 17 x 17 OFA fuel. Table 6.6.1.1-6 contains the results of the evaluation using the maximum pellet diameter of 0.380 inch. Using the maximum pellet diameter provides for a more reactive system, since moderator is added (at the removed rod locations), to an assembly that contains more fuel. The most reactive removed fuel rod case occurs when 24 fuel rods are removed in the diamond shaped geometry shown in Figure 6.6.1.1-1, from the model containing the largest allowed pellet diameter. This case represents the bounding number and geometry of removed fuel rods for the Maine Yankee fuel assemblies. It results in a more reactive system than either the Maine Yankee hybrid 14 x 14 fuel accident case or the Westinghouse 17 x 17 OFA accident case assuming unrestricted loading. However, as shown in Table 6.6.1.1-6, when the loading of any assembly with less than 176 fuel rods or filler rods is restricted to the four corner fuel tubes, the reactivity of the worse case drops well below that of the Westinghouse 17 x 17 OFA fuel assemblies. Therefore, loading of Maine Yankee fuel assemblies with removed fuel rods, or with hollow Zircaloy rods, is restricted to the four corner fuel tube positions of the basket. With this loading restriction, the Westinghouse 17 x 17 OFA criticality evaluation remains bounding.

6.6.1.1.6 Assemblies with Fuel Rods in the Guide Tubes

A few of the Maine Yankee intact assemblies may contain up to two intact fuel rods in some of the guide tubes (i.e., allowing for the potential storage of individual intact fuel rods in an intact fuel assembly). To evaluate loading of these assemblies into the canister, an analysis adding 1 and then 2 intact fuel rods into 1, 2, 3 and then 5 guide tubes is made. Since the additional fuel rods are added to a fuel assembly, the evaluation considers a fuel assembly with up to 186 fuel rods. The results of the evaluation of these configurations are shown in Table 6.6.1.1-7. While higher in reactivity than the Maine Yankee hybrid base case, any fuel configuration with up to 2

fuel rods per guide tube is less reactive than the accident case for the Westinghouse 17 x 17 OFA fuel assemblies. Therefore, the Westinghouse 17 x 17 OFA fuel criticality evaluation is bounding.

Fuel rods may also be inserted in the guide tubes of fuel assemblies from which the fuel rods were removed (i.e., fuel rods removed from a fuel assembly and re-installed in the guide tubes of the same fuel assembly). The maximum number of fuel rods in these assemblies, including fuel rods in the guide tubes remains 176. These configurations are restricted to loading in a Maine Yankee fuel can in a corner fuel position in the basket. As shown in Section 6.6.1.1.5 for the removed fuel rods, the maximum reactivity of Maine Yankee assemblies containing 176 fuel rods in various configurations is bounded by the Westinghouse 17 x 17 OFA evaluation. These non-standard Maine Yankee assemblies are restricted to the corner fuel positions.

In addition to the fuel rods, some Maine Yankee assemblies may contain poison shim rods in guide tubes. These solid fill rods will serve as parasitic absorber and displace moderator and are, therefore, not included in the criticality model but are bounded by the evaluation performed.

6.6.1.1.7 Consolidated Fuel

The consolidated assemblies are a 17x17 array of rods with a pitch of 0.492 inches. Some of the locations contain solid fill rods and some are empty. To determine the reactivity of the consolidated fuel lattice with empty fuel rod positions, an analysis changing the location and the number of empty positions is performed. This consolidated fuel analysis considers 24 consolidated fuel lattices in the basket. All 24 consolidated fuel lattices are centered in the fuel tubes and have the same number and location of empty fuel rod positions. As shown in Section 6.6.1.1.5, the removed fuel rod configuration with a 0.380-inch pellet diameter provides a more reactive system than a system using the optimum pellet diameter from Section 6.6.1.1.2. The larger pellet cases are more reactive, since moderator is added at the empty fuel rod positions to an assembly that contains more fuel. Therefore, the consolidated assembly empty rod position evaluation is performed with the 0.380-inch pellet diameter.

The results of this evaluation are shown in Table 6.6.1.1-8. Configurations having more than 73 empty positions result in a more reactive system than the Westinghouse 17 x 17 OFA design basis fuel. The most reactive consolidated assembly case occurs with 113 empty rod positions in the geometry shown in Figure 6.6.1.1-2. However, when the loading of the consolidated fuel is

restricted to the four corner fuel tubes, the reactivity of the cask is lower than the accident condition of the cask loaded with Westinghouse 17x17 OFA assemblies. Therefore, loading of the consolidated fuel is restricted to the four corner fuel tube positions of the basket. With this loading restriction, the Westinghouse 17 x 17 OFA fuel criticality evaluation is bounding.

6.6.1.1.8 Damaged Fuel and Fuel Debris in the Maine Yankee Fuel Can

Damaged fuel assemblies are placed in a Maine Yankee fuel can prior to loading in the basket (see Drawings 412-501 and 412-502). The Maine Yankee fuel can has screened openings in the baseplate and the lid to permit drainage, vacuum drying and inerting of the can. This evaluation conservatively considers 100% of the fuel rods in the fuel can as damaged.

Fuel debris must be loaded in a rod or tube structure that is subsequently loaded into a Maine Yankee fuel can. The mass of fuel debris placed in the rod or tube is restricted to the mass equivalent of a fuel rod of an intact fuel assembly.

The Maine Yankee spent fuel inventory includes fuel assemblies with fuel rods inserted in the guide tubes of the assembly. If the integrity of the cladding of the fuel rods in the guide tubes cannot be ascertained, then those fuel rods are assumed to be damaged.

Damaged Fuel Evaluation

All of the spent fuel classified as damaged and all of the spent fuel not in its original lattice are stored in a Maine Yankee fuel can. This fuel is analyzed using a 100% fuel rod failure assumption. The screened fuel can is designed to preclude the release of pellets and gross particulate into the canister cavity. Evaluation of the canister with four Maine Yankee fuel cans containing CE 14 x 14 fuel assemblies that have up to 176 damaged fuel rods, or consolidated fuel consisting of up to 289 fuel rods, considers 100% dispersal of the fuel from these rods within the fuel can. The Maine Yankee fuel can is restricted to loading in one of the four corner positions of the basket.

All loose fuel in each analysis is modeled as a homogeneous mixture of fuel and water, of which the volume fractions of the fuel versus the water are varied from 0-100%. By varying the fuel fraction up to 100%, this evaluation addresses fuel masses significantly larger than those available in a standard or consolidated fuel assembly. First, loose fuel from damaged fuel rods within a fuel assembly is evaluated between the remaining rods of the most reactive missing rod array. The results of this analysis, provided in Table 6.6.1.1-9, show a slight decrease in the

reactivity of the system. Adding fuel to the already optimized H/U ratio of the bounding missing rod array reduces the reactivity of the system as this effectively returns the system to an undermoderated state. Second, loose fuel is considered above and below the active fuel region of this most reactive missing rod array. This analysis is performed within a finite cask model. The results of this study, provided in Table 6.6.1.1-10, show that any possible mixture combination of fuel and water above and below the active fuel region and, hence, above and below the BORAL sheet coverage, will not significantly increase the reactivity of the system beyond that of the missing rod array. Loose fuel is also considered to replace all contents of the Maine Yankee fuel can in each four corner fuel tube location. As shown in Table 6.6.1.1-11, the results of this study, which include modeling of the Maine Yankee fuel can, show that any mixture of fuel and water within this cavity will not significantly increase the reactivity of the system beyond that of the missing rod array.

Damaged fuel within the fuel can may also result from a loss of integrity of a consolidated fuel assembly. As described in Section 6.6.1.1.7, the consolidated assembly missing rod study shows that a potentially higher reactivity heterogeneous configuration does not increase the overall reactivity of the system beyond that of loading 24 Westinghouse 17 x 17 OFA assemblies when this configuration is restricted to the four corner locations. The homogeneous mixture study of loose fuel and water replacing the contents of the Maine Yankee fuel can (in each of the four corner fuel tube locations) considers more fuel than is present in the 289 fuel rod consolidated assembly. This study shows that a homogeneous mixture at an optimal H/U ratio within the fuel can also does not affect the reactivity of the system.

The transport cask loaded with the Westinghouse 17 x 17 OFA fuel assemblies is subcritical. Therefore, it is inherent that a statistically equivalent, or less reactive, canister loading of four Maine Yankee fuel cans containing assemblies with up to 176 damaged rods, or consolidated assemblies with up to 289 rods and 20 of the most reactive Maine Yankee fuel assemblies, is also subcritical. Therefore, assemblies with up to 176 damaged rods and consolidated assemblies with up to 289 rods are allowable contents as long as they are loaded into Maine Yankee fuel cans.

Fuel Debris Evaluation

Prior to loading fuel debris into the screened Maine Yankee fuel can, fuel debris must be placed into a rod type structure. Placing the debris into rods confines the spent nuclear material to a known volume and allows the fuel debris to be treated identically to the damaged fuel for criticality analysis.

Based on the discussion presented in Section 6.6.1.1.1, the maximum k_s of the UMS® canister with fuel debris will be less than 0.95, including associated uncertainty and bias.

6.6.1.1.9 Fuel Assemblies with Start-up Sources or Other Non-Fuel Components Inserted in a Guide Tube

Maine Yankee fuel assemblies are evaluated for criticality safety with components inserted in the center or corner guide tubes of the fuel assembly. These components include start-up sources, Control Element Assembly (CEA) fingertips, and a 24-inch ICI segment. Start-up sources are inserted in the center guide tube. The CEA fingertips and ICI segment must be inserted in a corner guide tube that is closed at the bottom end of the assembly.

Assemblies with Start-up Sources

Maine Yankee has three Pu-Be sources and two Sb-Be sources that will be installed in the center guide tubes of 14 x 14 assemblies that subsequently must be loaded in one of the four corner fuel positions of the basket. Each source is designed to fit in the center guide tube of an assembly. All five of these start-up sources contain Sb-Be pellets, which are 50% Be by volume. The moderation potential of the beryllium (Be) is evaluated to ensure that this material will not increase the reactivity of the system beyond that reported for the accident condition. The antimony (Sb) content is insignificant and is not considered. The start-up source is assumed to remain within the center guide tube for all conditions. The base case infinite height model used for comparison is the bounding Maine Yankee fuel assembly with 24 empty rod positions as reported in Table 6.6.1.1-6. The center guide tube of this model is filled with 50% water and 50% beryllium. The analysis assumes that assemblies with start-up sources are loaded in all four of the basket corner fuel positions. This configuration, resulting in a system reactivity, $k_{eff} \pm \sigma$ of 0.91085 ± 0.00087, shows that loading Sb-Be sources or the used Pu-Be sources into the center guide tubes of the assemblies in the four corner locations of the basket does not significantly change the reactivity of the system.

One of the three Pu-Be sources was never irradiated. Analysis of this source is equivalent to assuming that the spent Pu-Be sources are fresh. The unused source consists of two capsules that have a total of 1.4 grams of plutonium. All of this material is conservatively assumed to be in one capsule and is modeled as ^{239}Pu. The diameter of this capsule is 0.270 inch and its length is 9.75 inches. This corresponds to a capsule volume of approximately 9.148 cubic centimeters. Thus, the 1.4 grams of ^{239}Pu occupies ~0.77% of the volume at a density of 19.84 g/cc. This

material composition is then conservatively assumed to fill the entire center guide tube, which models considerably more ^{239}Pu than is actually present within the Pu-Be source. The remaining volume of the guide tube is analyzed at various fractions of Be, water and/or void to ensure that any combination of these materials is considered. The results of these analyses, provided in Table 6.6.1.1-12, show that loading a fresh Pu-Be start-up source into the center guide tube of each of the four corner assemblies does not significantly change the reactivity of the system.

Fuel Assemblies with Inserted CEA Fingertips or ICI Segment

Maine Yankee fuel assemblies may have CEA fingertips or an ICI segment inserted in one of the four corner guide tubes of a 14 x 14 assembly. The ICI segment is approximately 24 inches long. These components do not contain any fissile material or moderating material. Therefore, it is conservative to ignore these components, as they displace moderator when the basket is flooded, reducing reactivity.

6.6.1.1.10 Transport Cask Top End Drop Event

The exposed fuel evaluation performed for the design basis Westinghouse 17 x 17 OFA fuel in Section 6.4.5 bounds that of the less reactive Maine Yankee fuel.

6.6.1.1.11 Maine Yankee Criticality Results and Fuel Loading Restrictions

The criticality analyses for the Maine Yankee site specific fuel demonstrates that the UMS® basket loaded with these fuel assemblies results in a system that is less reactive than loading the basket with the Westinghouse 17 x 17 OFA fuel assemblies, provided that loading is restricted to the four corner fuel tube positions in the basket for:

- All 14 x 14 fuel assemblies with less than 176 fuel rods or solid filler rods
- All 14 x 14 fuel assemblies with hollow rods
- All 17 x 17 consolidated fuel lattices
- All 14 x 14 fuel assemblies with fuel rods in the guide tubes and a maximum of 176 fuel rods or solid rods and fuel rods

The following Maine Yankee fuels are not restricted as to loading position within the basket:

- All 14x14 fuel assemblies with 176 fuel rods or solid filler rods at a maximum enrichment of 4.2 wt % ^{235}U.
- Variably enriched fuel with a maximum fuel rod enrichment of 4.21 wt % ^{235}U with a maximum planar average enrichment of 3.99 wt % ^{235}U.
- Fuel with solid stainless steel filler rods, solid Zircaloy filler rods or solid poison shim rods in any location.
- Fuel with annular axial end blankets of up to 4.2 wt % ^{235}U.
- Fuel with a maximum of two intact fuel rods in each guide tube for a total of 186 fuel rods.

Assemblies defined as unrestricted may be loaded into the basket in any basket location and may be mixed in the same basket. While not analyzed in detail, CEAs and ICI thimble assemblies may be loaded into any intact assemblies. The CEA fingertips and ICI segment may be loaded in the corner guide posts of any intact fuel assembly provided that a CEA flow plug is also installed in the fuel assembly to close the top of the guide tubes. The basket loading position of these assemblies is not restricted. These components displace a significant amount of water in the fuel lattice while adding parasitic absorber, thereby reducing system reactivity.

Based on the evaluation of Maine Yankee fuel assemblies with start-up sources, the following loading restrictions for criticality control apply:

- Any Maine Yankee fuel assembly having a component evaluated in this section inserted in a guide tube must be loaded in one of the four corner fuel loading positions of the basket. Corner positions are also peripheral positions and are marked "P" in the figure in Section 1.3.1.1.1.
- Start-up sources containing plutonium or beryllium shall be restricted to loading in fuel assemblies classified as intact and must be loaded in a center guide tube.
- Only one start-up source may be loaded into any intact fuel assembly.
- Up to four intact fuel assemblies with inserted start-up sources may be loaded in any canister using the corner positions of the basket.

When loaded in accordance with these restrictions, the evaluated components do not significantly increase the reactivity of the system.

Figure 6.6.1.1-1 24 Removed Fuel Rods - Diamond Shaped Geometry, Maine Yankee Site Specific Fuel

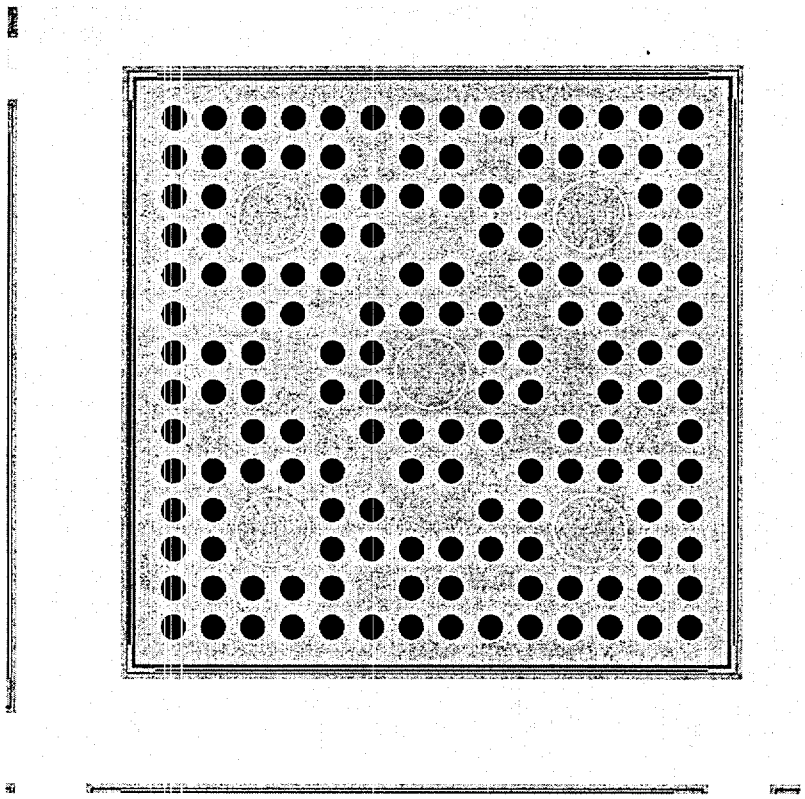

Figure 6.6.1.1-2 Consolidated Fuel Geometry, 113 Empty Fuel Rod Positions, Maine Yankee Site Specific Fuel

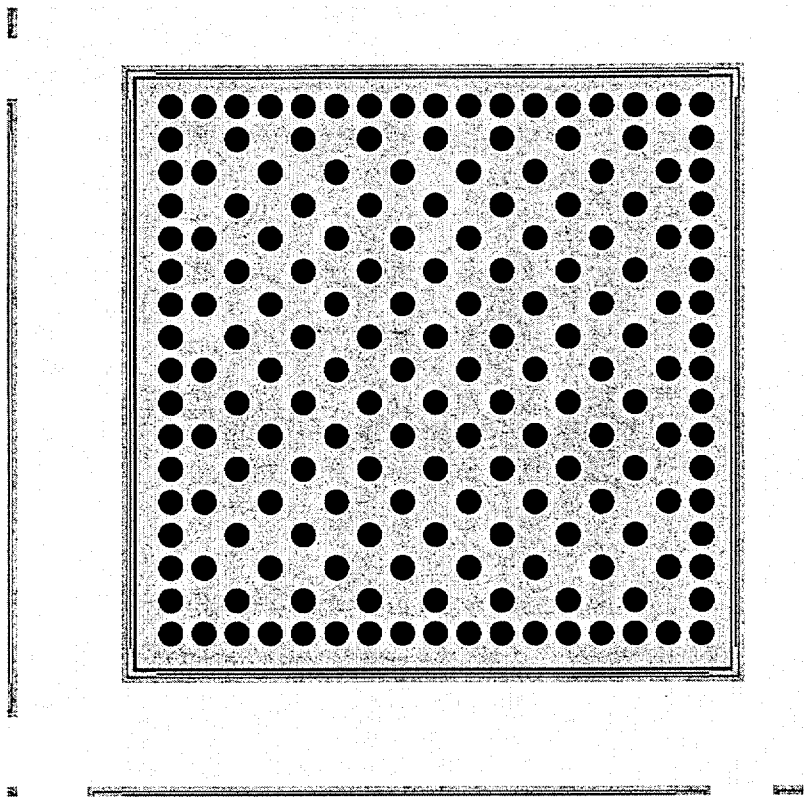

Table 6.6.1.1-1 Maine Yankee Standard Fuel Characteristics

Fuel Class[1]	Vendor	Array	Version	Number of Fuel Rods	Pitch (in.)	Rod Diameter (in.)	Clad ID (in.)	Clad Thickness (in.)	Pellet Diameter (in.)	GT[2] Thickness (in.)
1	CE	14x14	Std.	160[3]-176	0.570-0.590	0.438-0.442	0.3825-0.3895	0.024-0.028	0.376-0.380	0.036-0.040
1	Ex/ANF	14x14	CE	164[4]-176	0.580	0.438-0.442	0.3715-0.3795	0.0294-0.031	0.3695-0.3705	0.036-0.040
1	WE	14x14	CE	176	0.575-0.585	0.438-0.442	0.3825-0.3855	0.0262-0.028	0.376-0.377	0.034-0.038

1. All fuel rods are Zircaloy clad.
2. Guide tube thickness.
3. Up to 16 fuel rod positions may have solid filler rods or burnable poison rods.
4. Up to 12 fuel rod positions may have solid filler rods or burnable poison rods.

Table 6.6.1.1-2 Maine Yankee Most Reactive Fuel Dimensions

Parameter	Bounding Dimensional Value
Maximum Rod Enrichment[1]	4.2 wt % ^{235}U
Maximum Number of Fuel Rods[2]	176
Maximum Pitch (in.)	0.590
Maximum Active Length (in.)	N/A – Infinite Model
Minimum Clad OD (in.)	0.4375
Maximum Clad ID (in.)	0.3895
Minimum Clad Thickness (in.)	0.024
Maximum Pellet Diameter (in.)	0.3800 - Study
Minimum Guide Tube OD (in.)	1.108
Maximum Guide Tube ID (in.)	1.040
Minimum Guide Tube Thickness (in.)	0.034

1. Variably enriched fuel assemblies may have a maximum fuel rod enrichment of 4.21 wt % ^{235}U with a maximum planar average enrichment of 3.99 wt % ^{235}U.
2. Assemblies with less than 176 fuel rods or solid dummy rods are addressed after the determination of the most reactive dimensions.

Table 6.6.1.1-3 Maine Yankee Pellet Diameter Study

Diameter (inches)	k-eff	σ	k-eff +2σ
0.3800	0.95585	0.00085	0.95755
0.3779	0.95784	0.00080	0.95944
0.3758	0.95714	0.00085	0.95884
0.3737	0.95863	0.00082	0.96027
0.3716	0.95862	0.00084	0.96030
0.3695	0.95855	0.00083	0.96021
0.3674	0.95863	0.00085	0.96033
0.3653	0.95982	0.00084	0.96150
0.3632	0.95854	0.00088	0.96030
0.3611	0.95966	0.00083	0.96132
0.3590	0.95990	0.00084	0.96158
0.3569	0.96082	0.00082	0.96246
0.3548	0.96053	0.00083	0.96219
0.3527	0.96104	0.00082	0.96268
0.3506	0.95964	0.00087	0.96138
0.3485	0.95993	0.00086	0.96165
0.3464	0.95916	0.00084	0.96084
0.3443	0.95847	0.00083	0.96013
0.3422	0.95876	0.00083	0.96042
0.3401	0.95865	0.00081	0.96027
0.3380	0.95734	0.00084	0.95902

Table 6.6.1.1-4 Maine Yankee Annular Fuel Results

Case Description	k_{eff}	σ	$k_{eff} + 2\sigma$
All pellets with a diameter of 0.3527 inches	0.90896	0.00083	0.91061
Annular pellet diameter changed to 0.3800 inches	0.91013	0.00087	0.91187

Table 6.6.1.1-5 Maine Yankee Removed Fuel Rod Results with Small Pellet Diameter

Number of Removed Rods	Number of Fuel Rods	k_{eff}	σ	$k_{eff}+2\sigma$
4	172	0.91171	0.00088	0.91347
4	172	0.91292	0.00086	0.91464
4	172	0.91479	0.00081	0.91640
4	172	0.91125	0.00087	0.91299
6	170	0.91418	0.00087	0.91592
6	170	0.91264	0.00085	0.91435
6	170	0.91314	0.00086	0.91487
6	170	0.90322	0.00086	0.90493
8	168	0.91555	0.00087	0.91729
8	168	0.91490	0.00093	0.91676
8	168	0.91457	0.00088	0.91633
8	168	0.91590	0.00087	0.91764
8	168	0.89729	0.00088	0.89905
12	164	0.91654	0.00086	0.91827
12	164	0.91469	0.00085	0.91639
12	164	0.91149	0.00083	0.91315
16	160	0.91725	0.00084	0.91893
16	160	0.91567	0.00084	0.91735
16	160	0.90986	0.00088	0.91162
16	160	0.90849	0.00083	0.91015
16	160	0.90704	0.00086	0.90876
24	152	0.91572	0.00083	0.91739
32	144	0.91037	0.00088	0.91213
48	128	0.89385	0.00085	0.89554
48	128	0.84727	0.00079	0.84886
64	112	0.79602	0.00083	0.79768
96	80	0.69249	0.00077	0.69402
Westinghouse 17x17 OFA		0.9192	0.0009	0.9210

Table 6.6.1.1-6 Maine Yankee Removed Fuel Rod Results with Maximum Pellet Diameter

Number of Removed Rods	Number of Fuel Rods	k_{eff}	σ	$k_{eff} + 2\sigma$
4	172	0.91078	0.00086	0.91250
4	172	0.90916	0.00085	0.91085
4	172	0.91164	0.00087	0.91338
4	172	0.90809	0.00085	0.90979
6	170	0.91223	0.00085	0.91393
6	170	0.91223	0.00080	0.91384
6	170	0.91270	0.00086	0.91442
6	170	0.90245	0.00086	0.90416
6	170	0.89801	0.00086	0.89972
8	168	0.91567	0.00085	0.91736
8	168	0.91448	0.00085	0.91618
8	168	0.91355	0.00086	0.91526
8	168	0.91293	0.00085	0.91463
12	164	0.91639	0.00090	0.91818
12	164	0.91803	0.00086	0.91974
12	164	0.91235	0.00083	0.91401
16	160	0.91665	0.00091	0.91847
16	160	0.92136	0.00087	0.92310
16	160	0.91231	0.00084	0.91400
16	160	0.90883	0.00087	0.91057
24	152	0.92227	0.00087	0.92400
32	144	0.92164	0.00088	0.92340
48	128	0.91212	0.00081	0.91373
48	128	0.86308	0.00082	0.86472
64	112	0.81978	0.00080	0.82138
88	88	0.72087	0.00083	0.72247
24 (Four Corners)	152	0.91153	0.00085	0.91323
Westinghouse 17x17 OFA		0.9192	0.0009	0.9210

Table 6.6.1.1-7 Maine Yankee Fuel Rods in Guide Tubes Results

Number of Guide Tubes with Rods	Number of Rods in Each	k_{eff}	σ	$k_{eff} + 2\sigma$
1	1	0.91102	0.00089	0.91280
2	1	0.91059	0.00088	0.91234
3	1	0.91172	0.00087	0.91346
5	1	0.91411	0.00086	0.91583
1	2	0.91169	0.00090	0.91349
2	2	0.91201	0.00087	0.91375
3	2	0.91173	0.00086	0.91344
5	2	0.91357	0.00086	0.91529
Design Basis Westinghouse 17x17 OFA		0.9192	0.0009	0.9210

Table 6.6.1.1-8 Maine Yankee Consolidated Fuel Empty Fuel Rod Position Results

Number of Empty Positions	Number of Fuel Rods	k_{eff}	σ	$k_{eff} + 2\sigma$
4	285	0.79684	0.00082	0.79848
9	280	0.80455	0.00081	0.80616
9	280	0.80812	0.00079	0.80970
13	276	0.81573	0.00083	0.81739
24	265	0.84187	0.00080	0.84347
25	264	0.84017	0.00083	0.84182
25	264	0.84634	0.00081	0.84795
25	264	0.84583	0.00083	0.84750
25	264	0.85524	0.00083	0.85690
25	264	0.83396	0.00081	0.83558
25	264	0.84625	0.00083	0.84790
27	262	0.85438	0.00083	0.85604
29	260	0.85179	0.00081	0.85340
31	258	0.85930	0.00084	0.86098
33	256	0.86407	0.00082	0.86571
35	254	0.86740	0.00082	0.86904
37	252	0.87372	0.00084	0.87541
45	244	0.88630	0.00081	0.88793
45	244	0.87687	0.00079	0.87844
52	237	0.90062	0.00083	0.90228
57	232	0.87975	0.000870	0.88149
61	258	0.89055	0.00083	0.89221
73	216	0.90967	0.00082	0.91131
84	205	0.93261	0.00091	0.93443
85	204	0.94326	0.00086	0.94499
113	176	0.95626	0.00084	0.95794
117	172	0.95373	0.00088	0.95549
119	170	0.95315	0.00085	0.95485
125	164	0.95020	0.00086	0.95192
141	148	0.94348	0.00086	0.94521
145	144	0.93868	0.00089	0.94047
113 (Four Corners)	176	0.91292	0.00087	0.91466
Design Basis Westinghouse 17x17 OFA		0.9192	0.0009	0.9210

Table 6.6.1.1-9 Fuel Can Infinite Height Model Results of Fuel - Water Mixture Between Rods

Volume Fraction of UO_2 in Water	k_{eff}	Δk_{eff} to 24 (Four Corners)[1]
0.000	0.91090	-0.00063
0.001	0.91138	-0.00015
0.002	0.91120	-0.00033
0.003	0.91177	0.00024
0.004	0.91285	0.00132
0.005	0.90908	-0.00245
0.006	0.91001	-0.00152
0.007	0.90895	-0.00258
0.008	0.91005	-0.00148
0.009	0.90986	-0.00167
0.010	0.90864	-0.00289
0.020	0.91003	-0.00150
0.030	0.90963	-0.00190
0.040	0.91063	-0.00090
0.050	0.90931	-0.00222
0.060	0.90765	-0.00388
0.070	0.90753	-0.00400
0.080	0.91088	-0.00065
0.090	0.91122	-0.00031
0.100	0.90879	-0.00274
0.150	0.90968	-0.00185
0.200	0.90952	-0.00201
0.250	0.90815	-0.00338
0.300	0.90748	-0.00405
0.350	0.90581	-0.00572
0.400	0.90963	-0.00190
0.450	0.90547	-0.00606
0.500	0.90603	-0.00550
0.550	0.90753	-0.00400
0.600	0.90674	-0.00479
0.650	0.90589	-0.00564
0.700	0.90594	-0.00559
0.750	0.90568	-0.00585
0.800	0.90532	-0.00621
0.850	0.90693	-0.00460
0.900	0.90639	-0.00514
0.950	0.90684	-0.00469
1.000	0.90677	-0.00476

1. See Table 6.6.1.1-6.

Table 6.6.1.1-10 Fuel Can Finite Model Results of Fuel - Water Mixture Outside BORAL Coverage

Volume Fraction of UO_2 in Water	k_{eff}	Δk_{eff} to 0.00 UO_2 in Water	Δk_{eff} to 24 (Four Corners)[1]
0.00	0.91045[2]	NA	-0.00108
0.05	0.90781	-0.00264	-0.00372
0.10	0.90978	-0.00067	-0.00175
0.15	0.91048	0.00003	-0.00105
0.20	0.90916	-0.00129	-0.00237
0.25	0.90834	-0.00211	-0.00319
0.30	0.90935	-0.00110	-0.00218
0.35	0.90786	-0.00259	-0.00367
0.40	0.90892	-0.00153	-0.00261
0.45	0.91015	-0.00030	-0.00138
0.50	0.91011	-0.00034	-0.00142
0.55	0.91003	-0.00042	-0.00150
0.60	0.90874	-0.00171	-0.00279
0.65	0.91165	0.00120	0.00012
0.70	0.90977	-0.00068	-0.00176
0.75	0.90813	-0.00232	-0.00340
0.80	0.90909	-0.00136	-0.00244
0.85	0.91028	-0.00017	-0.00125
0.90	0.91061	0.00016	-0.00092
0.95	0.91129	0.00084	-0.00024
1.00	0.91076	0.00031	-0.00077

1. See Table 6.6.1.1-6.
2. $\sigma = 0.00084$.

Table 6.6.1.1-11 Fuel Can Finite Model Results of Replacing All Rods with Fuel - Water Mixture

Volume Fraction of UO_2 in Water	k_{eff}	Δk_{eff} to 24 (Four Corners) Finite Height Model[1]	Δk_{eff} to 24 (Four Corners) Infinite Height Model[2]
0	0.90071	-0.00974	-0.01082
5	0.90194	-0.00851	-0.00959
10	0.90584	-0.00461	-0.00569
15	0.90837	-0.00208	-0.00316
20	0.91008	-0.00037	-0.00145
25	0.91086	0.00041	-0.00067
30	0.90964	-0.00081	-0.00189
35	0.90828	-0.00217	-0.00325
40	0.90805	-0.00240	-0.00348
45	0.90730	-0.00315	-0.00423
50	0.90637	-0.00408	-0.00516
55	0.90672	-0.00373	-0.00481
60	0.90649	-0.00396	-0.00504
65	0.90632	-0.00413	-0.00521
70	0.90435	-0.00610	-0.00718
75	0.90792	-0.00253	-0.00361
80	0.90376	-0.00669	-0.00777
85	0.90528	-0.00517	-0.00625
90	0.90454	-0.00591	-0.00699
95	0.90360	-0.00685	-0.00793
100	0.90416	-0.00629	-0.00737

1. The k_{eff} comparison basis for this column is the finite height model with the four corner locations of the basket loaded with Maine Yankee assemblies in the most reactive missing rod geometry. This case is the first case presented in Table 6.6.1.1-10 with 0% UO_2 in the water above and below the active fuel of the missing rod array.
2. The k_{eff} comparison basis for this column is the infinite height model with the four corner locations of the basket loaded with Maine Yankee assemblies in the most reactive missing rod geometry, the first case presented in Table 6.6.1.1-6 labeled "24 (Four Corners)," k_{eff} = 0.91153.

Table 6.6.1.1-12 Infinite Height Analysis of Maine Yankee Start-up Sources

Pu Vf	Be Vf	H2O Vf	Void Vf	k_{eff}	sd	k_{eff}+2sd	ΔK*
0	0.5	0.5	0	0.91085	0.00087	0.91259	-0.00068
0.00771371	0.99228629	0	0	0.91034	0.00089	0.91212	-0.00119
0.00771371	0.9	0.09228629	0	0.91151	0.00087	0.91325	-0.00002
0.00771371	0.8	0.19228629	0	0.91138	0.00087	0.91312	-0.00015
0.00771371	0.7	0.29228629	0	0.91042	0.00085	0.91212	-0.00111
0.00771371	0.6	0.39228629	0	0.91231	0.00086	0.91403	0.00078
0.00771371	0.5	0.49228629	0	0.90922	0.00083	0.91088	-0.00231
0.00771371	0.4	0.59228629	0	0.91197	0.00087	0.91371	0.00044
0.00771371	0.3	0.69228629	0	0.91203	0.00086	0.91375	0.00050
0.00771371	0.2	0.79228629	0	0.90922	0.00084	0.91090	-0.00231
0.00771371	0.1	0.89228629	0	0.91140	0.00085	0.91310	-0.00013
0.00771371	0	0.99228629	0	0.91149	0.00086	0.91321	-0.00004
0.00771371	0.9	0	0.09228629	0.91075	0.00087	0.91249	-0.00078
0.00771371	0.8	0	0.19228629	0.91143	0.00091	0.91325	-0.00010
0.00771371	0.7	0	0.29228629	0.91182	0.00086	0.91354	0.00029
0.00771371	0.6	0	0.39228629	0.91072	0.00082	0.91236	-0.00081
0.00771371	0.5	0	0.49228629	0.90984	0.00085	0.91154	-0.00169
0.00771371	0.4	0	0.59228629	0.90982	0.00091	0.91164	-0.00171
0.00771371	0.3	0	0.69228629	0.91055	0.00087	0.91229	-0.00098
0.00771371	0.2	0	0.79228629	0.91054	0.00085	0.91224	-0.00099
0.00771371	0.1	0	0.89228629	0.91006	0.00088	0.91182	-0.00147
0.00771371	0	0	0.99228629	0.90957	0.00086	0.91129	-0.00196

*Change in reactivity from case "24 (Four Corners)" in Table 6.6.1.1-6.

THIS PAGE INTENTIONALLY LEFT BLANK

26. Attach a regulated gas (nitrogen, helium or air) supply line to the vent port. Install a valved fitting on the drain port and ensure the valve is closed. Pressurize the canister to 35 psia (approximately 20.5 psig) and hold the pressure. There must be no loss of pressure for 10 minutes.
27. Release the pressure. Visually examine the shield lid to canister shell weld for indications of defects. Perform a liquid penetrant examination of the final weld surface. Record the results of the examinations.
28. Attach the suction pump to the drain line. Ensure that the vent line is open. Using the pump, remove the remaining free water from the canister cavity. Note the time that the last free water is removed from the canister cavity.

    Caution: Radiation levels at the top and sides of the transfer cask may rise as water is removed.

    Note: A pressure regulated gas (nitrogen, helium or air) attached to the vent valve may be used to assist water removal from the canister cavity. The pressure must be less than 20 psig.
29. Attach the vacuum equipment to the vent and drain ports. Dry any free standing water in the vent and drain port recesses.
30. Operate the vacuum equipment until a vacuum of 3 mm of mercury exists in the canister.
31. Verify that no water remains in the canister by holding the vacuum for 30 minutes. If water is present in the cavity, the pressure will rise as the water vaporizes.
32. Backfill the canister cavity with helium having a minimum purity of 99.9% to a pressure of one atmosphere (0 psig).

    Note: As an option, an informational helium leak test may be conducted at this point of the procedure using the following steps (the record leak test is performed at Step 49):

    32a. Backfill the canister cavity with helium having a minimum purity of 99.9% to a pressure of 15 psig.

    32b. Using a helium leak detector ("sniffer" detector) with a test sensitivity of 5×10^{-5} cm^3/sec (helium), survey the weld joining the shield lid and canister shell.

    32c. At the completion of the survey, vent the canister helium pressure to one atmosphere (0 psig).
33. Restart the vacuum equipment and operate until a vacuum of 3 mm of mercury exists in the canister.
34. Backfill the canister with helium having a minimum purity of 99.9% to a pressure of one atmosphere (0 psig).

35. Disconnect the vacuum and helium supply lines from the vent and drain ports. Dry any residual water that may be present in the vent and drain port cavities.
36. Install the vent and drain port covers.
37. Complete the root pass weld of the drain port cover to the shield lid.
38. Prepare the weld and perform a liquid penetrant examination of the root pass. Record the results.
39. Complete welding of the drain port cover to the shield lid.
40. Prepare the weld and perform a liquid penetrant examination of the drain port cover weld final pass. Record the results.
41. Complete the root pass weld of the vent port cover to the shield lid.
42. Prepare the weld and perform a liquid penetrant examination of the root pass. Record the results.
43. Complete welding of the vent port cover to the shield lid.
44. Prepare the weld and perform a liquid penetrant examination of the weld final surface. Record the results.
45. Remove any supplemental shielding used during shield lid closure activities.
46. Install the helium leak test fixture.
47. Attach the vacuum line and leak detector to the leak test fixture fitting.
48. Operate the vacuum system to establish a vacuum in the leak test fixture.
49. Operate the helium leak detector for 15 minutes to verify that there is no indication of a helium leak exceeding 2×10^{-7} cm^3/second.
50. Release the vacuum and disconnect the vacuum and leak detector line from the fixture.
51. Remove the leak test fixture.
52. Attach a three-legged sling to the structural lid using the swivel hoist rings.

    Caution: Ensure that the hoist rings are fully seated against the structural lid. Verify that the spacer ring is in place on the structural lid.

    Note: Verify that the structural lid is stamped or otherwise marked to provide traceability of the canister contents.
53. Using the cask handling crane or the auxiliary hook, install the structural lid in the top of the canister. Verify that the structural lid does not protrude above the canister shell. If so, remove the lid and inspect the surface of the shield lid for the cause of the interference. Verify that the gap in the spacer ring is not aligned with the shield lid alignment key. Remove the hoist rings.
54. Install the automatic welding equipment on the structural lid.